

**Structural and functional distinctions between auditory centers revealed
with MRI in living humans**

by

Irina S. Sigalovsky

B.S. Biomedical Engineering
Boston University, 1996

Submitted to the Harvard-M.I.T. Division of Health Sciences and Technology in partial
fulfillment of the requirements for the degree of

DOCTOR OF PHILOSOPHY

at the

MASSACHUSETTS INSTITUTE OF TECHNOLOGY

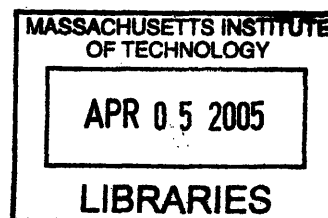
February 2005

© 2005 Massachusetts Institute of Technology
All rights reserved

Signature of Author:
Harvard-M.I.T. Division of Health Sciences and Technology
January 9, 2005

Certified by:
Jennifer R. Melcher, Ph.D.
Assistant Professor of Otology and Laryngology, Harvard Medical School
Thesis Supervisor

Accepted By:
Martha L. Gray, Ph.D.
Edward Hood Taplin Professor of Medical and Electrical Engineering
Co-Director, Harvard-M.I.T. Division of Health Sciences and Technology



ARCHIVES



Structural and functional distinctions between auditory centers revealed with MRI in living humans

by

Irina S. Sigalovsky

Submitted to the Harvard-M.I.T Division of Health Sciences and Technology on
January 9, 2005 in partial fulfillment of the requirements for the degree of
Doctor of Philosophy

ABSTRACT

From brainstem to cortex, sound is processed in centers that are functionally and structurally distinct. In animals, invasive electrophysiology and histology has revealed these distinctions and, consequently, organizational principles behind sound processing. In humans, however, comparable demonstrations are sparse. This thesis presents three MRI studies that provide new information regarding structural and functional distinctions between auditory centers in living humans.

The first study compared the effect of a fundamental acoustic variable, sound level, on the population neural activity of auditory brainstem, thalamus and cortex. Brainstem and cortex exhibited contrasting sensitivities to sound level (growth in activation followed by saturation in brainstem vs. plateau then growth in cortex), with thalamus showing intermediate properties.

The second study identified functional distinctions between cortical areas by spatially mapping the temporal properties of fMRI responses. Using a continuous noise stimulus, we found sustained responses on Heschl's gyrus flanked medially and laterally by more phasic activity. This pattern suggests that transient activity marking the beginning and end of a sound is most pronounced in non-primary areas of auditory cortex. The region of sustained responses may correspond to primary and primary-like areas. Thus, it may present a physiological marker for these areas in neuroimaging studies, something that has long been needed in the auditory neuroimaging field.

The third study examined whether auditory cortical areas can be distinguished - in the living human brain - based on classical features of cortical gray matter previously resolvable only in postmortem tissue. By mapping the imaging parameter R1, we identified regions of heavily myelinated gray matter that may correspond to primary auditory cortex. We further found greater gray matter myelination of the left temporal lobe, which may be a substrate for higher fidelity temporal processing on the left, and for left-hemispheric speech and language specializations. Being able to resolve gray matter structure in-vivo opens the way to relating cortical physiology and structure directly in living humans in ways previously possible only in animals.

Thesis Supervisor: Jennifer R. Melcher, Ph.D.

Title: Assistant Professor of Otology and Laryngology, Harvard Medical School

ACKNOWLEDGEMENTS

I would like to take this opportunity to express my gratitude to many people that made this journey such a transforming, enriching and, yes, enjoyable experience. Your advice and support are the main reason that, despite overwhelming experience of being a graduate student for so many (MANY) years, I consider myself fortunate to spend all this time in such nurturing environment as EPL.

First, I would like to give my very special thanks to my supervisor (and, even more importantly, advisor) Jennifer Melcher. Being her student is both challenging and rewarding in so many ways. Her contribution to my scientific development is tremendous. I especially appreciate the opportunity of frequent interactions provided by an “always open door” attitude on Jennifer’s side. Jennifer could certainly be credited with teaching me to think and write scientifically (i.e. describe facts in a logical manner and base conclusions on the facts). This is in contrast to the freelance writing style (i.e., pretty description of imaginary facts) I adopted prior to my graduate years. I hope to think that our complimentary personalities and ways of thinking have produced a number of creative accomplishments.

I would also like to thank my thesis committee for the time invested in sharing their expertise and reviewing this thesis. Special thanks to John Guinan, Jr. for offering his valuable and always detailed advise on multiple projects over the years. Thank you to Dr. Levine for exposing me to the fascinating world of patients and for being such a calming presence in the crazy world. Finally, thanks to Joe Mandeville for providing a much needed expertise on technical aspects of MRI.

Barbara Kiang, of course, deserves a very special thanks for extensive help with many things, ranging from making figures to fixing mistakes in my English. Huge thanks to Dianna Sands who is a unique person and represents to me that rare kind of a highly efficient administrator with a human face. I would also like to thank Nelson Kiang for teaching me to deal with the truth and to see beyond visible. He was, is and will be the ultimate teacher, beyond boundaries of a particular field or school of thought.

I also greatly appreciate the help of our wonderful technical support, Ish Stefanof-Wagner, Frank Cardarelli and Dave Steffens at EPL, and Paul Rines and Dave Coven at CNY. Throughout these years, many people helped me with technical MRI-related issues. Among these individuals are Bruce Fischl, David Salat, Doug Greve and Brian Quinn from the Martinos Imaging Center in Charlestown. Big thanks to the administrative staff at HST (MIT) who has been very helpful and friendly throughout these years.

During these years, I was fortunate to meet people who will, I hope, be my friends for life. These, of course, include Courtney Lane, Chandran Seshagiri, Radha Kalluri, Annette Tabernen, Vitaly Napadow, Jorge Jovicich, Rick Hoge, Alexander Cutschulk, Jocelyn Songer, Domenica Karavitaki, Evan Chen and many others.

Of course, my work would not exist without many people who offered their time to participate in my studies as subjects. Thank you, my friends, my relatives, my subjects.

Last, but certainly not least, I want to express my love and countless "Thank you" to my family. It is to my parents, my sister, my husband and my biggest love of all, Maya, that I owe my happiness and fortune. Their support and unconditional love are the true treasures I will value forever.

Irina Sigalovsky
January 9, 2005

The work in this thesis was supported by NIH/NIDCD PO1DC00119, T32DC00038, and Martinos Scholarship.

Table of Contents

Introduction	11
Thesis structure and chapter overview.....	13
References.....	15

Chapter I: Sound level representations in the auditory brainstem, thalamus and cortex of humans as seen with fMRI

Introduction.....	17
Methods.....	19
<i>Subjects</i>	
<i>Acoustic stimulation</i>	
<i>Task</i>	
<i>Mitigation of scanner acoustic noise</i>	
<i>Imaging</i>	
<i>Detecting activation</i>	
<i>Defining regions of interest</i>	
<i>Quantification of activation</i>	
Results.....	23
<i>Activation vs. stimulus level in brainstem structures: CN, SOC and IC</i>	
<i>Activation vs. stimulus level in the thalamus: MGB</i>	
<i>Activation vs. stimulus level in cortical areas: HGpm, HGal, PT and AMA</i>	
<i>Location of active voxels within cortical areas</i>	
Discussion.....	27
<i>Growth in population neural activity with sound level: subcortical vs. cortical centers</i>	
<i>Growth in activation with level: neural interpretations</i>	
<i>Dependencies of waveshape on sound level in cortex and thalamus, but not brainstem: neural interpretations</i>	
<i>Comparison to previous imaging and evoked potential studies of sound level dependencies</i>	
<i>Conclusions</i>	
References.....	35
Figure Captions.....	40
Figures.....	43

Chapter II: Spatio-temporal patterns of fMRI activation in the human auditory cortex

Introduction.....	51
Methods.....	54
<i>Subjects</i>	

<i>Acoustic stimuli</i>	
<i>Stimulus delivery</i>	
<i>Instructions to subject</i>	
<i>Imaging</i>	
<i>Functional data analysis</i>	
<i>Defining regions of interest</i>	
<i>Quantifying response waveshape</i>	
<i>Creating maps of waveshape index</i>	
Results.....	58
<i>Spatial maps of waveshape index (WI)</i>	
<i>Spatial variations in waveshape index: repeatability across subjects</i>	
<i>Response waveforms for different cortical areas</i>	
<i>Dependencies on sound intensity</i>	
<i>No difference in waveshape between the postero-medial and antero-lateral parts of Heschl's gyrus</i>	
<i>Differences in waveshape between PT and AMA</i>	
<i>Variability in waveshape index within PT</i>	
Discussion.....	61
<i>Sustained waveshape regions: relationship to primary auditory cortex</i>	
<i>Spatial variations in waveshape outside Heschl's gyrus: differentiation of non-primary areas</i>	
<i>Comparison to previous studies</i>	
<i>Optimizing regional differences in waveshape</i>	
<i>Spatial variations in waveshape: a reflection of differences in neural activity or hemodynamics?</i>	
<i>Functional significance of spatial variations in response waveshape</i>	
References.....	68
Figure Captions.....	71
Figures.....	73

Chapter III: Imaging gray matter myelin content of human auditory cortex suggests that a major architectonic division can be resolved in-vivo

Introduction.....	79
Methods.....	82
<i>Imaging</i>	
<i>Segmentation of the cortical gray matter</i>	
<i>Estimating gray matter R1</i>	
<i>Mapping and visualizing gray matter R1</i>	
<i>Defining regions of interest (ROIs)</i>	
<i>Validity of the techniques</i>	
Results.....	86
<i>Spatial variations in gray matter R1</i>	
<i>Regions of highest R1 on the superior temporal lobe</i>	
<i>Hemispheric differences</i>	
Discussion.....	87

*High R1 on Heschl's gyrus: A marker for koniocortex?
Hemispheric differences and functional interpretations
Implications and significance*

References.....	94
Figure Captions.....	99
Figures.....	101

Chapter IV: Imaging auditory gray matter thickness

Introduction.....	109
Methods.....	110
<i>Subjects</i>	
<i>Imaging</i>	
<i>Segmentation of the cortical gray matter</i>	
<i>Estimating and mapping gray matter thickness</i>	
<i>Defining regions of interest</i>	
Results.....	111
Discussion.....	112
References.....	114
Figure Captions.....	115
Figures.....	117

Chapter V: Contrasting sensitivity of inferior colliculus and auditory cortex to music and continuous noise studied using fMRI

Introduction.....	121
Methods.....	122
<i>Subjects</i>	
<i>Acoustic stimulation</i>	
<i>Task</i>	
<i>Mitigation of scanner acoustic noise</i>	
<i>Imaging</i>	
<i>Detecting activation</i>	
<i>Defining regions of interest</i>	
<i>Calculating response waveforms</i>	
<i>Response quantification</i>	
Results.....	125
<i>Effect of stimulus type on response waveshape</i>	
<i>Effect of stimulus type on response amplitude</i>	
Discussion.....	126
References.....	128
Figure Captions.....	129
Figures.....	131

Chapter VI: Summary	133
References.....	138
Figure Caption.....	139
Figure.....	141
Biography	143

Introduction

The ability to study brain structure and function in living humans using non-invasive techniques such as MRI has opened new doors to understanding normal and pathological workings of the human brain. Functional MRI (fMRI) is a relatively new technique (Kwong et al. 1992; Ogawa et al 1992) and provides a view of population neural, largely synaptic, activity (Logothetis et al., 2001). Because of its adequate spatial resolution (millimeters) but low temporal resolution (seconds), fMRI is sometimes viewed as complimentary to microelectrode recordings in animals and high-temporal-resolution, low-spatial-resolution EEG/MEG recordings in humans. However, its unparalleled versatility and ability to assess neural activity over the whole brain at once have been instrumental in revealing a great deal of new information about how the brain functions (e.g., understanding multi-sensory integration).

While the non-invasive and versatile nature of fMRI has led to its widespread use by neuroscientists and clinicians, it has been significantly under-utilized by the auditory community for a number of reasons. Some of the challenges of imaging the auditory system include (1) the acoustically noisy environment of the MRI scanners, which may saturate and/or alter neural activity in response to the intended stimulus (e.g., Bandettini et al., 1998, Talavage et al., 1999, Edmister et al., 1999), (2) a large number of small auditory nuclei deep in the brain susceptible to the cardiac-related, pulsatile brainstem motion (Guimaraes et al., 1998), and (3) relatively low metabolic changes associated with neural activity in auditory nuclei. The solutions to these challenges have been developed (Guimaraes et al., 1998, Edmister et al., 1998, Hall et al., 1999, Ravicz and Melcher, 2001), but, at the same time, these solutions have increased experimental complexity and lowered the efficiency of data acquisition. This most likely explains why many fundamental questions about human auditory system (e.g., “Where are the borders of the primary auditory cortex?”) remain unanswered. The situation, however, also presents an opportunity to ask (and answer) such questions.

This thesis consists of several studies that ask the following basic questions about the human auditory system: (1) How does sound level affect the population neural activity of auditory brainstem, thalamus and cortex? (2) What can temporal properties of

the fMRI responses tell us about physiological differences between different areas of the auditory cortex? (3) Can MRI be used to differentiate auditory cortical areas using classical, histologically-derived anatomical criteria in living humans using MRI?

Chronologically, each of these questions was motivated by findings and/or issues raised by the preceding one. For example, our findings from the study on sound level representations (Chapter I) revealed that, for some stimuli, fMRI response waveshape changes across the auditory pathway, from brainstem to thalamus to cortex. This finding prompted the question of whether the changes in fMRI response waveshape continue in the auditory cortex, from primary to non-primary areas. An ability to differentiate auditory cortical areas based on the temporal properties of fMRI responses could reveal physiological differences between these areas as well as provide physiological markers. While our results suggest that, indeed, regional variations in the fMRI response waveshape might provide a marker for the primary auditory cortex (Chapter II), our interpretations were limited by the fact that fMRI response waveshape has no analog in the animal literature.

In particular, at present, there is no way, either physiological or anatomical, to identify primary auditory cortex in living humans. For lack of a better alternative, neuroimaging studies have traditionally used gross anatomical landmarks, a standardized coordinate system (Talairach and Tournoux, 1988), or probabilistic atlases to define primary auditory cortex in their subjects (Rademacher et al., 2001, Morosan et al., 2001). These three approaches, however, provide only an approximate localization of cortical areas because of the considerable inter-subject variability in size and position of auditory areas relative to gross anatomy (Rademacher et al., 2001, Morosan et al., 2001, Hackett et al., 2001), and can prove especially faulty in clinical populations with abnormal gross anatomy (e.g., in dyslexia, see Leonard et al, 1993).

Thus, our third study (Chapter III) was motivated by the need for a marker of the primary auditory cortex in individual living humans. Unlike in the first two studies, which used functional MRI, we utilized the newly-evolving area of structural MRI in this study. In particular, we used the sensitivity of MR parameters to the myelin content of the tissue to examine whether differences in gray matter myelin content between major auditory areas could be resolved in-vivo.

In overview, the work presented here examines diverse aspects of the human auditory system ranging from looking for a structural and functional marker of the primary auditory cortex to examining sound level representations across different structures of the auditory pathway. The diversity of topics in this thesis is a testament to the fact that scientific investigations are a mixture of, on one hand, specific aims and hypotheses, and, on the other hand, a journey with unexpected detours to understand unpredicted experimental outcomes. It is also a testament to the rapid development of MR technology that allowed asking (and answering) questions that seemed impossible at the beginning of my dissertation work.

Thesis structure and chapter overview

This thesis is composed of the introduction and six chapters with the last chapter providing a summary discussion. Each of the first five chapters is written as a self-contained paper.

In Chapter I, we measured how a fundamental acoustic variable, sound level, affects the population neural activity of auditory brainstem, thalamus and cortex. Brainstem and cortex exhibited contrasting sensitivities to sound level (fast growth in activation followed by slower growth in brainstem vs. slow growth then fast growth and spread of activation in cortex), with thalamus showing intermediate properties. The combination of our data and previous studies suggests that loudness is reflected in the amount of population neural activity of subcortical, but not cortical, centers.

In Chapter II, we identified functional differences between cortical areas by spatially mapping the temporal properties of fMRI responses. Using a continuous noise stimulus, we found sustained responses on Heschl's gyrus flanked medially and laterally by more phasic activity. This pattern suggests that transient activity marking the beginning and end of a sound is most pronounced in non-primary areas of auditory cortex. The region of sustained responses, because of its location and extent, appears to correspond to primary and primary-like areas. Thus, the region of sustained responses may present a physiological marker for the primary and primary-like areas in

neuroimaging studies, something that has long been needed in the auditory neuroimaging field.

In Chapter III, we examined whether auditory cortical areas can be distinguished - in the living human brain - based on classical anatomical features of cortical gray matter previously resolvable only in postmortem tissue. By mapping the imaging parameter R1, we identified regions of heavily myelinated gray matter that may correspond to primary auditory cortex. In addition, we found greater gray matter myelination of the left temporal lobe than on the right, which may be a substrate for higher fidelity temporal processing on the left side, and for left-hemispheric speech and language specializations. Being able to resolve gray matter structure in-vivo opens the way to relating cortical physiology and structure directly in individual living humans in ways previously possible only in animals.

In Chapter IV, we examined spatial variations in the thickness of the auditory gray matter. Our results show that thickness co-varies with curvature of the cortical surface and generally increases towards the temporal pole, both trends being consistent with histological data.

In Chapter V, we compared fMRI activation to two stimuli with different temporal characteristics in the inferior colliculus and auditory cortex. In particular, we used broadband continuous noise and orchestral music to demonstrate contrasting sensitivities to these stimuli in these two major auditory structures. We found that while music produced stronger activation than noise in the auditory cortex, the reverse was true in the inferior colliculus.

The final chapter of the thesis, Chapter VI, reflects on ways in which functional and structural data from the same individual can be combined in the future to understand organizational principles behind auditory function and dysfunction, development and learning.

References

- Bandettini, P. A., A. Jesmanowicz, et al. (1998). "Functional MRI of brain activation induced by scanner acoustic noise." Magn Reson Med **39**(3): 410-6.
- Bandettini, P. A., K. K. Kwong, et al. (1997). "Characterization of cerebral blood oxygenation and flow changes during prolonged brain activation." Hum Brain Mapp **5**(2): 93-109.
- Guimaraes, A. R., J. R. Melcher, et al. (1998). "Imaging subcortical auditory activity in humans." Hum Brain Mapp **6**(1): 33-41.
- Edmister, W. B., T. M. Talavage, et al. (1999). "Improved auditory cortex imaging using clustered volume acquisitions." Hum Brain Mapp **7**(2): 89-97.
- Hackett, T. A., T. M. Preuss, et al. (2001). "Architectonic identification of the core region in auditory cortex of macaques, chimpanzees, and humans." J Comp Neurol **441**(3): 197-222.
- Hall, D. A., M. P. Haggard, et al. (1999). "'Sparse' temporal sampling in auditory fMRI." Hum Brain Mapp **7**(3): 213-23.
- Kwong, K. K., J. W. Belliveau, et al. (1992). "Dynamic magnetic resonance imaging of human brain activity during primary sensory stimulation." Proc Natl Acad Sci U S A **89**(12): 5675-9.
- Leonard, C. M., K. K. Voeller, et al. (1993). "Anomalous cerebral structure in dyslexia revealed with magnetic resonance imaging." Arch Neurol **50**(5): 461-9.
- Logothetis, N. K., J. Pauls, et al. (2001). "Neurophysiological investigation of the basis of the fMRI signal." Nature **412**(6843): 150-7.
- Morosan, P., J. Rademacher, et al. (2001). "Human primary auditory cortex: cytoarchitectonic subdivisions and mapping into a spatial reference system." Neuroimage **13**(4): 684-701.
- Ogawa, S., D. W. Tank, et al. (1992). "Intrinsic signal changes accompanying sensory stimulation: functional brain mapping with magnetic resonance imaging." Proc Natl Acad Sci U S A **89**(13): 5951-5.
- Rademacher, J., P. Morosan, et al. (2001). "Probabilistic mapping and volume measurement of human primary auditory cortex." Neuroimage **13**(4): 669-83.
- Ravicz, M. E. and J. R. Melcher (2001). "Isolating the auditory system from acoustic noise during functional magnetic resonance imaging: examination of noise conduction through the ear canal, head, and body." J Acoust Soc Am **109**(1): 216-31.
- Ravicz, M. E., J. R. Melcher, et al. (2000). "Acoustic noise during functional magnetic resonance imaging." J Acoust Soc Am **108**(4): 1683-96.
- Talairach, J. and P. Tournoux (1988). Co-planar stereotaxic atlas of the human brain, Thieme Medical Publishers, New York.
- Talavage, T. M., W. B. Edmister, et al. (1999). "Quantitative assessment of auditory cortex responses induced by imager acoustic noise." Hum Brain Mapp **7**(2): 79-88.

Chapter I.

Sound level representations in the auditory brainstem, thalamus and cortex of humans as seen with fMRI

Introduction

Sound level is an acoustic variable fundamental to virtually every major aspect of auditory perception from sound detection to speech recognition. As such, the neural representations of sound level have been extensively studied in both animals and humans, although important open questions remain. The goal of this fMRI study is to address aspects of sound level representation in the human CNS that have not been previously examined, particularly focusing on how these representations vary across major auditory processing stages from cochlear nucleus to cortex.

Neurophysiological studies in animals have revealed a variety of ways in which sound level may be encoded in the auditory system. For example, increases in spike rate, spread of excitation and decreases in response latency with increasing sound level have been demonstrated for single unit and gross neural activity throughout the auditory pathway (Kiang et al., 1965, Sachs and Abbas, 1974, Pfeiffer and Kim, 1975, Evans, 1981, Aitkin, 1991; Brugge et al., 1969, Phillips et al., 1985). While monotonic increase in neural activity with increasing sound level is more typical for the lower stages of the auditory pathway, a non-monotonic level dependency (e.g., a neuron responding best to a narrow range of intensities) becomes increasingly prevalent at the higher stages of the pathway as inhibitory processes influence the shape of the rate-intensity functions (Rose et al., 1963, Brugge et al., 1969, Brugge and Merzenich, 1973; Young and Brownell,

1976, Phillips and Irvine, 1981, Phillips et al, 1985, Semple and Kitzes, 1985; Shofner and Young, 1985). The occurrence of the non-monotonic units has led to suggestions of a place code for “best” level in the central auditory system, or amplitopy (Brugge and Merzenich, 1973), although to date, this has only been definitively demonstrated in bats (Suga and Manabe, 1982).

Unlike microelectrode recordings, imaging techniques such as fMRI and PET are well suited for studying neuronal populations (which becomes progressively important at the higher stages of the auditory pathway) and allow studying sounds processing in humans non-invasively. As such, they provide new and complimentary information to microelectrode recordings in animals. However, despite a large number of imaging papers on sound level dependencies in the human auditory pathway (Millen et al., 1995, Jancke et al., 1998, Lockwood et al., 1999, Hall et al., 2001, Brechmann et al., 2002, Bilecen et al., 2002, Hart et al., 2002, Hart et al., 2003), important gaps in knowledge remain. First, all but one study (Lockwood et al., 1999) focused on sound level representation in the auditory cortex, and thus, sound level representation in the subcortical auditory structures remains largely unresolved in humans. Second, imaging studies have used only pure tone, complex tone and speech stimuli, so the level dependencies for spectrally continuous, broadband stimuli remain unknown. Third, no imaging study paid attention to the temporal aspects of level coding. It has been demonstrated (Giraud et al., 2000; Harms and Melcher, 2002; Siefritz et al., 2002) that auditory cortex can show fMRI activation with a wide range of temporal waveshapes, from highly sustained (response remains elevated throughout stimulus presentation) to highly phasic (response peaks just after stimulus onset and offset). These data highlight the importance of examining temporal aspects of fMRI responses and raise a possibility that different parts of the BOLD response waveform may show different sensitivity to sound level.

The present fMRI study complements the previous imaging work by examining the sound-level dependence of activation in structures throughout the auditory pathway using broadband, continuous noise as the stimulus and considering the temporal waveshape as well as the magnitude of activation. Our data suggest that sound level is

represented differently in the population neural activity of subcortical and cortical auditory centers.

Portions of this work were presented at the Sixth International Tinnitus Seminar (1999), the 25th annual meeting of the Association for Research in Otolaryngology (2001), and the 7th International conferences on Functional Mapping of the Human Brain (2001).

Methods

Subjects

Five subjects (24 to 38 years; 4 male; all right-handed) each participated in one imaging session. Subjects had no known neurological disorders and no tinnitus. Hearing thresholds of all subjects were normal (< 20 dB HL) at all standard audiological frequencies from 250 to 8000 Hz.

This study was approved by the institutional committees on the use of human subjects at the Massachusetts Institute of Technology, Massachusetts Eye and Ear Infirmary, and Massachusetts General Hospital. All subjects gave their written informed consent.

Acoustic stimulation

Broadband continuous noise was presented binaurally at 30, 50 and 70 dB sensation level (SL; 50-99 dB SPL) referenced to threshold measured in the scanner room separately for each ear. Stimuli at all levels were clearly audible during functional imaging and did not exceed the subject's comfort level.

Stimuli were alternately turned on for 30 s and off for 30 s in a standard fMRI block paradigm. Four on/off repetitions comprised a scanning "run". For every imaging session, subjects were presented with 4 runs at each stimulus level. Stimuli were

generated by a digital-to-analog board (running under LabVIEW), amplified, and fed to a pair of audio piezoelectric transducers housed in earmuffs worn by the subject.

Task

Subjects were instructed not to move and to attend to the stimuli.

Mitigation of scanner acoustic noise

The effects of the acoustic noise produced by the scanner gradient coils during functional imaging were reduced by (1) using clustered imaging with a long inter-acquisition interval TR (Hall et al., 1999, Edmister et al., 1999), (2) using earmuffs that attenuated the gradient noise by approximately 30 dB (Ravicz and Melcher, 2001). Additionally, the scanner coolant pump, which generates on-going low-frequency noise, was turned off during functional imaging (and threshold measurement).

Imaging

Subjects were imaged in a 3 Tesla (Siemens Allegra) scanner using a transmit/receive head coil. In each imaging session: (1) Contiguous sagittal images of the whole head were acquired. (2) The brain slices to be functionally imaged were selected based on the sagittal images. Eleven parallel near-coronal slices covered the brainstem, thalamus and temporal lobe. (3) T1-weighted, high resolution anatomical images were acquired of the selected brain slices for subsequent overlay of the functional data (thickness = 4mm; gap = 1mm; in-plane resolution = 0.78x0.78 mm; TR = 700ms; TI = 930ms; TE = 12ms). (4) Functional images were acquired using a blood oxygenation level-dependent (BOLD) sequence (gradient echo, TE = 30 ms, flip = 90°, slice thickness = 4 mm; gap = 1 mm, in-plane resolution = 3.125x3.125 mm). Images of the eleven selected slices were acquired in brief (< 1 s) clusters with a TR of approximately 8 s (Figure 1.1). For each stimulus level, data were collected with 0, 2, 4 and 6s delays relative to the start of the run, so the effective temporal sampling interval within the overall data set was approximately 2 s. Four runs (one for each delay) were collected at each stimulus level, yielding 156 images per level. Functional imaging was performed using cardiac gating to improve the detection of activation in brainstem structures

(Guimaraes et al. 1998). In particular, image acquisition was synchronized to the first QRS complex following a minimum inter-image interval of 7.5s, thus yielding a TR of 8036 ± 305 ms.

Detecting activation

The functional image data were first corrected for any head movements that may have occurred over the course of the imaging session using standard software (SPM95; Friston et al, 1995). Activation was then detected using a general linear model which operated on a set of basis functions designed to reflect different temporal components of fMRI activation in the auditory system (Harms and Melcher, 2003). This approach models the signal vs. time within each voxel as a weighted sum of basis functions, and identifies “active” voxels based on the goodness of fit of this model. Activation maps were created for each stimulus and sound level by estimating (using an F-statistic; Fomby et al, 1984), for every voxel, whether the amplitude of any of the basis functions is significantly different from zero.

Defining regions of interest

Activation was analyzed within regions of interest (ROIs) defined using gross anatomical landmarks and measurements obtained from atlases based on postmortem tissue (described in Hawley et al., submitted). ROIs were first identified in the high-resolution, T1-weighted MRI images (in-plane resolution 0.78 x 0.78 mm). They were then down-sampled to the lower resolution of the functional images (3.125 x 3.125 mm) to yield the ROIs used for all subsequent analyses.

Cortical ROIs were defined based on 3D reconstructions of the temporal lobes for each subject (created using FreeSurfer, Fischl and Sereno, 1999, Dale et al., 1999; Figure 1.2). HGpm was defined as the postero-medial two-thirds of the first (i.e., most anterior) Heschl’s gyrus. HGal was the remaining antero-lateral one-third of the first Heschl’s gyrus. PT covers the superior temporal cortex lateral and posterior to the transverse temporal sulcus (without extending onto the lateral face of the temporal lobe). Posteriorly it was limited by the vertical wall of the temporo-parietal cortex, and anteriorly it extended to the antero-lateral limit of the most lateral Heschl’s gyrus (either

first or second). AMA was located antero-medial to Heschl's gyrus. It was limited medially by the circular sulcus, and anteriorly by an imaginary line extending perpendicularly from the circular sulcus to the anterior limit of the first Heschl's gyrus. Whenever there was a second Heschl's gyrus (6/10 hemispheres), it was excluded from the analyses.

The ROIs for subcortical structures were defined as follows. The CN ROI was located immediately rostral to the pontomedullary junction at the caudal edge of the pons (Figure 1.3, bottom). The medial and lateral limits were 6.5 and 15 mm from the midline. The SOC ROI (located medial and rostral to the CN) was approximately 7 mm rostral to the pontomedullary junction and had medial and lateral limits 4 mm and 8.5 mm from the midline (Figure 1.3, second from the bottom). The ICs were readily identified as distinct anatomical circular areas (Figure 1.3, third from the bottom). The MGB ROI lay at the caudal edge of the thalamus abutting the ambient cistern (Figure 1.3, fourth from the bottom). The lateral edge of the midbrain defined the medial boundary of this ROI. The lateral boundary was defined to be two-thirds of the distance from the lateral edge of the midbrain to the lateral edge of the ambient cistern measured at its superior border.

Quantification of activation

Within each cortical ROI, activation was quantified for voxels that achieved significant ($p < 0.001$) change in image signal for at least one sound level. For these voxels, an activation time course was calculated as a weighted sum of basis functions (weighting determined by the general linear model) averaged across voxels where amplitudes were converted to percent change relative to the baseline (an average across all stimulus "off" conditions at a given level). Activation magnitude was calculated from the time courses as (1) the time-average percent change over the 30 s stimulus presentation ("time-average" percent change), (2) the maximum percent change occurring within 12 s of stimulus onset ("onset" percent change), and (3) the maximum percent change within 12 s of stimulus offset ("offset" percent change). The extent of activation for each sound level was quantified as the number of voxels with $p < 0.001$.

Subcortically, the time course and magnitude of activation were quantified for the lowest, for a given sound level, p-value voxel within each ROI (this voxel was the same across levels in almost all cases). For each subject, structure, and at least 2 out of 3 stimulus levels, this voxel had a p-value less than 0.01 with one exception. One subject did not show SOC activation at any stimulus level ($p > 0.05$ for all voxels in the ROI) and was therefore excluded from the analyses. Activation extent was not examined for subcortical structures because the size of one functional voxel was comparable to the size of these nuclei (CN: 3x3x7 mm; SOC: 2x2x5; IC: 6x6x4; MGB: 5x5x7).

The temporal waveshape of activation was quantified using a single numerical value, a “waveshape index” (WI). The WI, calculated from the basis function amplitudes, describes responses on a continuum from completely sustained (WI = 0) to completely phasic (WI = 1) (details in Harms and Melcher, 2003).

Results

Broadband continuous noise reliably evoked activation in four subcortical structures (CN, SOC, IC, MGB; Figure 1.3) and four cortical areas (HGpm, HGal, AMA, and PT). The effect of stimulus level on fMRI activation in these auditory centers was assessed by examining the magnitude of activation, the temporal waveshape of activation and, in cortical areas (where activation extended beyond a single voxel), the extent of activation.

Activation vs. stimulus level in brainstem structures: CN, SOC, IC

The effect of level in the CN, SOC, and IC is illustrated by the activation time courses for 30 and 70 dB SL noise in Figure 1.4 (left). In all three structures, the magnitude of activation was greater at 70dB as compared to 30dB. Since the increase in magnitude with increasing level occurred uniformly throughout the stimulus presentation, response waveshape remained the same (highly sustained) regardless of level. Thus, the

magnitude of activation, but not the temporal waveshape, was sensitive to level in the brainstem structures imaged.

The increase in magnitude with increasing level was statistically significant in all three brainstem centers as determined by an analysis of two measures: percent signal change time-averaged over the stimulus (“time-average” percent change) and the maximum percent change in a 12 s window beginning at stimulus onset (“onset” percent change). Both measures increased significantly between 30 dB and one or both of the higher levels used (50, 70 dB; $p \leq 0.02$; Wilcoxon’s rank sum test).

Activation magnitude increased monotonically with level in the CN, SOC, and IC, but not always at a steady rate. On average, CN and IC showed 2.2 and 1.6-fold increases in onset percent change from 30 to 50 dB (CN: $p = 0.002$; IC: $p = 0.01$, rank sum), but only a (non-significant, $p > 0.5$) 1.1-fold increase from 50 to 70 dB (Figure 1.5). Time average percent change (not shown) also showed a greater increase from 30 to 50 dB (CN: 2.4-fold, $p = 0.0005$; IC: 1.7-fold, $p = 0.02$), than from 50 to 70 (CN: 1.2-fold, $p = 0.4$, 1.1-fold, $p = 0.9$). Consistent with these average trends, most individual CNs and ICs showed a greater increase from 30 to 50 dB than from 50 to 70 dB (time-average: CN: 8/10, IC: 9/10; onset: CN: 7/10, IC: 6/10). Unlike the CN and IC, the SOC showed an increase in activation magnitude from 30 to 50 dB that was about the same as from 50 to 70 dB (~1.4-fold). Overall, the data indicate a growth in activation magnitude with increasing level in brainstem centers, but suggest a slower rate of growth (i.e., saturation) at higher levels (50 – 70 dB) in the CN and IC.

Activation vs. stimulus level in the thalamus: MGB

In contrast to brainstem structures, the MGB showed level dependencies in both the temporal waveshape and the magnitude of activation, as illustrated by the activation time courses in Figure 1.4. In this structure, an increase in stimulus level resulted in an increase in magnitude that was most pronounced near the beginning of the stimulus. The magnitude increase corresponded to a significant increase in onset percent change (from 30 to 70 dB; $p = 0.006$, rank sum test). Time-average percent change did not change significantly with level because the increase in magnitude near the beginning of the stimulus was “washed out” by the lack of change near the end.

The increase in onset percent change with level in MGB was, on average, greater between 30 and 50 dB (2.0-fold, $p = 0.03$; rank sum) than between 50 and 70 dB (1.2-fold, $p = 0.5$) with most (8/10) individual MGBs showing the same trend (Figure 1.5). Thus, as in the CN and IC, onset percent change in the MGB increased with increasing level, but showed signs of saturation at higher levels.

Activation vs. stimulus level in cortical areas: HGpm, HGal, PT, AMA

In contrast to the highly sustained temporal waveshapes of activation seen at all stimulus levels in brainstem centers, cortical areas showed more phasic waveshapes at all levels and a tendency for waveshape to vary with level (Figure 1.4, right column). Cortical waveshapes at 30 dB were characterized by a prominent peak just after stimulus onset. As level increased, responses became even more phasic because this onset peak increased and an additional peak began to emerge just after stimulus offset (see especially the time-course for AMA). The shift toward more phasic waveshapes at higher levels was subtle, but highly repeatable in two cortical areas (PT and AMA), as demonstrated by an analysis of a quantitative measure of waveshape (WI). The WI almost always increased from 30 to 70 dB (or, in one case without 30 dB data, from 50 to 70 dB; PT: 9/10, $p = 0.06$; AMA: 8/10, $p = 0.05$).

All cortical areas showed increases in activation magnitude with increasing level, although the increases were somewhat less than those seen in subcortical centers (Figures 1.4 and 1.5, middle column). Onset percent change increased significantly from 30 to 70 dB SL in AMA, PT and HGal ($p < 0.02$), although not for HGpm ($p = 0.1$). The increase from 30 to 70 dB was more apparent in an analogous (to onset percent change) measure designed to capture the off peak in cortical activation time courses (offset percent change; $p < 0.008$). Using time-average percent change, AMA and HGpm showed a significant ($p < 0.02$) increase in activation magnitude from 30 to 70 dB, but PT and HGal did not ($p > 0.07$).

In contrast to subcortical auditory structures, activation magnitude in cortical areas showed no evidence of saturation. In fact, PT and AMA showed a greater increase in activation magnitude between 50 and 70 dB than between 30 and 50 dB. This trend was evident on average (AMA: 1.5-fold increase from 50 to 70 dB vs. 1.2-fold increase

from 30 to 50 dB; PT: 1.4- vs. 1.1-fold) and usually in individual cases (7/10 for both PT and AMA). The two areas on Heschl's gyrus, HGpm and HGal, showed a similar increase between 30 and 50 dB and between 50 and 70 dB on average (HGpm: 1.2-fold increase from 50 to 70 dB vs. 1.2-fold increase from 30 to 50 dB; HGal: 1.3- vs. 1.4-fold).

The extent of activation showed significant increases in most cortical areas (HGpm, PT, AMA). In every area, extent showed a greater increase between 50 and 70 dB than between 30 and 50 dB. This trend was strongest in AMA and PT (Figure 1.5, right column) where it was evident on average (AMA: 2.9-fold increase from 50 to 70 dB vs. 0.7-fold from 30 to 50 dB; PT: 1.6- vs. 1.1-fold) and in most individual instances (AMA: 10/10, $p = 0.0002$; PT: 8/10, $p = 0.05$). The two areas on Heschl's gyrus, HGpm and HGal, showed the same trend but more subtly (HGpm: 1.4-fold increase from 50 to 70 dB vs. 1.2-fold from 30 to 50; HGal: 1.3- vs. 1.1-fold), and the trend was only significant in HGpm (HGpm: 8/10, $p = 0.05$; HGal: 6/10, $p = 0.2$). Overall, activation extent increased from 30 to 70 dB in cortical areas, and showed signs of accelerated growth at higher levels, especially in PT and AMA.

Location of active voxels within cortical areas

Although not a primary goal for the present study, we also qualitatively examined the cortical data for systematic relationships between sound level and the location of activation (i.e., amplitopy). The location of the most significantly activated voxels did not show a systematic shift in position with increasing level in any cortical area and usually remained stationary across levels. Furthermore, we did not observe any systematic shifts in the overall activated volume. On the contrary, the activated volume appeared to grow approximately equally in all directions and showed a high degree of overlap across sound levels. In any given area, voxels activated at 70dB contained at least 74% of the voxels activated at 50dB, and at least 80% of the voxels activated at 30dB. In summary, for the stimulus and levels used, there was no obvious amplitopic organization in any cortical area.

Discussion

In this fMRI study we used broadband continuous noise to examine and compare sound level dependency at the different stages of the human auditory pathway. Our results show that while all examined structures exhibited sensitivity to sound level, there were distinct differences between brainstem, thalamic and cortical centers. In particular, in brainstem (CN, SOC and IC), level dependency was observed as an increase in response amplitude throughout the stimulus presentation, but there was no change in response waveshape. In thalamus (MGB), level dependency was observed as a change in both the amplitude and the waveshape of the response: responses became more phasic as the amplitude at the beginning of the stimulus grew much faster with increasing stimulus level than in the middle or at the end of the stimulus. Finally, in cortical areas, level dependency was observed as a change in the waveshape, extent and amplitude of activation. In particular, response amplitude at the stimulus onset and, especially, offset increased with increasing level (thus making responses more phasic).

Growth in population neural activity with sound level: subcortical vs. cortical centers

One way to contrast level dependencies in subcortical auditory structures and auditory cortex is to compare overall neural activity in these structures. Unlike microelectrode recordings, fMRI data reflect (through stimulus driven changes in hemodynamics) time-integrated, mostly synaptic, activity of large neuronal populations (Kwong et al., 1992, Ogawa et al., 1992, Logothetis et al, 2001). For subcortical structures, where the extent of activation was usually one voxel, the magnitude of fMRI activation of a single voxel provides an estimate of the total sound-evoked neural activity of the structure. Auditory cortex, on the other hand, encompasses multiple voxels, so total neural activity must be estimated across voxels. Our measurements of the magnitude of fMRI activation provide this estimate.

Figure 1.6 summarizes one of the main results of this study: The magnitude of fMRI activation in CN, IC and MGB grows at a slower rate at high levels (50-70 dB SL;

~75-100 dB SPL) compared to moderate levels (30-50 dB SL; ~50-75 dB SPL) (i.e., black bars are higher than white bars). In contrast, activation magnitude in the non-primary cortical areas PT and AMA grows at a greater rate at high compared to moderate sound levels (i.e., white bars are higher than black bars). This suggests that total neural activity in the brainstem and thalamic auditory structures grows at a slower rate at high compared to moderate levels, whereas the reverse is true in the non-primary areas of the auditory cortex. Note the overall progressive increase in the height of the white bars, as well as overall progressive decrease in the height of the black bars suggesting that shape of the level function changes progressively along the higher stages of the auditory pathway (i.e., shape of level function in the primary and primary-like areas on Heschl's gyrus, HGpm and HGal, is intermediate between those of subcortical structures and non-primary auditory areas).

To summarize, the shape of the level function differed across stages of the auditory pathway: subcortical auditory structures showed evidence of saturation, non-primary cortical areas showed an accelerated rate of growth in activation at high sound levels and primary (HGpm) and primary-like (HGal) areas on Heschl's gyrus showed intermediate behavior.

Growth of activation with level: neural interpretations

The main body of work on level dependencies in the auditory system comes from microelectrode recordings in animals. Comparing fMRI and neurophysiological data can provide useful (and complimentary) insights into how the auditory system processes sound level besides methodological (e.g., microelectrode recordings are usually limited to a small number of cells, reflect action potentials and are biased towards large cells) and species differences.

At the periphery of the central auditory pathway, population neural activity in the auditory nerve increases monotonically as sound level increases for both broadband (Ruggero et al., 1973) and narrowband sounds (Zwislocki, 1973, Geisler et al., 1974, Sachs and Abbas, 1974), until it saturates at high levels due to inherent limitations in the release of neurotransmitter and the number of neurons (e.g., Kiang et al., 1965, Smith and

Brachman, 1980, Westerman and Smith, 1984). Consistent with the fact that fMRI reflects synaptic activity, our results suggest that fMRI activation in CN, which receives inputs from the auditory nerve, reflects population neural activity of the auditory nerve: fMRI activation increases monotonically and then shows signs of saturation at the higher levels.

Our data suggest that population neural activity in IC and MGB might also reflect the same simple dependence on sound level predicted from the auditory nerve data despite the fact that many individual units in these structures and projecting to these structures have been shown to exhibit complex non-linear response properties like non-monotonic rate-level functions (Rose et al., 1963, Semple and Kitzes, 1985, Aitkin, 1991). However, it has been found in the IC, for example, that the proportion of neurons with monotonic rate-level functions is greater in response to broadband than to narrowband stimulus (Aitkin, 1991). Therefore, we might expect that population neural activity in IC and MGB would exhibit more monotonic-like behavior in response to broadband noise than it would to narrowband (e.g., tonal) stimuli.

Unlike subcortical auditory structures, auditory cortex did not show saturation in fMRI activation at high stimulus levels. Instead, total fMRI activation changed relatively little at moderate levels, but increased significantly at high levels, especially in the non-primary areas of the auditory cortex. Such behavior of level function cannot be predicted from the auditory nerve models and suggests that population neural activity in the auditory cortex (as seen with fMRI) may be dominated by complexities and non-linearities of individual cortical neurons. Below we consider several possible explanations for the slower change in activation with increasing level at moderate compared to high levels.

One possible explanation is that different neuronal populations preferentially respond to sounds of moderate and high levels. For example, non-monotonic neurons may dominate responses to sounds of moderate intensities, while monotonic neurons may dominate responses to sounds of high intensities. If this were the case, the overall neural activity in the auditory cortex would increase more slowly as sound level increases in the moderate range because the effect of non-monotonic units on the overall level function is

to flatten it out. Neurophysiological studies of auditory cortex using broadband stimuli are sparse (Phillips et al., 1985, Phillips and Cynader, 1985, Imig et al., 1990, Clarey et al., 1994), and there is not nearly enough data to either support or reject the proposal above conclusively. However, there is some evidence that non-monotonic neurons respond predominately at lower levels, while monotonic neurons responded predominately at higher levels in response to noise bursts (Clarey et al., 1994).

Another possible explanation for slow growth in fMRI activation at moderate sound levels in the auditory cortex may come from the differential effects of attention at different sound levels. For example, subject may pay more attention (and thus produce more “attention-driven” activation) to the stimulus at 30 dB SL level (clearly audible, but soft in the presence of scanner-generated noise) than to the 50 and 70dB SL levels. If this were the case, than greater “sound-evoked” activation at 50 dB SL may be cancelled out by greater “attention-driven” activation at 30 dB, thus producing similar amounts of total (“sound-evoked” plus “attention-driven”) activation at 30 and 50 dB SL. Alternatively, a significant increase in activation from 50 to 70 dB SL could be caused by subject paying more attention to the loudest sound at 70 dB SL compared to 30 or 50 dB SL (and thus produce more “attention-driven” activation at 70 dB SL). It is further reasonable to assume that effects of attention, a high level cognitive process, would be more evident in the auditory cortex, rather than subcortical auditory structures. Thus, effect of attention might be more evident in the level function of the auditory cortex than subcortical structures.

Finally, interesting behavior of the level function in the auditory cortex may reflect dominant representation of other stimulus characteristics in the population neural activity. In other words, level dependency in cortical fMRI responses may be obscured and/or dominated by complexities introduced to the fMRI response by other sound characteristics (e.g., temporal envelope). For example, while some cortical neurons maybe sensitive to changes in sound level, other sound characteristics may fundamentally determine population neural activity seen in the fMRI response.

Dependencies of waveshape on sound level in cortex and thalamus, but not brainstem: neural interpretations

fMRI response waveshape reflects neural activity integrated over time scale of seconds in response to a long-duration (e.g., 30s in the present study) stimulus. Our data show that fMRI responses in CN, SOC and IC to continuous noise remain sustained throughout stimulus presentation and show no change in waveshape with increases in sound level. This suggests that neural activity in these brainstem structures remains sustained and equally sensitive to changes in stimulus level throughout the 30s-long window of stimulus presentation.

In contrast, responses of the auditory cortex to continuous noise show phasic features and become even more phasic as stimulus level increases. In particular, the amplitude of the response increases at the stimulus onset and offset with increasing level while amplitude in the middle of stimulus presentation does not change (e.g., in PT) or even decreases (e.g., in AMA). While these changes in waveshape of the cortical responses with changes in sound level are rather subtle (e.g., compared with differences in waveshape between brainstem and cortex), they are highly repeatable across subjects. This suggests that neural activity in the auditory cortex is most sensitive to level changes at the onset and offset of continuous noise (i.e., when cortex is most responsive to this particular stimulus). An interesting question for future studies is whether the same result (greatest sensitivity to level at the stimulus onset and offset) holds for stimuli that show sustained responses in cortex (e.g., music).

Our results also show that changes in waveshape with increasing level are more pronounced in the non-primary areas of PT and AMA than in the primary areas of Heschl's gyrus. These differences between cortical areas are discussed in more details in Chapter II.

In the auditory thalamus, dependence of the fMRI waveshape on level appears to be intermediate between that of the auditory brainstem and cortex. In particular, in MGB, response amplitude increased with increasing stimulus level at the onset of the stimulus, but not throughout (as in brainstem) or at the offset (as in cortex) of the stimulus. This suggests that neural activity in MGB is most sensitive to level changes at the onset of continuous noise.

Comparison to previous imaging and evoked potential studies of sound level dependencies

To our knowledge, this is the first study (either imaging, evoked potentials or microelectrode) that directly compares sensitivity to sound level across different stages of the auditory pathway, from cochlear nucleus to cortex. While PET study by Lockwood et al (1999) reported activation in the auditory midbrain and thalamus, it did not directly compare level sensitivity across structures, nor did it allow precise localization of activation due to limited spatial resolution. We can, however, compare our data on sound level representations in the auditory cortex to that of other studies.

Unlike the present study, most of the previous imaging studies on sound level dependencies for non-speech sounds used narrowband stimuli. Despite the stimulus difference, however, these previous studies, like the present one, found increases in the extent of fMRI activation with increasing level (Jancke et al., 1998, Lockwood et al., 1999, Hall et al., 2001, Brechmann et al., 2002, Bilecen et al., 2002, Hart et al., 2003). Many also showed increases in the magnitude of activation (Lockwood et al., 1999, Hall et al., 2001, Hart et al., 2003, Brechmann et al., 2002).

Another aspect of sound level representations in the auditory cortex that has been addressed, but not resolved in neuroimaging studies is the existence of the amplitopic organization in the human auditory cortex. In neurophysiological studies in animals, while there is evidence that non-monotonic units in the auditory cortex may be clustered according to their best SPL (Schreiner and Mendelson, 1990, Schreiner et al., 1992, Heil et al., 1994, Clarey et al., 1994), there have been no data suggesting amplitopic organization in any mammals other than bats (Suga and Manabe, 1982). Several imaging studies addressed the question of amplitopy in the human auditory cortex by either tracking the peak activated voxel (Lockwood et al, 1999, Hart et al., 2002) or center of activation (Bilecen et al., 2002). The results could be described as heterogeneous at best: Consistent with the results of the present study, Hart et al (2002) did not find any evidence for a shift in the location of peak activated voxel with changes in level in any examined cortical area. Lockwood et al (1999) found partial evidence for

a shift in the location of peak activated voxel: in the medial-inferior portion of the auditory cortex, the location changed in the inferior to superior direction with increasing sound level on the ipsilateral side of stimulation only. Bilecen et al (2002), on the other hand, found a bilateral shift in the center of activation in the ventral to dorsal and lateral to medial directions with increasing sound level. Heterogeneity of the results could at least partially be explained by the fact that tracking the location of the peak activated voxel alone might not be an adequate measure of amplitopy. In particular, peak voxel in fMRI activation (e.g., voxel with the greatest change in BOLD signal) might not correspond to the actual peak in neural activity due to several factors including proximity of a large draining vein, etc. The present study tried to address the issue by using several complimentary measures, including tracking the position of the most significantly activated voxel as well as the overall activated volume. By either measure, we did not observe any systematic shifts indicating no obvious amplitopic organization. To summarize, the existence of the amplitopy of the human auditory cortex (as well as other mammals but bats) remains a question yet to be answered

Conclusions

Our data suggest that sound level representations in the population neural activity of auditory brainstem structures, as seen with fMRI, reflect sound level representation of the population neural activity of the auditory nerve: population neural activity increases as sound level increases. In contrast, the population neural activity in the auditory cortex shows response complexities that may reflect sub-ordinance of sound level representation to the representation of other sound features (e. g., temporal characteristics) and/or attention. Our results further suggest that sound level representations in the auditory thalamus reflect its intermediate position between brainstem and cortex.

The present study reinforces the notion of dichotomy between auditory brainstem and cortex (as well as the intermediate nature of thalamic responses) demonstrated by previous studies in our group on the representations of sound repetition rate (Harms and Melcher, 2002) and bandwidth (Hawley et al., 2002). In particular, a monotonic increase in fMRI activation was observed in the auditory brainstem when these parameters, repetition rate and bandwidth, increased in value. In contrast, cortical dependencies on

rate and bandwidth exhibited complex non-linear behavior. Thus, the present and previous data from our group together suggest that population neural activity in the brainstem auditory structures reflects, to a first approximation, the amount of energy in the stimulus: the more sound goes in, the greater the response.

References

- Aitkin, L. (1991). "Rate-level functions of neurons in the inferior colliculus of cats measured with the use of free-field sound stimuli." J Neurophysiol **65**(2): 383-92.
- Antinoro, F., P. H. Skinner, et al. (1969). "Relation between sound intensity and amplitude of the AER at different stimulus frequencies." J Acoust Soc Am **46**(6): 1433-6.
- Bilecen, D., E. Seifritz, et al. (2002). "Amplitopicity of the human auditory cortex: an fMRI study." Neuroimage **17**(2): 710-8.
- Borgmann, C., B. Ross, et al. (2001). "Human auditory middle latency responses: influence of stimulus type and intensity." Hear Res **158**(1-2): 57-64.
- Brechmann, A., F. Baumgart, et al. (2002). "Sound-level-dependent representation of frequency modulations in human auditory cortex: a low-noise fMRI study." J Neurophysiol **87**(1): 423-33.
- Brugge, J. F., N. A. Dubrovsky, et al. (1969). "Sensitivity of single neurons in auditory cortex of cat to binaural tonal stimulation; effects of varying interaural time and intensity." J Neurophysiol **32**(6): 1005-24.
- Brugge, J. F. and M. M. Merzenich (1973). "Responses of neurons in auditory cortex of the macaque monkey to monaural and binaural stimulation." J Neurophysiol **36**(6): 1138-58.
- Cacace, A. T., R. Dowman, et al. (1988). "T complex hemispheric asymmetries: effects of stimulus intensity." Hear Res **34**(3): 225-32.
- Clarey, J. C., P. Barone, et al. (1994). "Functional organization of sound direction and sound pressure level in primary auditory cortex of the cat." J Neurophysiol **72**(5): 2383-405.
- Dale, A. M., B. Fischl, et al. (1999). "Cortical surface-based analysis. I. Segmentation and surface reconstruction." Neuroimage **9**(2): 179-94.
- Edmister, W. B., T. M. Talavage, et al. (1999). "Improved auditory cortex imaging using clustered volume acquisitions." Hum Brain Mapp **7**(2): 89-97.
- Ehret, G. and M. M. Merzenich (1988). "Complex sound analysis (frequency resolution, filtering and spectral integration) by single units of the inferior colliculus of the cat." Brain Res **472**(2): 139-63.
- Evans, E. F. (1981). The dynamic range problem: place and time coding at the level of the cochlear nerve and nucleus. Neuronal mechanisms of hearing. J. a. A. Syka, L.M. New York, Plenum: 69-85.
- Fischl, B., M. I. Sereno, et al. (1999). "Cortical surface-based analysis. II: Inflation, flattening, and a surface-based coordinate system." Neuroimage **9**(2): 195-207.
- Fomby, T. B., Hill, R.C., Johnson, S.R. (1984). Advanced econometric methods. New York, Springer-Verlag.
- Friston, K. J., Ashburner, J., Frith, C.D., Poline, J.-B., Frackowiak, R.S.J (1995a). "Spatial registration and normalization of images." Hum Brain Mapp **2**: 165-189.
- Friston, K. J., Holmes, A.P., Worsley, K.J., Poline, J.-P., Frith, C.D., Frackowiak, R.S.J. (1995b). "Statistical parametric maps in functional imaging: A general linear approach." Hum Brain Mapp **2**: 189-210.
- Friston, K. J., S. Williams, et al. (1996). "Movement-related effects in fMRI time-series." Magn Reson

Med **35**(3): 346-55.

Geisler, C. D., W. S. Rhode, et al. (1974). "Responses to tonal stimuli of single auditory nerve fibers and their relationship to basilar membrane motion in the squirrel monkey." J Neurophysiol **37**(6): 1156-72.

Giraud, A. L., C. Lorenzi, et al. (2000). "Representation of the temporal envelope of sounds in the human brain." J Neurophysiol **84**(3): 1588-98.

Greenwood, D. D. and J. M. Goldberg (1970). "Response of neurons in the cochlear nuclei to variations in noise bandwidth and to tone-noise combinations." J Acoust Soc Am **47**(4): 1022-40.

Guimaraes, A. R., J. R. Melcher, et al. (1998). "Imaging subcortical auditory activity in humans." Hum Brain Mapp **6**(1): 33-41.

Guinan, J. J., Jr. and K. M. Stankovic (1996). "Medial efferent inhibition produces the largest equivalent attenuations at moderate to high sound levels in cat auditory-nerve fibers." J Acoust Soc Am **100**(3): 1680-90.

Gutschalk, A., R. D. Patterson, et al. (2002). "Sustained magnetic fields reveal separate sites for sound level and temporal regularity in human auditory cortex." Neuroimage **15**(1): 207-16.

Hall, D. A., M. P. Haggard, et al. (1999). "'Sparse' temporal sampling in auditory fMRI." Hum Brain Mapp **7**(3): 213-23.

Hall, D. A., M. P. Haggard, et al. (2001). "Functional magnetic resonance imaging measurements of sound-level encoding in the absence of background scanner noise." J Acoust Soc Am **109**(4): 1559-70.

Harms, M. P., I. S. Sigalovsky, et al. (2001). Temporal dynamics of fMRI responses in human auditory cortex: dependence on stimulus type. Assoc Res Otolaryngology.

Harms, M. P. and J. R. Melcher (2002). "Sound repetition rate in the human auditory pathway: representations in the waveshape and amplitude of fMRI activation." J Neurophysiol **88**(3): 1433-50.

Harms, M. P. and J. R. Melcher (2003). "Detection and quantification of a wide range of fMRI temporal responses using a physiologically-motivated basis set." Hum Brain Mapp **20**(3): 168-83.

Harms, M. P., J. J. Guinan Jr, et al. (2005). "Short-term sound temporal envelope characteristics determine multisecond time-patterns of activity in human auditory cortex as shown by FMRI." J Neurophysiol **93**(1): 210-22.

Hart, H. C., D. A. Hall, et al. (2003). "The sound-level-dependent growth in the extent of fMRI activation in Heschl's gyrus is different for low- and high-frequency tones." Hear Res **179**(1-2): 104-12.

Hart, H. C., A. R. Palmer, et al. (2002). "Heschl's gyrus is more sensitive to tone level than non-primary auditory cortex." Hear Res **171**(1-2): 177-190.

Hawley, M. L. and J. R. Melcher (2002). Representation of sound bandwidth in the human auditory system using fMRI. Assoc Res Otolaryngology.

Hawley, M. L. and J. R. Melcher (2002). Representation of Sound Bandwidth in the Human Auditory System Using fMRI. Abstracts of Assoc. Res. Otolaryngol., St. Petersburg, Florida.

Heil, P., R. Rajan, et al. (1994). "Topographic representation of tone intensity along the isofrequency axis of cat primary auditory cortex." Hear Res **76**(1-2): 188-202.

Imig, T. J., W. A. Irons, et al. (1990). "Single-unit selectivity to azimuthal direction and sound pressure

- level of noise bursts in cat high-frequency primary auditory cortex." J Neurophysiol **63**(6): 1448-66.
- Jancke, L., N. J. Shah, et al. (1998). "Intensity coding of auditory stimuli: an fMRI study." Neuropsychologia **36**(9): 875-83.
- Kiang, N. Y., B. C. Fullerton, et al. (1984). "Artificial stimulation of the auditory system." Adv Audiol **1**: 6-17.
- Kiang, N. Y. S., Watanabe, T., Thomas, E.C., Clark, L.F. (1965). Response patterns of single fibers in the cat's auditory nerve. MIT Research Monograph. Cambridge, Massachusetts. **35**.
- Kwong, K. K., J. W. Belliveau, et al. (1992). "Dynamic magnetic resonance imaging of human brain activity during primary sensory stimulation." Proc Natl Acad Sci U S A **89**(12): 5675-9.
- Lasota, K. J., J. L. Ulmer, et al. (2003). "Intensity-dependent activation of the primary auditory cortex in functional magnetic resonance imaging." J Comput Assist Tomogr **27**(2): 213-8.
- Lieberman, M. C. (1978). "Auditory-nerve response from cats raised in a low-noise chamber." J Acoust Soc Am **63**(2): 442-55.
- Lockwood, A. H., R. J. Salvi, et al. (1999). "The functional anatomy of the normal human auditory system: responses to 0.5 and 4.0 kHz tones at varied intensities." Cereb Cortex **9**(1): 65-76.
- Logothetis, N. K., J. Pauls, et al. (2001). "Neurophysiological investigation of the basis of the fMRI signal." Nature **412**(6843): 150-7.
- Millen, S. J., V. M. Haughton, et al. (1995). "Functional magnetic resonance imaging of the central auditory pathway following speech and pure-tone stimuli." Laryngoscope **105**(12 Pt 1): 1305-10.
- Morel, A., P. E. Garraghty, et al. (1993). "Tonotopic organization, architectonic fields, and connections of auditory cortex in macaque monkeys." J Comp Neurol **335**(3): 437-59.
- Ogawa, S., R. S. Menon, et al. (1993). "Functional brain mapping by blood oxygenation level-dependent contrast magnetic resonance imaging. A comparison of signal characteristics with a biophysical model." Biophys J **64**(3): 803-12.
- Pfeiffer, R. R. and D. O. Kim (1975). "Cochlear nerve fiber responses: distribution along the cochlear partition." J Acoust Soc Am **58**(4): 867-9.
- Phillips, D. P. (1987). "Stimulus intensity and loudness recruitment: neural correlates." J Acoust Soc Am **82**(1): 1-12.
- Phillips, D. P. and M. S. Cynader (1985). "Some neural mechanisms in the cat's auditory cortex underlying sensitivity to combined tone and wide-spectrum noise stimuli." Hear Res **18**(1): 87-102.
- Phillips, D. P. and S. E. Hall (1986). "Spike-rate intensity functions of cat cortical neurons studied with combined tone-noise stimuli." J Acoust Soc Am **80**(1): 177-87.
- Phillips, D. P. and D. R. Irvine (1981). "Responses of single neurons in physiologically defined area AI of cat cerebral cortex: sensitivity to interaural intensity differences." Hear Res **4**(3-4): 299-307.
- Phillips, D. P. and D. R. Irvine (1981). "Responses of single neurons in physiologically defined primary auditory cortex (AI) of the cat: frequency tuning and responses to intensity." J Neurophysiol **45**(1): 48-58.
- Phillips, D. P., S. S. Orman, et al. (1985). "Neurons in the cat's primary auditory cortex distinguished by their responses to tones and wide-spectrum noise." Hear Res **18**(1): 73-86.

- Phillips, D. P., M. N. Semple, et al. (1994). "Level-dependent representation of stimulus frequency in cat primary auditory cortex." Exp Brain Res **102**(2): 210-26.
- Poremba, A., R. C. Saunders, et al. (2003). "Functional mapping of the primate auditory system." Science **299**(5606): 568-72.
- Ravicz, M. E. and J. R. Melcher (2001). "Isolating the auditory system from acoustic noise during functional magnetic resonance imaging: examination of noise conduction through the ear canal, head, and body." J Acoust Soc Am **109**(1): 216-31.
- Ravicz, M. E., J. R. Melcher, et al. (2000). "Acoustic noise during functional magnetic resonance imaging." J Acoust Soc Am **108**(4): 1683-96.
- Reese, T. G., T. L. Davis, et al. (1995). "Automated shimming at 1.5 T using echo-planar image frequency maps." J Magn Reson Imaging **5**(6): 739-45.
- Relkin, E. M. and J. R. Doucet (1997). "Is loudness simply proportional to the auditory nerve spike count?" J Acoust Soc Am **101**(5 Pt 1): 2735-40.
- Rhode, W. S., C. D. Geisler, et al. (1978). "Auditory nerve fiber response to wide-band noise and tone combinations." J Neurophysiol **41**(3): 692-704.
- Rose, J. E., D. D. Greenwood, et al. (1963). "Some discharge characteristics of single neurons in the inferior colliculus of the cat. II. Tonotopical organization, relation of spike counts to tone intensity, and firing patterns of single elements." J Neurophysiol **26**: 294-320.
- Ruggero, M. A. (1973). "Response to noise of auditory nerve fibers in the squirrel monkey." J Neurophysiol **36**(4): 569-87.
- Sachs, M. B. and P. J. Abbas (1974). "Rate versus level functions for auditory-nerve fibers in cats: tone-burst stimuli." J Acoust Soc Am **56**(6): 1835-47.
- Schalk, T. B. and M. B. Sachs (1980). "Nonlinearities in auditory-nerve fiber responses to bandlimited noise." J Acoust Soc Am **67**(3): 903-13.
- Scheich, H., F. Baumgart, et al. (1998). "Functional magnetic resonance imaging of a human auditory cortex area involved in foreground-background decomposition." Eur J Neurosci **10**(2): 803-9.
- Schreiner, C. E. and J. R. Mendelson (1990). "Functional topography of cat primary auditory cortex: distribution of integrated excitation." J Neurophysiol **64**(5): 1442-59.
- Seifritz, E., F. Esposito, et al. (2002). "Spatiotemporal pattern of neural processing in the human auditory cortex." Science **297**(5587): 1706-8.
- Semple, M. N. and L. M. Kitzes (1985). "Single-unit responses in the inferior colliculus: different consequences of contralateral and ipsilateral auditory stimulation." J Neurophysiol **53**(6): 1467-82.
- Shofner, W. P. and E. D. Young (1985). "Excitatory/inhibitory response types in the cochlear nucleus: relationships to discharge patterns and responses to electrical stimulation of the auditory nerve." J Neurophysiol **54**(4): 917-39.
- Smith, R. (1988). Encoding of sound intensity by auditory neurons. Auditory function: neurobiological bases of hearing. G. Edelman, Gall, WE, Cowan, WM. New York, John Wiley & Sons.
- Smith, R. L. and M. L. Brachman (1980). "Operating range and maximum response of single auditory

nerve fibers." Brain Res **184**(2): 499-505.

Suga, N. and T. Manabe (1982). "Neural basis of amplitude-spectrum representation in auditory cortex of the mustached bat." J Neurophysiol **47**(2): 225-55.

Vasama, J. P., J. P. Makela, et al. (1995). "Effects of intensity variation on human auditory evoked magnetic fields." Acta Otolaryngol **115**(5): 616-21.

Westerman, L. A. and R. L. Smith (1984). "Rapid and short-term adaptation in auditory nerve responses." Hear Res **15**(3): 249-60.

Young, E. D. and W. E. Brownell (1976). "Responses to tones and noise of single cells in dorsal cochlear nucleus of unanesthetized cats." J Neurophysiol **39**(2): 282-300.

Zwislocki, J. J. (1973). "On intensity characteristics of sensory receptors: a generalized function." Kybernetik **12**(3): 169-83.

Figure Captions:

Figure 1.1. The experimental paradigm. **Top:** Broadband continuous noise was presented during four 30 s-long epochs (gray) separated by 30 s-long “stimulus off” periods. **Bottom:** Images of eleven slices were acquired in clusters (vertical lines) spaces by a long TR. The first cluster was delayed by Δ seconds (0, 2, 4, or 6 s) relative to the start of the run.

Figure 1.2. Regions of interest in auditory cortex superimposed on a 3D reconstruction of the superior temporal lobe (left hemisphere, Subj. 1)

Figure 1.3. Activation in major auditory centers throughout the human auditory pathway. The stimulus was broadband continuous noise presented binaurally. Panels on the right are enlargements of the insets on the left. Activation (color) is thresholded at $p < 0.001$ and is superimposed on a T1-weighted anatomical (grayscale) image. Both activation and anatomical data are from individual brains (different subjects). Stimulus level: 70 dB SL (for all but one panel) or 50 dB (IC panel). In the SOC panel, the small blue circles inferior and lateral to the SOC reflect activation in the CNs, which happened to be partly intersected by this slice.

Figure 1.4. Time course of activation for different auditory structures at 30 (dashed line) and 70 (solid line) dB SL. Each time course is an average across subjects, hemispheres, and sound presentations. Gray shading shows \pm one standard error (across hemispheres) for 70 dB time course, and crossed hatching shows \pm one standard error for 30 dB time course.

Figure 1.5. Individual (thin lines) and averaged across subjects and hemispheres (thick line) level functions for different auditory structures. Left and middle columns show activation magnitude as a function of sound level for subcortical structures and cortical areas, respectively. Right column shows extent of activation as a function of sound level for four areas of the auditory cortex. For every structure, individual level functions were adjusted vertically in order to remove inter-subject variability in the absolute magnitude of the response by (1) subtracting mean across levels for the individual case at every level and then (2) adding mean across levels averaged across cases at every level. Averaged level function was not affected by this procedure. Note that, for activation magnitude, vertical scale is the same for subcortical structures and cortical areas.

Figure 1.6. Change in total activation in different auditory structures. For every structure, black column shows change in activation from 30 to 50 dB (normalized by total change in activation, i.e., from 30 to 70 dB). White column shows change in activation

from 50 to 70 dB (normalized by change in activation from 30 to 70 dB). Normalization was done so that relative change in activation could be compared across structures. Note that brainstem and thalamic structures generally show greater change in total activation at moderate levels (30 to 50 dB) whereas non-primary cortical areas PT and AMA show a greater change at high levels (50 to 70 dB).

Experimental paradigm

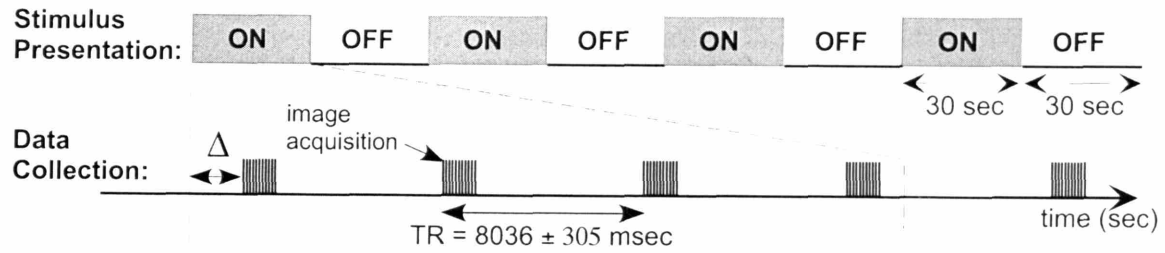


Figure 1.1.

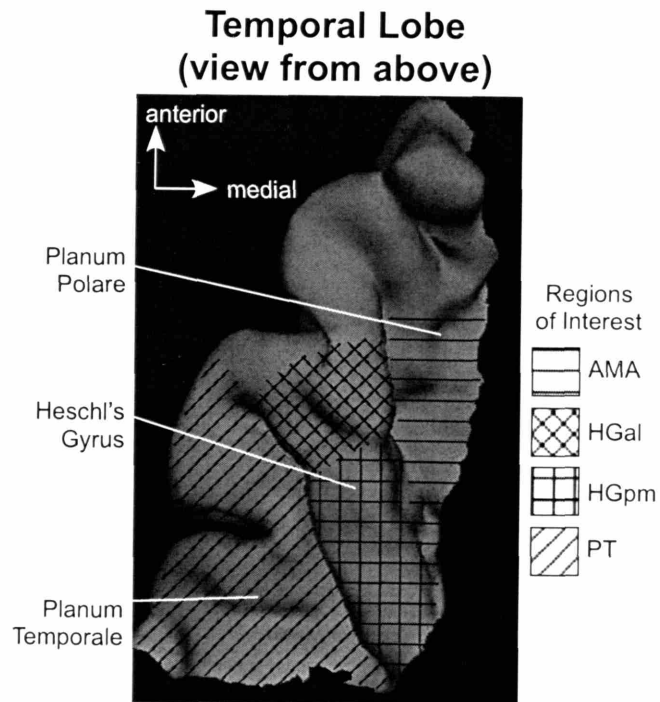


Figure 1.2.

Activation to Broadband Noise

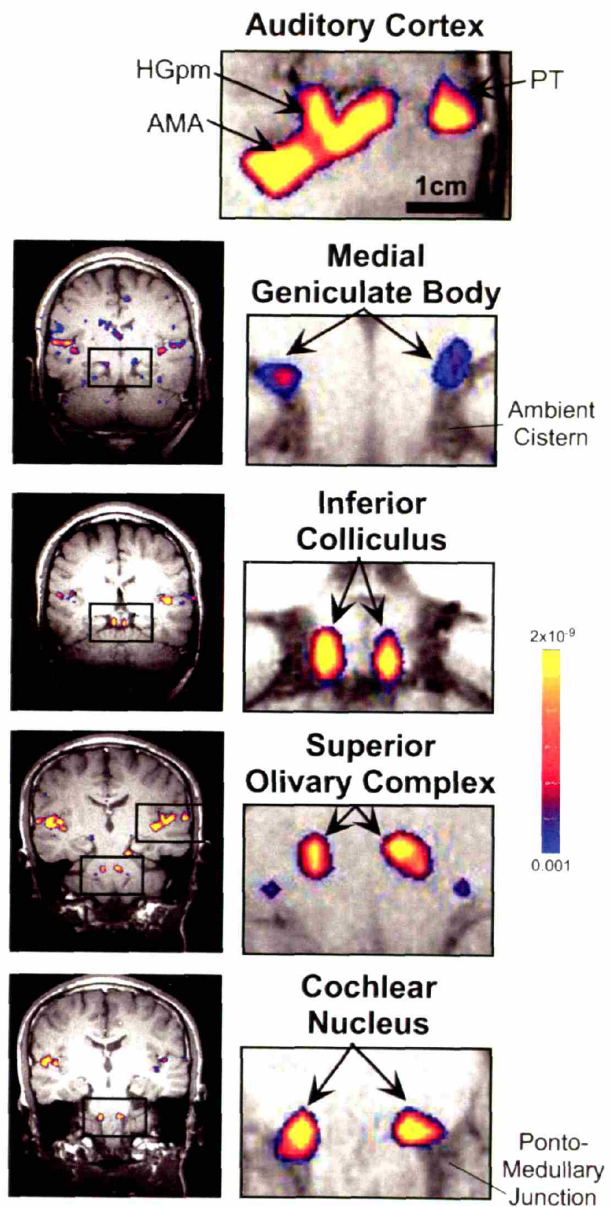
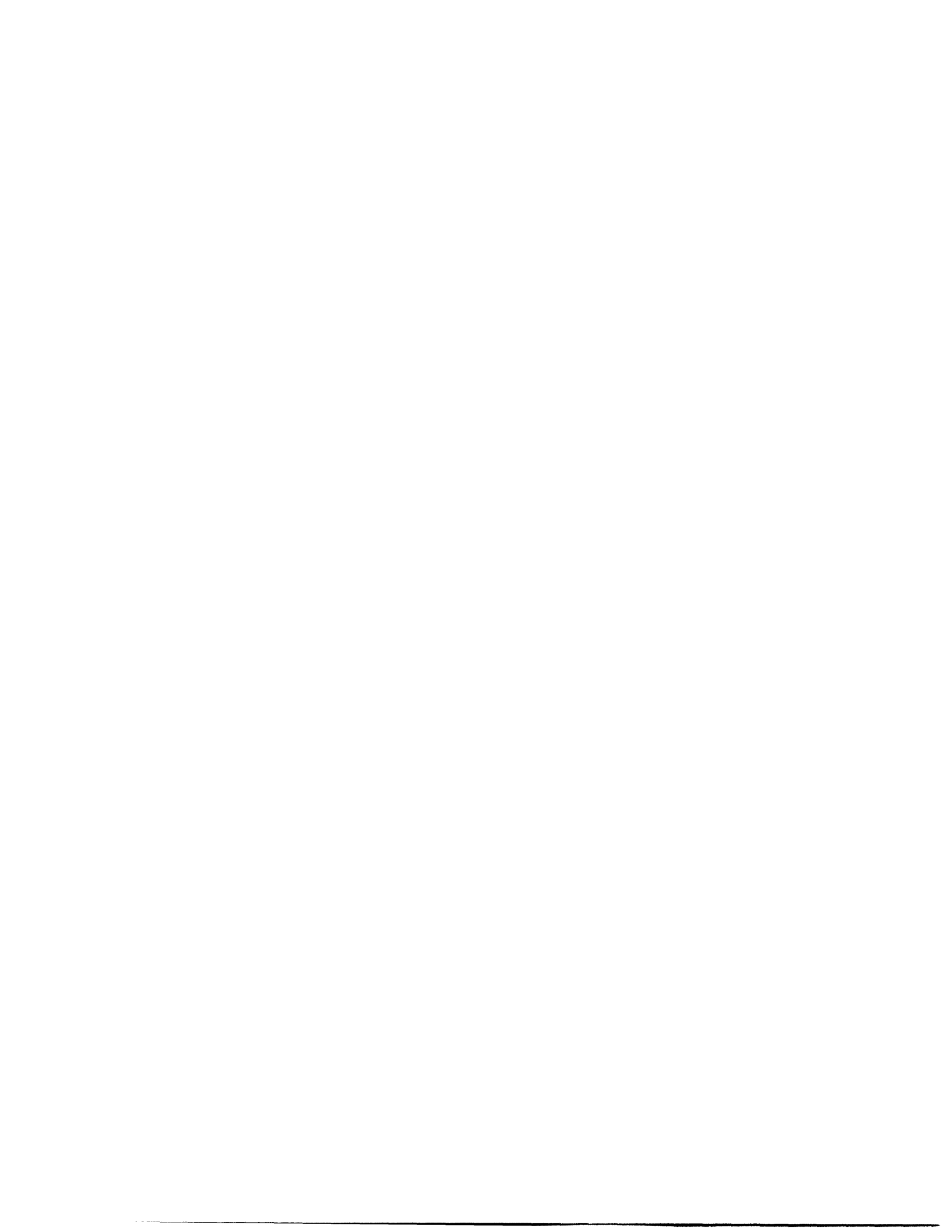


Figure 1.3.



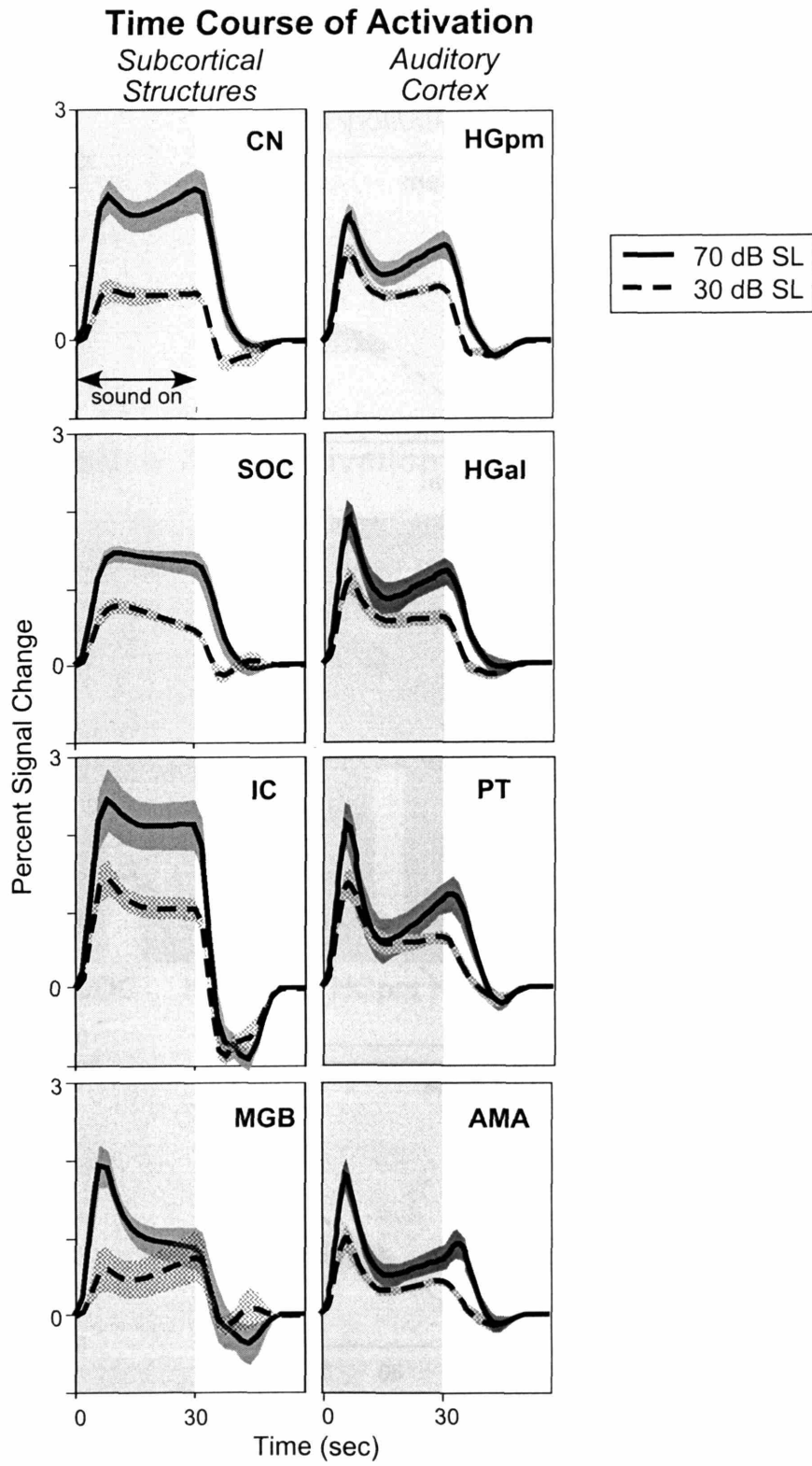


Figure 1.4.

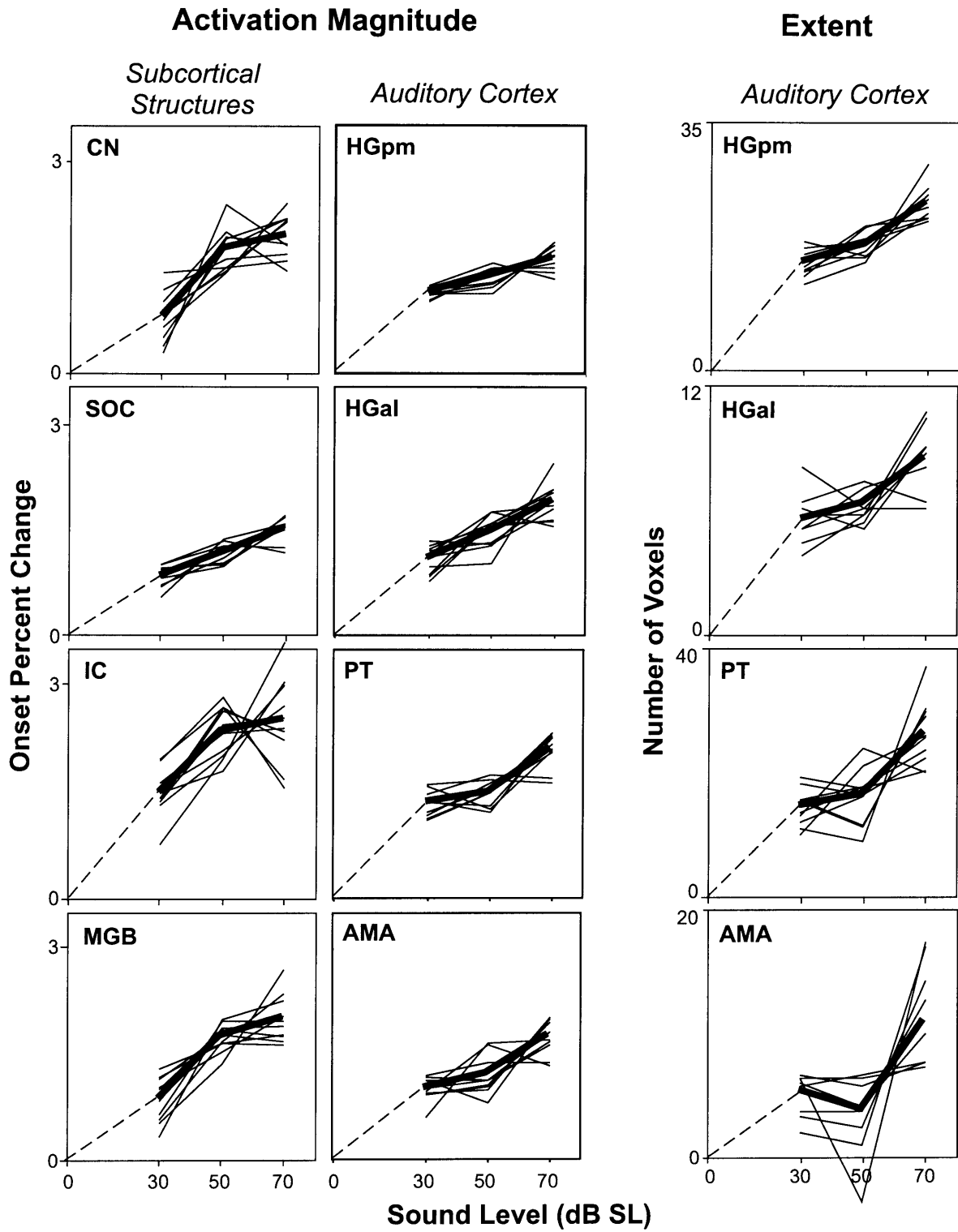


Figure 1.5.

Growth in Total Activation vs. Structure

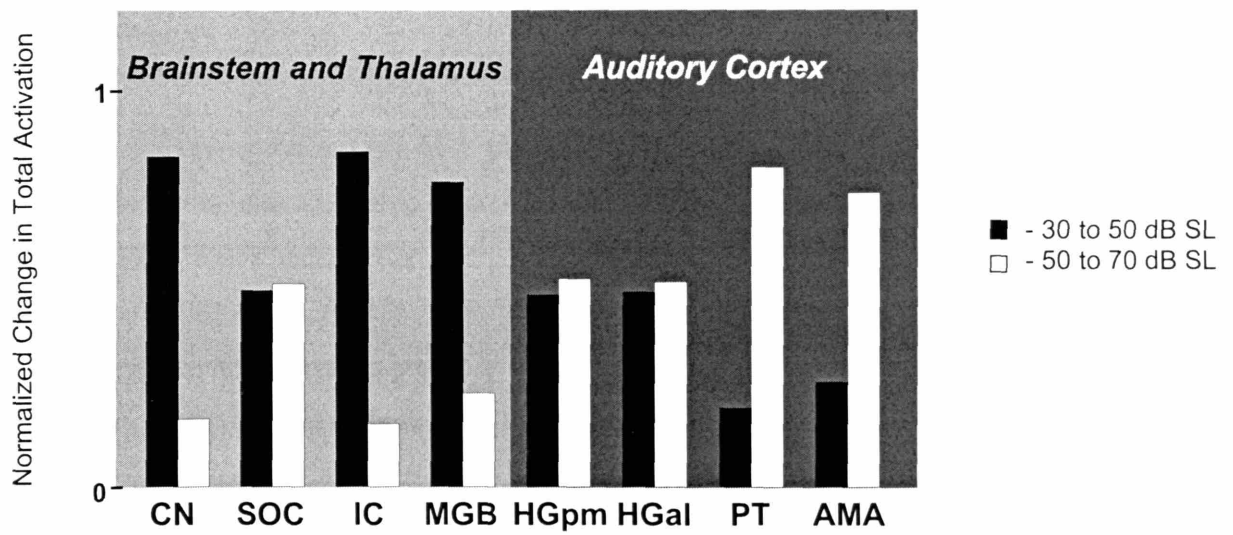


Figure 1.6.

Chapter II.

Spatio-temporal patterns of fMRI activation in human auditory cortex

Introduction

Sound-evoked neural activity on a millisecond time-scale differs between auditory cortical areas indicating area-to-area differences in how sound is represented (Morel et al., 1993, Rauschecker et al., 1995, Mendelson et al., 1997, Recanzone et al., 2000, Tian et al., 2001). Recent fMRI data for human auditory cortex indicates that there may also be regional differences in sound-evoked neural time-patterns on a much longer time-scale (10's of seconds; Seifritz et al., 2002; Harms et al., 2004). These data show that the temporal waveshape of fMRI activation varies spatially within auditory cortex. The purpose of the present study is to extend our understanding of the spatio-temporal fMRI activation patterns that arise in response to sound.

The first mapping of spatio-temporal patterns of fMRI activation in auditory cortex was published by Seifritz et al. (2002). Using an independent components analysis, this study detected cortical activation produced by a stimulus based on scanner noise (essentially a 10/s burst train) and decomposed the temporal waveshape of fMRI activation into two main components. One component corresponded to sustained activity (i.e., elevated image signal throughout the stimulus), while the other corresponded to transient activity at stimulus onset (i.e., a signal peak shortly after stimulus onset). When mapped along the surface of the superior temporal lobe, the sustained component dominated activation on Heschl's gyri, a region that typically includes the bulk of primary

auditory cortex (von Economo, 1929, Hopf, 1968, Galaburda and Sanides, 1980, Rivier and Clarke, 1997, Morosan et al., 2001, Rademacher et al., 2001, Hackett et al., 2001, Wallace et al., 2002). The transient component dominated in planum polare and planum temporale, a region containing non-primary cortical areas of diverse functionality (von Economo, 1929, Rivier and Clarke, 1997, Brugge et al., 2003). The spatial distribution of components suggests functional distinctions between cortical areas that may correspond to classically-defined anatomical distinctions. Specifically, the central "sustained" region surrounded by a "transient" region is reminiscent of the organization of auditory cortex into a core region of koniocortical gray matter (i.e., gray matter with cytoarchitectonic features of primary cortex), surrounded by a belt region (i.e., with cytoarchitectonic features of non-primary cortex)(Galaburda and Pandya, 1983, Kaas and Hackett, 2000).

In parallel with Seifritz et al, two other studies discovered that the temporal waveshape of fMRI activation in auditory cortex varies from sustained to transient along another, non-spatial dimension. Giraud et al (2000) reported that fMRI activation in response to amplitude-modulated noise is sustained for low modulation rates, but becomes increasingly transient at higher rates. Harms and Melcher (2002) reported similar results for noise burst trains but, unlike the other work, they discovered transient activity occurring at the offset, as well as onset, of sounds. Specifically, they showed that the fMRI activation for prolonged (30 s) trains of noise bursts is sustained throughout the train for low (2/s) burst rates, but at high (35/s) rates became highly phasic, showing distinct peaks just after train onset and offset. Subsequently, it was shown that the transition from sustained to phasic responses depends strongly on the temporal envelope characteristics of the stimulus (sound time fraction, as well as rate; Harms et al., 2004). The same study showed that waveshape on Heschl's gyrus (the first, or more anterior, when there were two) was more sustained while that of PT was more phasic. It was further found that responses were more sustained on Heschl's gyrus for continuous noise and higher-rate trains of bursts or clicks, but not for low-rate trains. This finding implies that any functional distinctions between cortical areas that may be implied by differences in fMRI waveshape pertain to some sounds, but not others.

While the previous work clearly demonstrates that fMRI waveshape varies spatially within human auditory cortex, the variations have yet to be examined in some fundamental ways. Seifritz et al. demonstrated a waveshape difference between Heschl's gyrus and surrounding cortical regions in averaged data, but did not demonstrate whether the difference can be discerned reliably in individuals. Ability to discern functionally different cortical areas reliably in the individual subjects is important considering significant variability in size and relative position of auditory areas (Penhune et al., 1996, Rademacher et al., 2001, Hackett et al., 2001). In addition, their approach of mapping independent components, while elegant, does not provide an appreciation for how the actual activation waveforms vary across areas. While the data of Harms et al. address some of these issues, they are limited in that they pertain almost exclusively to the posterior aspect of auditory cortex. Neither study tested the hypothesis that the region of sustained responses on Heschl's gyri corresponds to the anatomically-defined core region of auditory cortex, nor did they examine whether there are systematic spatial variations in waveshape beyond the most obvious distinction between Heschl's gyri and surrounding regions.

The present study extends the previous work by (1) determining whether the difference in fMRI waveshape between Heschl's gyrus and adjacent regions can be seen reliably and mapped in individual subjects (2) examining the manner and degree to which waveshape differs between auditory cortical regions, (3) beginning to test whether the region of sustained responses on Heschl's gyri corresponds to the core region of auditory cortex and, (4) examining whether there might be systematic spatial variations within regions surrounding Heschl's gyrus that might indicate functionally distinct areas. Our approach involves spatially mapping and quantifying the temporal waveshape of fMRI activation in response to continuous broadband noise. We chose this stimulus because it showed some of the largest waveshape differences between Heschl's gyrus and adjacent regions in the Harms et al study and because it is more easily replicated and controlled than the scanner noise stimulus used by Seifritz et al. Since some of the Harms et al. data suggest that the degree to which waveshape differs between cortical regions might depend on sound intensity, we presented continuous noise at several levels. Activation

was detected using a general linear model and basis functions designed to capture different features of sustained and phasic waveforms (Harms and Melcher, 2003). The temporal waveshape of fMRI activation was quantified in terms of an index derived from the basis function amplitudes so as to weight the relative amounts of transient and sustained activity.

Methods

Subjects

Five subjects (24 - 38 yrs., mean = 29) each participated in an imaging session. Subjects (four male, all right-handed) had no known neurological disorders and had normal hearing thresholds (<20 dB HL) at all standard audiological frequencies (250 - 8000 Hz).

This study was approved by the institutional committees on the use of human subjects at the Massachusetts Institute of Technology, Massachusetts Eye and Ear Infirmary, and Massachusetts General Hospital. All subjects gave their written informed consent.

Acoustic stimuli

Broadband continuous noise (cutoff = 10kHz) was presented binaurally at 30, 50 and 70 dB SL (50-99 dB SPL). Threshold was measured in the scanner room separately for each ear. The intermittent acoustic noise during functional imaging (beeps at maximum level of ~ 85 dB SPL at the ear) was not present during threshold measurement, nor was the noise of the scanner coolant pump (the pump was turned off during both threshold measurement and functional imaging). The stimulus at all levels was clearly audible during functional imaging and did not exceed subject's comfort level at the highest intensity.

The stimuli were alternately played for 30 s and turned off for 30 s in a standard fMRI block design. Each scanning run consisted of four stimulus on/off repetitions at the same sound level. Four runs were presented at each stimulus level.

Stimulus delivery

Stimuli were generated by a digital-to-analog board (running under LabVIEW), amplified, and fed to a pair of audio piezoelectric transducers housed in earmuffs worn by the subject. The earmuffs attenuated the scanner-generated acoustic noise by approximately 30 dB (Ravicz and Melcher, 2001).

Instructions to subject

Subjects were instructed not to move and to attend to the stimuli. They reported their alertness on a qualitative scale ranging from 1 (fell asleep during run) to 5 (highly alert) at the end of each scanning run. Alertness ratings were always 3-5.

Imaging

Subjects were imaged using a 3 Tesla head-only scanner (Siemens Allegra) and transmit/receive head coil. Each imaging session lasted approximately 1.5 hours and included the following:

- Contiguous sagittal images of the whole head were acquired.
- The brain slices to be functionally imaged were selected using the sagittal images as a reference. Eleven near-coronal slices (4 mm thick, 1mm gap between slices) were selected to cover the entire temporal lobe, which houses auditory cortex.
- T1-weighted, high resolution anatomical images were acquired of the selected brain slices for subsequent overlay of the functional data (slice thickness = 4mm, 1mm gap; in-plane resolution = 0.78x0.78mm; TR = 700ms; TI = 930ms; TE = 12ms).
- Functional images of the selected slices were acquired using a blood oxygenation level-dependent (BOLD) sequence (gradient echo; TE = 30 ms; flip = 90°; slice thickness = 4 mm, 1 mm gap; in-plane resolution = 3.125x3.125 mm).

The scanner acoustic noise associated with image acquisition was handled by acquiring images in a brief (< 1 s) cluster and leaving a long time interval between clusters (TR ~8 s) (Hall et al, 1999, Edmister et al. 1999). The data for each stimulus level were collected with 0, 2, 4 and 6 s delays relative to the start of the stimulus (four

runs total), so that the effective temporal resolution in the overall data was approximately 2 s, instead of approximately 8 s.

These same experiments examined subcortical as well as cortical structures (subcortical data to be presented in a separate publication). Therefore, functional imaging was performed using cardiac gating which increases the detectability of activation in brainstem structures (Guimaraes et al. 1998). Image acquisitions were synchronized to the subject's electrocardiogram (i.e., the first QRS complex following a minimum inter-image interval of 7.5 s). The inter-image intervals (TR) were recorded so that the precise timing of the image acquisitions relative to the sound stimulus could be taken into account in subsequent analyses. Because of the long TR, variations in image signal strength (i.e., T1 effects) from acquisition to acquisition due to fluctuations in heart rate were insignificant and did not require correction.

Functional data analysis

The functional data were first corrected for any head movements that may have occurred over the course of the imaging session (SPM95; Friston et al). Activation was then detected using a general linear model and a set of basis functions designed to detect responses ranging from sustained to phasic (Harms and Melcher, 2003). The five basis functions reflect empirically observed aspects of the responses (*Onset, Sustained, Ramp, Offset* and *Undershoot*). Activation maps were created by estimating (using an F-statistic; Fomby et al, 1984), for every voxel, whether the amplitude of any of the basis functions is significantly different from zero. All subsequent analyses were performed on voxels with $p < 0.001$ (not corrected for multiple comparisons). Response waveforms were calculated as a weighted sum of the basis functions (weighting determined by the GLM).

Defining regions of interest

The superior temporal plane was divided into the following regions of interest (ROIs; Figure 2.1). HGpm was defined as the postero-medial two-thirds of the first Heschl's gyrus (HG), a region typically associated with auditory koniocortex. HGal was the remaining antero-lateral one-third of the first Heschl's gyrus. Planum temporale (PT)

was defined as the superior temporal cortex lateral and posterior to the transverse temporal sulcus. Posteriorly, it was limited by the vertical wall of the temporo-parietal cortex. Anteriorly, it was limited by the lateral edge of the most lateral Heschl's gyrus. An antero-medial area (AMA) was defined as cortex antero-medial to first Heschl's gyrus. This ROI was limited medially by the circular sulcus, and anteriorly by an imaginary line extending perpendicularly from the circular sulcus to the anterior limit of first Heschl's gyrus. In cases with a second Heschl's gyrus, this gyrus defined a fifth ROI (HG2).

The ROIs were delimited in 3D, using a reconstruction of the temporal lobe obtained from the sagittal images, for every hemisphere. They were then cross-referenced onto the high-resolution T1-weighted images (0.78 x 0.78mm) from the same subject. These "high-resolution" ROIs were then down-sampled to the lower resolution of the functional images (3.1 x 3.1mm) to yield the ROIs used for all subsequent analyses.

Quantifying response waveshape

Response waveshape for every voxel was quantified using a single numerical value, a "waveshape index" (WI) which was designed to describe responses on a continuum from sustained to phasic (Harms and Melcher, 2003).

$$WI = \frac{1}{2} \left(\frac{Onset + Offset}{Mid + \max(Onset, Offset)} \right) \in [0,1],$$

where *Onset* and *Offset* are the amplitudes of the onset and offset basis functions. *Mid*, a measure of the response near the middle of the stimulus presentation, is the sum of the amplitude of the *Sustained* basis function plus one-half of the *Ramp*.

The WI approaches one when responses are highly phasic and zero when responses are highly sustained.

Creating Maps of Waveshape Index

For every hemisphere, WIs were mapped onto a 3D reconstruction of the temporal lobe for visual inspection. The mapping procedure included two steps. First, high resolution T1-weighted images in the plane of functional images were manually registered to the 3D anatomical data set from the same hemisphere using gross

anatomical landmarks clearly visible on the high-resolution MRI images (e.g., ventricles and scalp). Then, the same registration matrix was used to register low-resolution functional data onto a 3D reconstruction of the temporal lobe.

Results

Spatial maps of waveshape index (WI)

Broadband continuous noise produced robust cortical activation enabling response waveshape to be mapped over the superior temporal lobe in individual subjects. Sample maps of WI for three subjects at 70dB SL (also, at 30dB SL for one subject) are shown in Figure 2.2. These maps all indicate more sustained responses on Heschl's gyrus (especially the first when there are two; e.g., left-most panel in Fig. 2) and more phasic responses laterally in PT and medially in AMA (see especially maps for 70dB). Similar spatial patterns of waveshape were seen in every hemisphere studied.

Spatial variations in waveshape index: repeatability across subjects

The fact that the differences in waveshape between Heschl's gyrus and adjacent regions were highly repeatable across subjects can be seen from quantitative comparisons of WI. Compared to HG, PT almost always showed a higher WI indicating more phasic responses (Figure 2.3A, top; 30dB: $p < 0.01$; 50dB: $p < 0.08$; 70dB: $p < 0.005$; sign rank test). AMA also usually showed more phasic responses than HG (Figure 2.3A, bottom; 30dB: $p = 0.1$; 50dB: $p < 0.02$; 70dB: $p < 0.0005$).

A second Heschl's gyrus was observed in six out of the ten hemispheres, three on the left and three on the right. Response waveshape on HG2 was almost always more phasic than on HG (70dB: 6/6 cases; 50dB: 5/6 cases; 30dB: 4/6 cases), but the differences were not significant ($p > 0.3$ at all levels). On average, response waveshape in this area was intermediate between PT and HG.

Waveshape did not differ systematically between hemispheres for any region ($p > 0.25$ at all levels).

Response waveforms for different cortical areas

The meaning of the differences in WI between regions can be appreciated by examining the average response waveforms and underlying basis functions in Figure 2.4. The waveforms for PT and AMA are more phasic than those for HG because the transient basis functions (*Onset* and *Offset*; Figure 2.4, bottom) are greater in amplitude, while those representing on-going activity during the sound (*Sustained* and *Ramp*; Figure 2.4, middle) are less in PT and AMA compared to HG. Notice, that the waveform differences between regions are small (compared to differences between stimuli; Harms and Melcher, 2002). Importantly, however, the inter-region differences in waveform, while subtle, are highly repeatable across subjects (see Figure 2.3). Also, notice that, characteristically for broadband continuous noise (Harms and Melcher), waveshape for any of the ROIs is not drastically phasic. In particular, the response at the offset of the stimulus is subtle and manifests itself mainly as a prolongation in the post-stimulus signal decline in PT and AMA as compared to HG (Figure 2.4).

Dependencies on sound intensity

While the waveshape differences between regions were apparent at all sound intensities, the differences were most pronounced at the highest intensity. This trend is illustrated in the maps of WI for 70dB and 30dB for one subject in Figure 2.2 (two right-most panels). It is also evident from the following quantitative comparison of WI across cases. At 30dB, responses in PT and AMA were, on average, only slightly more phasic than those in HG (mean WI = 0.31 for PT and AMA, compared to 0.26 for HG) and the difference was only marginally significant and only in the comparison to PT (PT vs. HG: $p < 0.01$; AMA vs. HG: $p = 0.1$; Figure 2.5, right). In contrast, at 70dB, responses in PT and AMA were distinctly more phasic than those of HG (mean WI = 0.46 and 0.48 for PT and AMA, compared to 0.27 for HG) and the difference was highly significant (PT vs. HG: $p < 0.005$; AMA vs. HG: $p < 0.0005$; Figure 2.5, left). The results for 50dB were in between these two extremes (mean WI = 0.4 for PT and AMA, compared to 0.32 for HG; not shown). Note that the WIs for HG did not change significantly with increasing intensity, while those for PT and AMA increased. Thus, the distinction in waveshape

between regions increased with increasing sound intensity mainly because responses in PT and AMA, but not HG, became increasingly phasic.

No difference in waveshape between the postero-medial and antero-lateral parts of Heschl's gyrus

To test whether the region of more sustained responses on Heschl's gyrus corresponds to the auditory core, which is typically associated with the postero-medial two-thirds of Heschl's gyrus, we examined fMRI response waveshape within Heschl's gyrus in two ways.

First, individual maps of WI and basis functions components were visually examined for any consistent variations within HG. A visual inspection of WI, *Onset*, *Offset* and *Mid* (waveform midpoint measure) maps did not reveal any systematic variations within Heschl's gyrus. While there was some variability within Heschl's gyrus (e.g., small region of relatively more phasic responses on the anterior part of the first Heschl's gyrus for Subj. 1 in Figure 2.2), these variations were not repeatable across cases.

Second, fMRI response waveshape was quantitatively compared between the postero-medial two-thirds of HG (HGpm) and the remaining antero-lateral HG (HGAl) based on the evidence from histological literature that auditory koniocortex (an anatomical equivalent of the primary auditory cortex) largely overlaps postero-medial two-thirds of HG. WI values for HGpm did not differ systematically from those for HGAl (Figure 2.3, bottom; $p > 0.6$ at all sound intensities), indicating no difference in response waveshape between these two regions.

Differences in waveshape between PT and AMA

Even though WI did not differ between PT and AMA ($p > 0.5$ at all sound levels), these regions showed certain differences in the response waveshape. The main difference between these two regions was a significantly smaller amplitude of the sustained component of the response in AMA compared to PT ($p < 0.01$, across all levels) as reflected by, for example, the waveform midpoint measure *Mid* (Figure 2.6, middle). In addition, responses in AMA showed a non-significant ($p = 0.1$) tendency to be smaller at

the stimulus onset compared to PT (Figure 2.6, left). Thus, the difference in waveshape between AMA and PT was not reflected in the WI because differences at the onset and midpoint of the stimulus presentation counterbalanced each other. Finally, there was no difference ($p > 0.5$ for all sound levels) between AMA and PT in the response after the sound offset (Figure 2.6, right). To the extent that there was any difference at all, it was opposite to the other differences: the amplitude of the *Offset* component was, on average, greater for AMA compared to PT (Figure 2.4, middle). Thus, AMA showed a smaller response to noise than PT at the onset and throughout, but not offset, of the stimulus presentation.

Variability in waveshape index within PT

A visual inspection of WI maps for individual subjects revealed greater spatial variations in waveshape within PT compared to other areas (Figure 2.2). This qualitative observation was confirmed by a trend toward greater standard deviation in the WI of PT compared to other areas ($p < 0.09$; sign test, Figure 2.7). A consistent pattern of variations within PT could not be discerned, however, due to considerable variability in the WI patterns across cases. Thus, compared to other areas, PT showed greater variability both within and across subjects.

Discussion

Our results show spatio-temporal variations in fMRI response waveshape that are highly repeatable across subjects. In particular, we found that response waveshape is consistently more sustained on Heschl's gyrus and more phasic in the surrounding areas of *planae polare* and *temporale*, suggesting functional differences between these areas. This pattern becomes especially accentuated as stimulus level increases. Our results also show that regional variations in fMRI waveshape in response to a particular stimulus (broadband continuous noise in this study) are subtle, compared to differences in

waveshape that have been previously observed in response to different stimuli in a given area of auditory cortex (Harms et al., 2004). Importantly, however, while these variations are subtle, they are highly consistent and significant.

Sustained waveshape region: relationship to primary auditory cortex

Consistent with previous studies, our data show that the most significant differences in fMRI response waveshape are seen between Heschl's gyrus and surrounding regions. One way to interpret this finding, as suggested by Seifritz et al, is that such regional differentiation indicates a functional marker for the primary auditory cortex in humans. A more detailed comparison between fMRI and histological data, however, suggests a somewhat different picture.

Histological studies on human tissue have shown that, besides significant inter-subject variability, auditory koniocortex largely overlaps postero-medial two-thirds of Heschl's gyrus (Campbell, 1909, von Economo, 1929, Hopf, 1968, Galaburda and Sanides, 1980, Rivier and Clarke, 1997, Morosan et al., 2001, Rademacher et al., 2001, Hackett et al., 2001, Wallace et al., 2002) and, thus, does not typically include the anterior parts of the gyrus occupied by primary-like (or non-primary, depending on the author) areas (paAr in Galaburda and Sanides, ALA in Wallace et al, Te1.2 in Morosan et al). Our data, on the other hand, showed no consistent or significant variations within Heschl's gyrus. Specifically, we did not find differences between the postero-medial two-thirds and antero-lateral parts of Heschl's gyrus in either individual cases or on average. This evidence suggests that region of sustained responses on Heschl's gyrus does not correspond solely to the primary auditory cortex, but instead, may include both primary auditory cortex and primary-like (or, non-primary) areas of the anterior Heschl's gyrus. It remains to be tested whether this result is specific to broadband continuous noise or can be generalized to other stimuli. To conclude, our data indicate that rather than delimiting primary auditory cortex *per se*, the region of sustained responses may encompass both primary auditory cortex and primary-like area immediately anterior to it.

Spatial variations in waveshape outside Heschl's gyri: differentiation of non-primary areas

While the most prominent result of the present study is a region of more sustained responses on Heschl's gyrus flanked by more phasic responses medially and laterally, we also found differences in fMRI response waveshape within non-primary areas surrounding Heschl's gyrus. One noticeable difference, highly repeatable across subjects, was the difference in the temporal structure of the fMRI responses between AMA (part of planum polare) and PT (planum temporale). In particular, we found that response throughout, but not at the offset of stimulus presentation was smaller in the AMA compared to PT area indicating differences in sound processing between these two areas. One possible interpretation of this result is that relative contribution of the neuronal off-responses in AMA is stronger compared to PT (and, of course, HG) in response to broadband continuous noise. Such functional differences between AMA and PT would be consistent with organizational scheme of the auditory cortex that outlines differences in the structure of medial belt ("root" in Galaburda and Pandya, 1983) and lateral belt of the auditory cortex. Unfortunately, there have been virtually no examinations of the functional properties of medial belt in either humans or monkeys (e.g., due to technical difficulties associated with deep sulcal recordings in animals).

In addition to consistent differences between PT and AMA, we found some evidence for spatial variations in fMRI response waveshape within planum temporale. While spatial patterns within PT were difficult to quantify due to considerable inter-subject variability, this result may indicate presence of several functionally distinct fields within planum temporale. The relatively high inter-subject variability within PT is consistent with general notion that non-primary areas are more heterogeneous in extent and relative arrangement than primary areas (Galaburda and Sanides, 1980, Rivier and Clarke, 1997). This would be especially expected in the human auditory cortex given its specialization for music and language processing as well as broad spectrum in abilities to process these complex stimuli.

It remains to be tested whether variations within PT, as well as differences between PT and AMA, are specific to the stimulus used in this study or can be elicited (or maximized) by other stimuli. In any case, our data suggest that fMRI response waveshape could be potentially used to differentiate auditory cortex into functionally distinct areas beyond the 1st order core/belt distinction.

Comparison to previous studies

Spatial variations in fMRI response waveshape observed here in individual subjects have the same main features as the averaged map presented by Seifritz et al (2002): responses are more sustained on Heschl's gyrus than in the surrounding areas of planum polare and planum temporale. It is less clear, however, whether the magnitude of these regional differences is comparable between their and our studies. Looking at the map of relative contributions of sustained and transient components presented by Seifritz et al, it is easy to get an impression that responses on Heschl's gyrus are highly sustained, while responses in the surrounding areas are highly transient. Our results, on the other hand, show that regional variations in waveshape, while highly consistent and repeatable, are rather subtle. We believe, however, that this seeming discrepancy is a matter of data presentation, rather than the real difference in the results for the following reasons. The map presented by Seifritz et al. shows relative contributions of only two ICA components, and it is not clear how much other components contribute to the responses. On the other hand, scanner noise (essentially a train of 10Hz bursts) used by Seifritz et al. roughly falls in the range of sounds examined by Harms et al. (2004). None of the many various stimuli examined by Harms et al. (including 10 Hz stimulus trains) showed greater regional differences than found in the present study. Thus, it is also unlikely that regional variations produced by scanner noise are greater than observed here.

Naturally, our data are highly consistent with results by Harms et al. (2004) for continuous noise since experimental design and analysis in this study were nearly identical to theirs with one major difference: the whole extent of the auditory cortex was imaged in this study, while only a part of it was imaged by Harms et al.

Optimizing regional differences in waveshape

This and previous studies indicate that regional variations in fMRI response waveshape have a potential to be used for functional differentiation of the auditory cortex. The fact that regional variations in the time-patterns of the fMRI responses can be seen using either PCA (Seifritz et al., 2002) or GLM (this study and Harms et al., 2004) confirms that this phenomenon, while subtle, is real and robust to differences in

detection methodology. In this section we address how these regional variations can be maximized by optimizing experimental design.

Our choice of stimulus was governed by the fact that Harms et al. (2004) showed that fMRI responses to high-rate and/or continuous stimuli show greater spatial variations in the auditory cortex than responses to low-rate stimuli. The results of this study demonstrate that using high intensity stimuli is beneficial for maximizing differences between cortical regions. Taking these facts into consideration, we believe that broadband continuous noise of high intensity is a good choice for optimizing differences between Heschl's gyrus and surrounding areas.

On the other hand, continuous noise might not be an optimal stimulus for revealing differences within non-primary areas because it probably does not evoke maximally possible activation in planum temporale. It remains to be examined whether other stimuli that evoke widespread activation within planum temporale (e.g., music) are also capable of revealing spatio-temporal variations within these areas.

To conclude, the choice of stimulus for revealing functional differences between auditory areas may be dependent on a particular interest of the examiner (i.e., whether the purpose of the study is to differentiate primary-like from non-primary areas, or one non-primary area from another).

Spatial variations in waveshape: a reflection of differences in neural activity or hemodynamics?

In this section, we consider the possibility that observed spatial variations in response waveshape are due to differences in hemodynamic activity between cortical areas, rather than differences in the underlying neural activity. Regional differences in waveshape observed in the present study, while highly repeatable across subjects, are subtle and could be the same order of magnitude as regional differences in hemodynamics (Handwerker et al., 2004). Such regional differences in hemodynamics may arise from several factors including, for example, regional differences in the density of capillary beds (Harrison et al., 2002). In fact, a greater vascularization of primary sensory areas has been proposed as a general principle of cortical organization (see Logothetis and Wandell, 2004, for review).

Several lines of evidence, however, suggest that regional differences in waveshape observed in this study are not likely to be of hemodynamic origins. First, our data show that regional differences in response waveshape are more pronounced at high sound levels (i.e., responses become more phasic in AMA and PT, but not on Heschl's gyrus). We think that it is highly unlikely that local hemodynamics changes as a function of sound intensity. Second, it has been demonstrated that regional differences in fMRI response waveshape can be evoked by some, but not other stimuli (Harms et al., 2004, Sigalovsky, unpublished). We cannot, however, completely exclude the possibility that regional differences seen in this study arise, all or in part, from regional differences in hemodynamics because mechanisms behind such differences are not fully understood (i.e., they might be stimulus-driven).

To conclude, the question about the origins of spatial variations in fMRI response waveshape remains open. That said, for the purposes of delineation of auditory areas, it is irrelevant whether regional differences in fMRI waveshape are explained by regional differences in hemodynamics or neural activity. What is important is that these regional differences reflect the general organizational scheme of the human auditory cortex: primary and primary-like area on Heschl's gyrus flanked by non-primary areas on planae polare and temporale.

Functional significance of spatial variations in response waveshape

Spatio-temporal variations in fMRI responses suggest differences in sound processing between different auditory areas. As discussed by Harms and Melcher (2002), a decline in the BOLD signal following the onset of the stimulus suggests adaptation of neural activity, while an increase in the BOLD signal at the end of the stimulus suggests a form of off-response. Our data suggest that neural adaptation throughout the stimulus, as well as transient activity at the beginning and end of the stimulus, are more pronounced in the non-primary areas of planum polare and temporale than in the primary areas on HG.

From the perceptual point of view, transient activity in the auditory cortex has been suggested to be involved in the demarcation of auditory objects (Harms et al., 2004). If this hypothesis is correct, our data suggest that the demarcation of an auditory

object occurs to a greater degree in the non-primary areas of planum polare and planum temporale compared to the primary areas on Heschl's gyrus.

Interestingly, differences between various cortical areas found in this study in response to a particular stimulus are rather subtle compared to differences observed in a particular area in response to different stimuli (Harms et al., 2004). Thus, our data suggest that differences in the population neural activity evoked by different sounds in a particular area of the auditory cortex are greater than cross-regional differences in response to a particular sound. This, in turn, may indicate that the range of the response properties of a particular group of neurons in the auditory cortex is at least as broad and versatile as to represent properties of neurons from a different auditory area (on a multi-second time scale).

To summarize, we demonstrated that different areas of the auditory cortex can be distinguished based on the temporal properties of the fMRI responses and identified ways in which this can be done robustly in individual subjects. In the auditory neuroimaging field, at present, no functional (or structural) markers for the primary auditory cortex (e.g., tonotopy) have been conventionally established. A region of sustained responses on Heschl's gyrus may present one way to delineate primary and anterior to it primary-like area from adjacent non-primary auditory areas. This phenomenon, however, remains to be further investigated in order to understand how these functional differentiations can be reconciled in terms of structural data from histologically prepared human tissue and functional data observed in animals using microelectrode recordings or in humans using evoked potentials. In the near future, improvements in the MRI technology show promise to allow simultaneous acquisition of structural MRI data (e.g., myelin content of gray matter, see Chapter III) and functional MRI data in the individual living humans. Ability to discern cortical structure and function in the same subject would enable examining organization of the auditory cortex in ways that, until now, have been available only in animals.

References

- Brodman, K. (1909). Brodman's "Localisation in the cerebral cortex". London, Smith-Gordon.
- Brugge, J. F., I. O. Volkov, et al. (2003). "Functional connections between auditory cortex on Heschl's gyrus and on the lateral superior temporal gyrus in humans." J Neurophysiol **90**(6): 3750-63.
- Campbell, A. W. (1905). Histological studies on the localization of cerebral function. Cambridge, Cambridge University Press.
- Dale, A. M., B. Fischl, et al. (1999). "Cortical surface-based analysis. I. Segmentation and surface reconstruction." Neuroimage **9**(2): 179-94.
- Edmister, W. B., T. M. Talavage, et al. (1999). "Improved auditory cortex imaging using clustered volume acquisitions." Hum Brain Mapp **7**(2): 89-97.
- Fischl, B., M. I. Sereno, et al. (1999). "Cortical surface-based analysis. II: Inflation, flattening, and a surface-based coordinate system." Neuroimage **9**(2): 195-207.
- Fomby, T. B., Hill, R.C., Johnson, S.R. (1984). Advanced econometric methods. New York, Springer-Verlag.
- Friston, K. J., Ashburner, J., Frith, C.D., Poline, J.-B., Frackowiak, R.S.J (1995a). "Spatial registration and normalization of images." Hum Brain Mapp **2**: 165-189.
- Friston, K. J., C. D. Frith, et al. (1995c). "Characterizing dynamic brain responses with fMRI: a multivariate approach." Neuroimage **2**(2): 166-72.
- Friston, K. J., Holmes, A.P., Worsley, K.J., Poline, J.-P., Frith, C.D., Frackowiak, R.S.J. (1995b). "Statistical parametric maps in functional imaging: A general linear approach." Hum Brain Mapp **2**: 189-210.
- Friston, K. J., S. Williams, et al. (1996). "Movement-related effects in fMRI time-series." Magn Reson Med **35**(3): 346-55.
- Galaburda, A. and F. Sanides (1980). "Cytoarchitectonic organization of the human auditory cortex." J Comp Neurol **190**(3): 597-610.
- Galaburda, A. M. and D. N. Pandya (1983). "The intrinsic architectonic and connectional organization of the superior temporal region of the rhesus monkey." J Comp Neurol **221**(2): 169-84.
- Giraud, A. L., C. Lorenzi, et al. (2000). "Representation of the temporal envelope of sounds in the human brain." J Neurophysiol **84**(3): 1588-98.
- Guimaraes, A. R., J. R. Melcher, et al. (1998). "Imaging subcortical auditory activity in humans." Hum Brain Mapp **6**(1): 33-41.
- Hackett, T. A., T. M. Preuss, et al. (2001). "Architectonic identification of the core region in auditory cortex of macaques, chimpanzees, and humans." J Comp Neurol **441**(3): 197-222.
- Hall, D. A., M. P. Haggard, et al. (1999). "'Sparse' temporal sampling in auditory fMRI." Hum Brain Mapp **7**(3): 213-23.
- Handwerker, D. A., J. M. Ollinger, et al. (2004). "Variation of BOLD hemodynamic responses across subjects and brain regions and their effects on statistical analyses." Neuroimage **21**(4): 1639-51.

- Harms, M. P., J. J. Guinan Jr, et al. (2005). "Short-term sound temporal envelope characteristics determine multisecond time-patterns of activity in human auditory cortex as shown by fMRI." J Neurophysiol **93**(1): 210-22.
- Harms, M. P. and J. R. Melcher (2002). "Sound repetition rate in the human auditory pathway: representations in the waveshape and amplitude of fMRI activation." J Neurophysiol **88**(3): 1433-50.
- Harms, M. P. and J. R. Melcher (2003). "Detection and quantification of a wide range of fMRI temporal responses using a physiologically-motivated basis set." Hum Brain Mapp **20**(3): 168-83.
- Harrison, R. V., N. Harel, et al. (2002). "Blood capillary distribution correlates with hemodynamic-based functional imaging in cerebral cortex." Cereb Cortex **12**(3): 225-33.
- Herdman, A. T., A. Wollbrink, et al. (2003). "Determination of activation areas in the human auditory cortex by means of synthetic aperture magnetometry." Neuroimage **20**(2): 995-1005.
- Kaas, J. H. and T. A. Hackett (2000). "Subdivisions of auditory cortex and processing streams in primates." Proc Natl Acad Sci U S A **97**(22): 11793-9.
- Leonard, C. M., K. K. Voeller, et al. (1993). "Anomalous cerebral structure in dyslexia revealed with magnetic resonance imaging." Arch Neurol **50**(5): 461-9.
- Logothetis, N. K. and B. A. Wandell (2004). "Interpreting the BOLD signal." Annu Rev Physiol **66**: 735-69.
- Mendelson, J. R., C. E. Schreiner, et al. (1997). "Functional topography of cat primary auditory cortex: response latencies." J Comp Physiol [A] **181**(6): 615-33.
- Morel, A., P. E. Garraghty, et al. (1993). "Tonotopic organization, architectonic fields, and connections of auditory cortex in macaque monkeys." J Comp Neurol **335**(3): 437-59.
- Morosan, P., J. Rademacher, et al. (2001). "Human primary auditory cortex: cytoarchitectonic subdivisions and mapping into a spatial reference system." Neuroimage **13**(4): 684-701.
- Obata, T., T. T. Liu, et al. (2004). "Discrepancies between BOLD and flow dynamics in primary and supplementary motor areas: application of the balloon model to the interpretation of BOLD transients." Neuroimage **21**(1): 144-53.
- Penhune, V. B., R. J. Zatorre, et al. (1996). "Interhemispheric anatomical differences in human primary auditory cortex: probabilistic mapping and volume measurement from magnetic resonance scans." Cereb Cortex **6**(5): 661-72.
- Rademacher, J., V. S. Caviness, Jr., et al. (1993). "Topographical variation of the human primary cortices: implications for neuroimaging, brain mapping, and neurobiology." Cereb Cortex **3**(4): 313-29.
- Rademacher, J., P. Morosan, et al. (2001). "Probabilistic mapping and volume measurement of human primary auditory cortex." Neuroimage **13**(4): 669-83.
- Rauschecker, J. P., B. Tian, et al. (1995). "Processing of complex sounds in the macaque nonprimary auditory cortex." Science **268**(5207): 111-4.
- Ravicz, M. E. and J. R. Melcher (2001). "Isolating the auditory system from acoustic noise during functional magnetic resonance imaging: examination of noise conduction through the ear canal, head, and body." J Acoust Soc Am **109**(1): 216-31.

- Recanzone, G. H., D. C. Guard, et al. (2000). "Frequency and intensity response properties of single neurons in the auditory cortex of the behaving macaque monkey." J Neurophysiol **83**(4): 2315-31.
- Rivier, F. and S. Clarke (1997). "Cytochrome oxidase, acetylcholinesterase, and NADPH-diaphorase staining in human supratemporal and insular cortex: evidence for multiple auditory areas." Neuroimage **6**(4): 288-304.
- Ross, B., T. W. Picton, et al. (2002). "Temporal integration in the human auditory cortex as represented by the development of the steady-state magnetic field." Hear Res **165**(1-2): 68-84.
- Seifritz, E., F. Esposito, et al. (2002). "Spatiotemporal pattern of neural processing in the human auditory cortex." Science **297**(5587): 1706-8.
- Tian, B., D. Reser, et al. (2001). "Functional specialization in rhesus monkey auditory cortex." Science **292**(5515): 290-3.
- von Economo, C. (1929). The cytoarchitectonics of the human cerebral cortex. London, Oxford University Press.
- Wallace, M. N., P. W. Johnston, et al. (2002). "Histochemical identification of cortical areas in the auditory region of the human brain." Exp Brain Res **143**(4): 499-508.
- Wessinger, C. M., J. VanMeter, et al. (2001). "Hierarchical organization of the human auditory cortex revealed by functional magnetic resonance imaging." J Cogn Neurosci **13**(1): 1-7.

Figure Captions

Figure 2.1. Regions of interest displayed on a 3-D reconstruction of the right superior temporal lobe in one subject (#1).

Figure 2.2. Spatial maps of waveshape index (WI) on the superior temporal plane indicate generally more sustained responses on first Heschl's gyrus and more phasic responses in surrounding regions. Each panel shows right hemisphere data for a particular subject and sound level (70 or 30 dB SL). WI is indicated on a red (more sustained) to yellow (more phasic) color scale for every voxel with $p < 0.05$. This liberal threshold was used for visualization only (quantification of results was done at $p < 0.001$). Stimulus: broadband continuous noise presented binaurally.

Figure 2.3. A. WI in Heschl's gyrus vs. PT (top) and AMA (bottom). B. WI within Heschl's gyrus: postero-medial two-thirds (HGpm) vs. antero-lateral remainder (HGal). Greater value indicates more phasic response. Each circle represents a particular subject, hemisphere, and sound level.

Figure 2.4. Time course of activation (top) and its sustained (middle) and transient (bottom) components for three cortical areas. Stimulus level: 70dB SL. Time courses and individual components were weighted as determined by GLM and converted to percent change relative to baseline. Each time course is an average across subjects, hemispheres, stimulus presentations, and voxels with $p < 0.001$.

Figure 2.5. Mean WI in different auditory areas at 70 (left) and 30 (right) dB SL. Error bars indicate OSE.

Figure 2.6. Amplitude of waveform components in PT vs. AMA. *Onset* (left) and *Offset* (right) represent transient components of the response at the onset and offset of the stimulus, respectively. *Mid* (middle), a waveform amplitude midpoint measure, represents sustained component of the response. Greater value indicates more phasic response. Each circle represents a subject, hemisphere, and sound level.

Figure 2.7. Standard deviation of WI in different auditory areas (mean across sound levels).

Temporal Lobe (view from above)

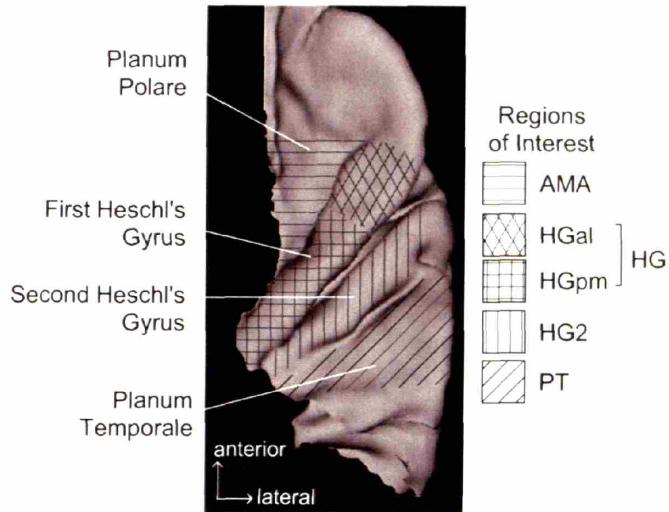


Figure 2.1.

Spatial Maps of Waveshape Index

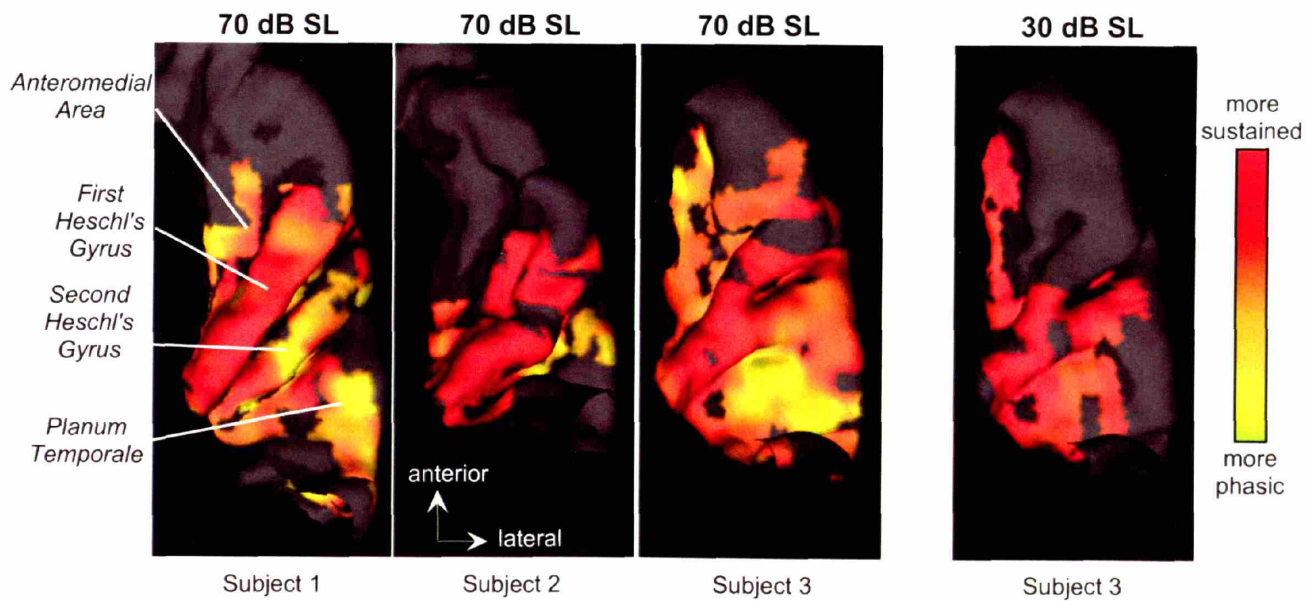
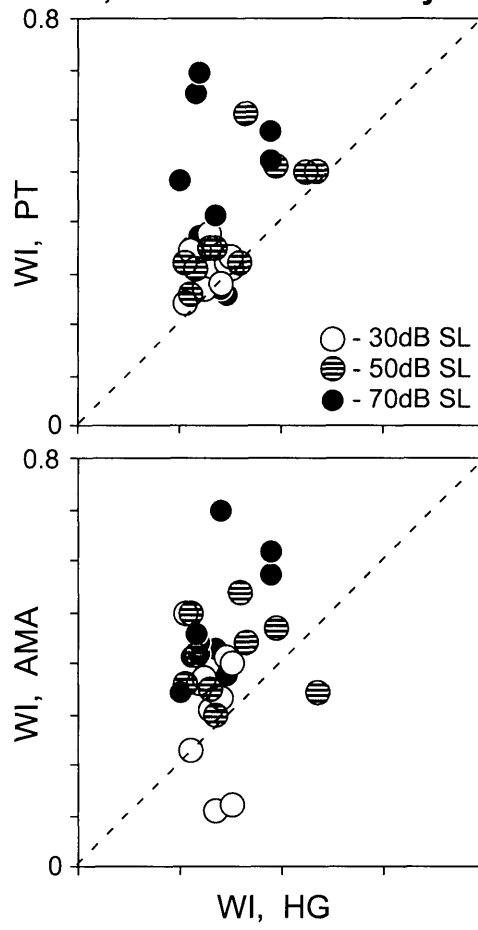


Figure 2.2.



**A. Waveshape Index:
PT, AMA vs. Heschl's Gyrus**



**B. Waveshape Index:
HGpm vs. HGal**

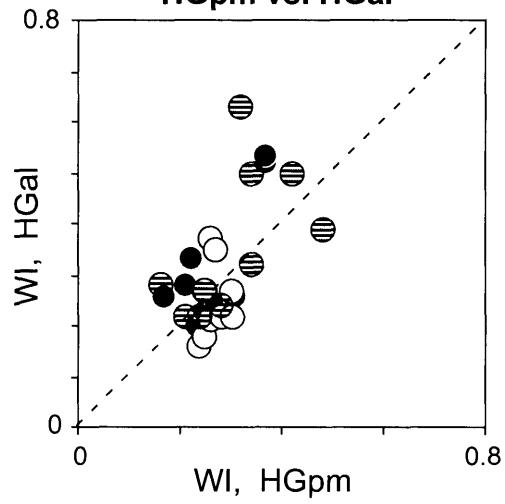


Figure 2.3.

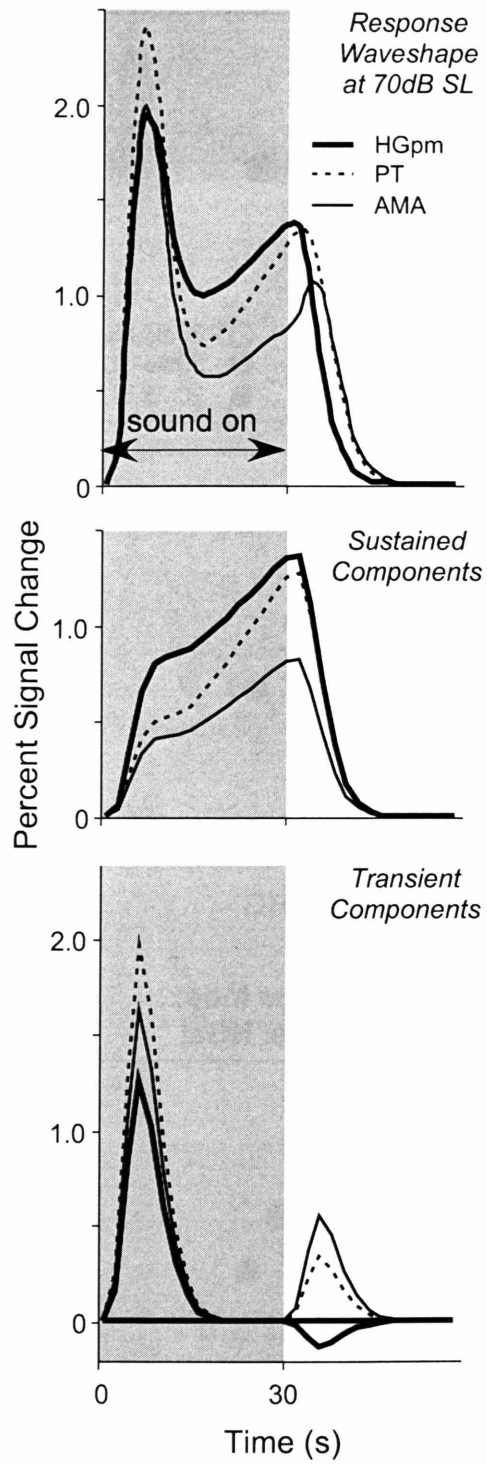


Figure 2.4.

Waveshape Index vs. Cortical Region

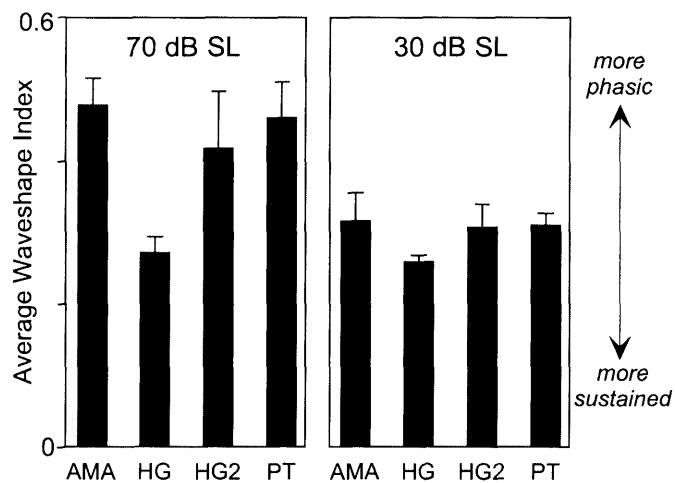


Figure 2.5.

Waveform Components Amplitude in AMA vs. PT

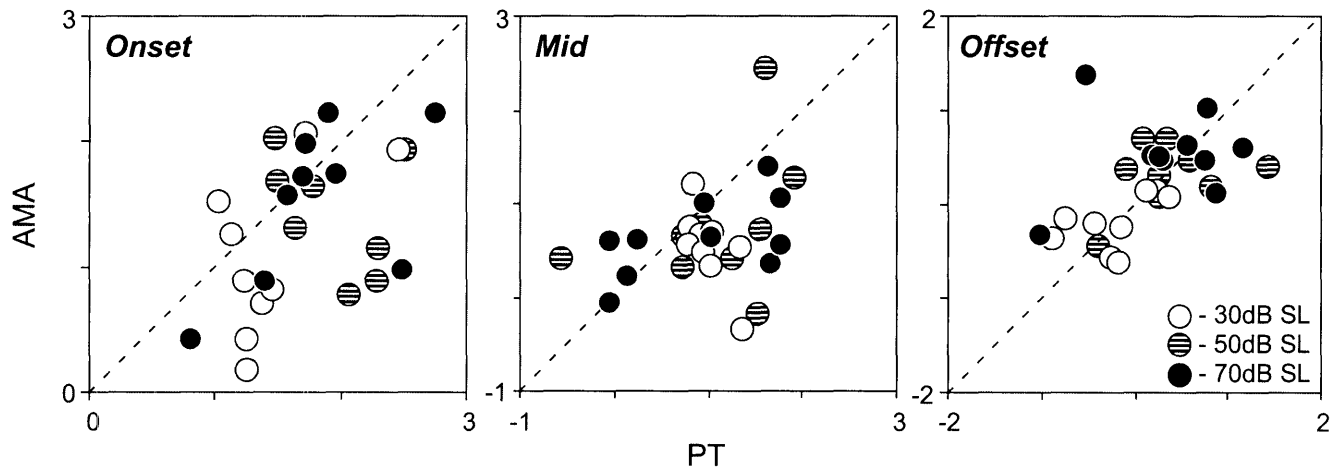


Figure 2.6.

Spatial Variability of Waveshape vs. Cortical Region

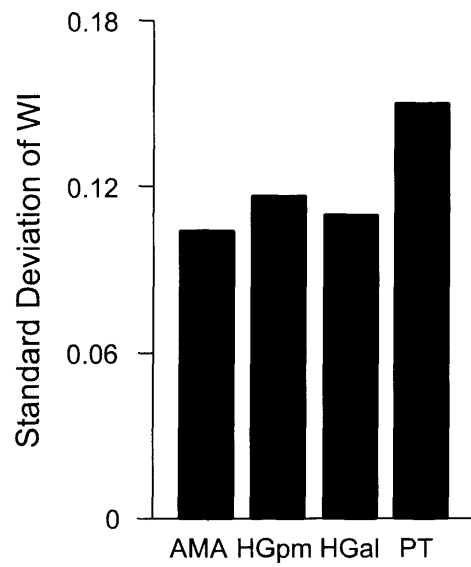


Figure 2.7.

Chapter III.

Imaging gray matter myelin content of human auditory cortex suggests that a major architectonic division can be resolved in-vivo

Introduction

In animals, examining structure/function relationships (i.e., a relationship between cellular architecture, connections, neuronal response properties and behavior) in the auditory cortex have provided basis for understanding the organizational principles of the auditory processing (Morel et al., 1993, Rauschecker et al., 1995, Mendelson et al., 1997, Recanzone et al., 2000, Tian et al., 2001). A major obstacle to understanding such relationships in the human auditory cortex has been the inability to anatomically differentiate cortical areas in vivo, in individual subjects. In neuroimaging studies the location of architectonic areas is often inferred from gross anatomical landmarks or by mapping atlases onto imaged brains (Talairach and Tournoux, 1988, Rademacher et al., 2001, Morosan et al., 2001). However, these approaches provide only an approximate localization since the spatial relationship between architectonics and gross morphology varies considerably across individuals (Rademacher et al., 2001, Morosan et al., 2001, Hackett et al., 2001) and may be especially faulty in pathological cases (Leonard et al., 1993). The present study begins to examine, for the first time, whether auditory cortical areas, and primary auditory cortex in particular, can be differentiated in-vivo in individual subjects. In particular, we exploit the sensitivity of MRI to myelin content to examine myelination patterns in the gray matter of the human auditory cortex.

Histological literature suggests that major divisions of the auditory cortex can be distinguished based on their myeloarchitecture. In both humans and non-human primates, the auditory cortical areas of the superior temporal lobe form several major distinctions: a core area with histological features of primary sensory cortex, and belt areas flanking the core medially and laterally and, a lateral parabelt area (e.g., Kaas et al., 1999). Myeloarchitectonic differences (i.e., differences in overall myelin content and laminar structure of the gray matter) between these areas and sub-areas thereof have been described since the beginning of the last century (Hopf, 1968). In this study we focus on the overall myelin content of the auditory gray matter because it is a grosser measure that can be acquired in short time using conventional scanners and protocols. Relevant to our examinations, auditory core has been characterized by high myelin content relative to less myelinated lateral belt and sparsely myelinated medial belt (Hopf, 1968, Hackett et al., 2001, Wallace et al., 2002). The goal of this study, then, is to examine whether the highly myelinated core can be identified in individual living humans.

Our interest in mapping myelin (rather than, for instance, cytoarchitecture) stems from the fact that MR parameters, such as T1, proton density and magnetization transfer ratio, are sensitive to myelin content. T1 reflects the amount of random tumbling of the water molecules in the tissue, which is restricted by the lattice of myelinated fibers and depends on their size, configuration and amount. For example, myelination differences between the gray and white matter account for the striking contrast between these two tissues in the conventional T1-weighted MRI images. While details of the relationship between myelin content and MR parameters are yet to be fully understood (e.g., cell body density, fiber configuration, manganese and iron depositories in the tissue may also contribute to signal intensity in MR images), a number of studies provide direct evidence that myelin is a primary contributor to MR image contrast (Walters et al., 2003, Eickhoff et al., 2003, Barbier et al., 2002, Mottershead et al., 2003). In particular, these studies directly compared ultra-high resolution MR images and myelin stains from the same postmortem specimen and found high correlation between MR signal and myelin content.

Rather than using image intensity in the T1-weighted images, we estimated T1 itself because, as an intrinsic parameter of the tissue, it is site and operator-independent. For convenience of data presentation, we use R1 ($R1 = 1/T1$) because of its direct

relationship with myelin content: R1 increases or decreases when myelin content increases or decreases. R1 of the gray matter was calculated by averaging R1 across the depth of the gray matter at finely spaced points along the cortical surface. Importantly, this was done in 3D, always perpendicular to the cortical surface, thus ensuring that the R1 estimate reflected an appropriate sampling of the gray matter layers and avoiding inaccuracies associated with the inclusion of neighboring gray matter of other type (as would occur in 2D slices oriented obliquely to the cortical surface). Gray matter R1 values were then mapped on the surface of the temporal lobe, which allowed examination of the gray matter R1 in a continuous manner. Such continuous mapping is essential for examining gross as well as local variations in the gray matter myelin content, and for identifying edges of different auditory areas.

Since gray matter R1 has never been mapped before, we first set out to examine the basic spatial patterns of R1 on the temporal lobe including differences between hemispheres, a comparison motivated by the well-known functional and anatomical asymmetries of the temporal lobe. This was done qualitatively by visually examining spatial maps and quantitatively through comparisons between different gross anatomically defined divisions of the temporal lobe. To address our primary goal of identifying a marker for auditory core, R1 maps were thresholded to isolate regions with highest R1 (i.e., highest myelin content) within temporal lobe to see whether they coincided with histological descriptions of the auditory core in humans: (1) overlap with postero-medial two-thirds of the Heschl's gyrus (the first when there are two), and (2) considerable variability in the extent and position relative to Heschl's gyrus.

At the end, spatial patterns in R1, that were highly repeatable across subjects, were identified in the temporal lobes of all subjects. In particular, a region of high R1 could be isolated in every hemisphere, suggesting that auditory core could be identified in individual humans in-vivo. Moreover, comparisons of R1 between hemispheres showed systematically greater R1 on the left in posterior parts of the superior temporal plane.

Methods

Five subjects (24 to 39 years, mean = 30 yrs.; 3 male; all right-handed) each participated in one imaging session. Subjects had no known neurological disorders and no tinnitus. Hearing thresholds of all subjects were normal (< 20 dB HL) at all standard audiological frequencies from 250 to 8000 Hz.

This study was approved by the institutional committees on the use of human subjects at the Massachusetts Institute of Technology, Massachusetts Eye and Ear Infirmary, and Massachusetts General Hospital. All subjects gave their written informed consent.

Imaging

Subjects were imaged using a 1.5 Tesla whole-body Siemens Sonata scanner and a transmit/receive head coil. In each imaging session, four scans of the whole head (1 slab; 128 sagittal slices; 8 min) were acquired using a standard excitation-recovery pulse sequence (3-D FLASH, TR = 20 ms, TE = 7.72 ms, resolution: 1.3 x 1.0 x 1.3 mm). Each scan used a different flip angle ($\alpha = 3, 5, 20$ and 30 degrees for subjs. 1 - 4 and 5, 10, 20 and 40 degrees for subj. 5). The four resulting data sets allowed an estimation of R1 (for each voxel in the brain) using the following relationship between image signal (S), pulse parameters (TR, TE, α), and intrinsic MR tissue properties (R1, R2 and proton density, PD; Nishimura, 1996):

$$S(TR, TE, \alpha, R1, R2, PD) = PD \sin \alpha \frac{1 - e^{-TR \cdot R1}}{1 - \cos \alpha e^{-TR \cdot R1}} e^{-TE \cdot R2}$$

Segmentation of the cortical gray matter

The cortical gray matter was segmented by estimating the boundaries between gray and white matter, and between gray matter and CSF (Figure 3.1). Since the contrast between gray and white matter was not optimal in any individual FLASH scan (with a given flip angle), the segmentation was performed on a synthesized T1-weighted volume derived from the multiple FLASH data sets so as to achieve high contrast between gray

and white matter (effective imaging parameters: TR = 20ms; alpha = 30 degrees; TE = 3 ms). The gray matter was segmented with subvoxel resolution (~0.1-0.3 mm) (Dale and Sereno, 1993; Dale et al, 1999; Fischl et al, 1999). Subvoxel resolution was achieved by utilizing information about neighboring voxels in the context of slowly (relative to image resolution) varying curvature of the brain and continuity of the cortical surface.

Because curvature of the brain varies slowly relative to the image resolution (i.e., is locally planar) and cortical surface is continuous, subvoxel accuracy in tissue classification can be achieved by utilizing information about neighboring voxels. In particular, the segmentation procedure detects the local plane-of-least-variance in the intensity and uses intensity information in this plane to optimize tissue classification.

Estimating gray matter R1

Gray matter R1 was estimated at finely-spaced points covering the cortical surface. A single R1 value was obtained for each point by averaging R1 across 80% of the depth of the gray matter starting from the gray/white matter border (Figure 3.1, black line). 80% instead of 100% was used to exclude superficial voxels, which represent a volume average of CSF and gray matter. In these voxels, considerable difference between R1 of CSF and gray matter could contaminate the estimate of the gray matter R1 (unlike the lesser difference between R1 of gray and white matters). However, the same qualitative results were obtained regardless of whether 80% or 100% was used. An important consideration is that R1 was determined in 3-D, rather than 2-D, and was always done perpendicular to the cortical surface.

Mapping and visualizing gray matter R1

For each subject, gray matter R1 was mapped over the cortical surface and viewed on reconstructions of the temporal lobes (created from the segmented gray matter using FreeSurfer, Fischl et al., 1999). The R1 maps were also viewed in a format that computationally inflates the cortex so that the cortical surface on gyri and in sulci can be viewed simultaneously (inflation performed using FreeSurfer; Dale and Sereno, 1993; Dale et al, 1999; Fischl et al, 1999). While this inflated representation is not used for data presentation, it was helpful in forming an initial impression of the global variations

in R1 over the temporal lobe. Note that all quantifications in this study were performed on the original, folded cortex.

To isolate regions of high R1, the R1 maps for each subject and hemisphere were processed as follows. First, the maps were thresholded to only show data for points with an R1 greater than ~60% of the difference between the minimum and the maximum R1 on the temporal lobe. The threshold was defined in the narrow range of values (determined separately for each hemisphere) where spatial change in R1 was rather abrupt, especially on the medial side of Heschl's gyrus. After thresholding, small (less than 50 mm²) isolated clusters of high R1 were removed for the ease of visual examination. This latter step resulted in the rejection of only 3-6 clusters per hemisphere (all located on Heschl's gyri and in planum temporale) and had only a minor effect on the maps.

Defining regions of interest (ROIs)

Gross anatomical landmarks were used to delineate the following ROIs on the superior temporal lobe (Figure 3.2): HGpm was defined as the postero-medial two-thirds of the first Heschl's gyrus. HGal was the remaining antero-lateral one-third of the first Heschl's gyrus. PT included the superior temporal cortex lateral and posterior to the transverse temporal sulcus. Posteriorly it was limited by the vertical wall of the temporo-parietal cortex, and anteriorly it extended to the antero-lateral limit of the most lateral Heschl's gyrus (either first or second). AMA was located antero-medial to Heschl's gyrus. It was limited medially by the circular sulcus, and anteriorly by an imaginary line extending perpendicularly from the anterior limit of the first Heschl's gyrus to the circular sulcus. HG2 was defined, when present, as a second most lateral Heschl's gyrus. STS included all of the gray matter within the superior temporal sulcus (both upper and lower lips). STG was defined as the lateral face of the superior temporal lobe extending from the anterior to the posterior limit of the STS.

Validity of the techniques

The methods for gray matter segmentation and spatial mapping have been described and tested previously in studies of gray matter thickness (Fischl et al, 2000,

Rosas et al, 2002). Estimating and mapping gray matter R1, while novel as an application, uses essentially the same methodologies except that gray matter segmentation was performed on data acquired using FLASH imaging sequence, rather than an MPAGE sequence which is typically used for segmentation because it is optimized for contrasting gray and white matter.

To check the quality of the gray matter segmentation from FLASH data, estimates of contrast-to-noise (CNR) from FLASH data were compared with estimates obtained using MPAGE data from the same subjects. CNR was defined as the difference between signals in the white and gray matter normalized by the background noise (for every hemisphere, sample values for gray and white matters were obtained near the gray/white matter border at 20 locations on the temporal lobe, whereas noise values were sampled outside the brain tissue). CNR estimates based on FLASH and MPAGE data were the same for three subjects (Subjs. 1,2 and 3). However, for two subjects (Subjs. 4 and 5) CNR estimates based on FLASH data were approximately 30% lower compared to estimates based on MPAGE data. Interestingly, for these two subjects, CNR estimates based on MPAGE data were also approximately 30% lower than for the other three subjects based on MPAGE data. These data suggest that data from subjects 1,2 and 3 have to be weighted as more reliable than from subjects 4 and 5 (e.g., in Figure 3.5). Importantly, all of our results on relative distribution of the gray matter R1 along the surface of the temporal lobe still hold for every hemisphere examined.

It is worth mentioning that the accuracy of gray/white matter segmentation may be somewhat compromised at the site of auditory koniocortex because of the high density of ascending fibers in primary sensory areas, which could obscure gray/white matter border if spatial resolution of the MR images is not sufficiently high (irrespective of the imaging protocol used). As a result, the myelin content of the auditory koniocortex on Heschl's gyrus (as well as differences between cortical areas) may be slightly underestimated.

Results

Spatial variations in gray matter R1

Sample maps of gray matter R1 on the surface of the superior temporal plane are shown for the left and right hemispheres of one subject in Figure 3.3. This subject is typical in that R1 was low, overall, on planum polare, intermediate on planum temporale and high on Heschl's gyrus, particularly the postero-medial aspect. In addition to these gross spatial variations, all hemispheres also showed variations within regions. For instance, R1 showed a fairly progressive increase from anterior to posterior within planum polare and extending onto the anterior parts of Heschl's gyrus. (Note that the maps in Figure 3.3 have been thresholded in contrast to highlight the gross variations, making these finer variations less apparent.) Within planum temporale, R1 varied spatially, although in a patchy way that was not obviously consistent across subjects.

Quantitative comparisons of R1 across ROIs on the superior temporal lobe confirmed regional differences in R1 seen qualitatively in the maps (Figure 3.4). For instance, R1 was lowest in AMA (located within planum polare; 10/10 hemispheres), greatest on Heschl's gyri (i.e., in HGpm, HGal, or HG2; 10/10 hemispheres), and intermediate between these extremes in PT (planum temporale; 10/10 hemispheres). Among the ROIs on Heschl's gyri, HGpm (corresponding to the postero-medial two-thirds of first Heschl's gyrus) showed the highest R1, on average, although the difference compared to the other two ROIs was not significant. HGpm (but not HGal or HG2) showed significantly greater R1 than any of the ROIs off Heschl's gyrus i.e., AMA ($p = 2 \times 10^{-7}$; paired t-test), PT ($p = 0.002$), STG ($p = 0.06$) and STS ($p = 6 \times 10^{-5}$). Thus, the ROI analysis confirmed a concentration of high R1 values on Heschl's gyri, particularly within the postero-medial two-thirds of the first (i.e., most anterior) gyrus.

Regions of highest R1 on the superior temporal lobe

Figure 3.5 displays R1 maps thresholded to isolate the regions of high R1 on the superior temporal lobe. High R1 regions were never seen in planum polare (except for the slight encroachment in the right hemisphere of subject 2). Nor were they seen on the

superior temporal gyrus, or within the superior temporal sulcus (not visible in Figure 3.5). Instead, the high R1 regions were located on Heschl's gyri and, in some hemispheres, planum temporale. In every hemisphere, there was a region of high R1 overlapping the posteromedial two-thirds of Heschl's gyrus (the first when there were two: subj. 4, right; 3, left; 5, left), although the position of this region relative to the gyrus differed across hemispheres and subjects.

Hemispheric differences

Hemispheric differences in gray matter R1 were identified by calculating an asymmetry index for each subject and ROI. In particular, for each ROI, asymmetry index was equal to the difference between R1 on the left and right (averaged across ROI) divided by the sum (Figure 3.6). For all ROIs, the mean asymmetry index was greater than zero, indicating greater R1 on the left. However, the degree of asymmetry differed across ROIs with PT and STS showing the strongest asymmetry (index > 0 in 5/5 subjects; $p < 0.008$, paired t-test comparison of left and right R1 values), HGpm and STG showing a lesser asymmetry (index > 0 in 4/5 subjects; $p = 0.05$). HGal and AMA did not show a significant asymmetry ($p > 0.7$). Thus, while gray matter R1 was generally greater on the left compared to the right, the asymmetry was most prominent in posterior regions of the superior temporal plane (PT, HGpm), on the STG, and within the STS.

Discussion

This study shows, for the first time, that gray matter R1 can be estimated and mapped over the surface of the temporal lobe in living humans. Cross-regional variations revealed by such mappings were highly repeatable across subjects. For instance, we found that R1 was always lowest overall on planum polare, intermediate on planum temporale and high on Heschl's gyri. We further found that the regions of highest R1 always overlapped the postero-medial aspects of Heschl's gyrus (the most anterior one

when there were two). Comparisons of R1 between hemispheres showed repeatable trends, namely systematically greater R1 on the left in posterior parts of the superior temporal plane, as well as STG and STS.

Given the strong relationship between R1 and myelin content, we interpret the observed spatial variations in R1 as variations in the overall myelin content of the gray matter. This interpretation is supported by the fact that the gross regional differences in R1 reported here (between planum polare, Heschl's gyri, and planum temporale) are in accordance with observations in myelin-stained postmortem tissue (Hopf, 1968, Hackett et al., 2001, Wallace et al., 2002). In particular, Heschl's gyrus has been consistently described as the most heavily myelinated region of the temporal lobe (Hopf, 1968) or among neighboring areas on the superior temporal plane (Hackett et al., 2001, Wallace et al., 2002). Cortex antero-medial to Heschl's gyrus, which includes planum polare, has been described as sparsely myelinated region, and areas immediately lateral and posterior to Heschl's gyrus (including planum temporale) have been described as less heavily myelinated than Heschl's gyrus (Hopf, 1968, Hackett et al., 2001, Wallace et al., 2002).

The present work, while in agreement with the pertinent histological data, provides a very different view of gray matter myelination on the human temporal lobe and does so in living humans. The previous observations in myelin-stained tissue are generally qualitative and are based on the discrete samples of the cortex, either closely spaced histological sections limited to sub-regions of the temporal lobe (Hackett et al., 2001, Wallace et al., 2002) or sparse samples from the large expanses of the temporal lobe (Hopf, 1968). The present study, by contrast, provides an assessment of gray matter myelination that is at once quantitative, spatially continuous, and inclusive of the entire temporal lobe. These attributes, as well as the acquisition of data in-vivo, were crucial to achieving the goals of the present study.

High R1 on Heschl's gyrus: A marker for koniocortex?

Within every temporal lobe examined, regions of high gray matter R1 were localized to Heschl's gyri and, in a few hemispheres, also to planum temporale. In all

cases, a region of high gray matter R1, its borders defined by the abrupt change in R1, overlapped the postero-medial two-thirds of the most anterior Heschl's gyrus. We interpret the regions of high R1 as the regions with heavy myelination of the gray matter. Heavy myelination is one of the prominent and well-documented characteristics of the auditory koniocortex (Hopf, 1968, Hackett et al., 2001, Wallace et al., 2002), which is typically localized to the postero-medial two-thirds of the most anterior Heschl's gyrus (Campbell, 1909, von Economo, 1929, Hopf, 1968, Galaburda and Sanides, 1980, Rivier and Clarke, 1997, Morosan et al., 2001, Rademacher et al., 2001, Hackett et al., 2001, Wallace et al., 2002). The placement of the high R1 regions on Heschl's gyrus, the abrupt nature of their borders and their interpretation as heavily myelinated areas leads us to suggest that the high R1 region(s) overlapping Heschl's gyrus (the first when there are two) coincides with some or all of auditory koniocortex.

While the present data are promising in indicating that auditory koniocortex can be identified approximately based on R1 mappings, it remains to be seen how closely these regions correspond to koniocortex as it would be defined histologically. The direct validation (e.g., by direct comparison of MR images and stained for myelin tissue from the same sample) is beyond the scope of this study, but we will consider histological evidence and methodological considerations that bare direct relevance on how borders of high R1 region may coincide with borders of auditory koniocortex. From the histology perspective, our data show evidence that the region(s) of high R1 may also include areas beyond koniocortex anteriorly. In some hemispheres (e.g., Subj. 2, left hemisphere and Subj. 4, right hemisphere, Figure 3.5), the regions of high R1 extend practically to the anterior edge of Heschl's gyrus, further than might be expected based on histological descriptions of auditory koniocortex. One possibility is that this reflects true inter-subject variability in the extent of the auditory koniocortex, which is well documented in histological literature (e.g., Rademacher et al., 2001, Hackett et al., 2001). Another and, perhaps, more likely, possibility is that gray matter myelin content information alone might not be sufficient to define anterior borders of the auditory koniocortex (e.g., myelin content in the auditory koniocortex and the anterior parts of HG can be similarly high, but other architectonic features can be different). In support of this idea, Wallace et al., (2002) describe similarly high myelin density in the auditory koniocortex and the most

anterior part of Heschl's gyrus (not auditory koniocortex), but differences in the laminar structure (e.g., unlike auditory koniocortex, anterior part of Heschl's gyrus showed no evidence of an internal stria of Baillarger). We suggest that other types of information (e.g., laminar profile of the gray matter) may be needed in addition to overall gray matter myelin content to define the anterior border of the auditory koniocortex. It should be noted, however, that obtaining laminar profile of the gray matter requires ultra-high resolution imaging and, at present, is typically done in high field (e.g., 7 Tesla) scanners over a long period of time. One of the advantages of the R1 mapping performed here is that the scans are short because of the relatively low spatial resolution and can be performed on low-field scanners so that the procedure is highly practical and can be included in any functional imaging study.

Given the pilot nature of the present study, it is important to realize that a number of methodological issues remain to be improved on by further optimizing certain aspects of data acquisition and analysis. In particular, our data suggest that improving the accuracy of gray matter segmentation would improve the odds of the accurate identification of auditory cortex. For example, as mentioned in the Methods section, two subjects (Subjs. 4 and 5) were distinguishable from the others (Subjs. 1-3) in that the gray matter segmentation may have been less accurate because of the lower contrast-to-noise ratio in these subjects. It turns out that these are the same subjects (Subjs. 4 and 5, Figure 3.5) for whom the disparities with histology mainly occur: the regions of high R1 do not extend as far postero-medially on Heschl's gyrus as one might expect from the previous histological work and also occur in the non-primary areas of planum temporale. Overall, our data suggest that (1) there is inter-subject variability in the cortical gray matter tissue properties, and (2) the gray matter segmentation was of sufficient quality for some, but not other subjects. From the methodological perspective, this suggests that in the future experiments, data acquisition and analysis protocols might have to be (1) tailored to a particular subject to optimize tissue contrast in this subject, and/or (2) further improved to achieve sufficient quality of gray matter segmentation for a wide range of input variables (e.g., different values for tissue parameters in different subjects).

In general, the accuracy of gray matter segmentation can be improved by increasing tissue contrast, which, in turn, can be improved in several ways. A straight-

forward way to improve tissue contrast is to acquire more data to increase signal-to-noise ratio or to increase the resolution of the images. However, both proposals would require additional imaging time. Extra imaging time is not desirable in general, but especially if, as suggested, the technique is to be included in auditory neuroimaging studies as a standard “quick koniocortex localizer” scan. An alternative way to increase tissue contrast is to further optimize and custom-tailor scanning and analysis protocols (e.g., parameters for the synthesized T1-weighted volume on which segmentation is performed). Additionally, we suggest implementing a real-time contrast-to-noise estimation during imaging as a quality assurance and time saving mechanism (e.g., some subjects may require less data to achieve sufficient tissue contrast than others).

In conclusion, we suggest that the region (regions) of high R1 on Heschl’s gyrus indicates an approximate marker for the auditory koniocortex, but additional information (e.g., laminar profile) and technical improvements (e.g., increased accuracy of gray matter segmentation) may be needed to define its borders with greater accuracy and reliability.

Hemispheric differences and functional interpretations

The present study provides evidence, for the first time, for a left-right difference in the myelination of the gray matter of the temporal lobe and does so in living humans. As such, it compliments a wealth of previous data documenting hemispheric differences in gross morphology or gray matter microstructure of the posterior temporal plane and Heschl’s gyri (gross morphology: Geschwind and Levitsky, 1968, Galaburda et al., 1978, Penhune et al., 1996, Leonard et al., 1998; microstructure: Seldon, 1981a, 1981b, 1982, Hutsler and Gazzaniga, 1996, Anderson et al., 1999, Galuske et al., 2000, Buxoeveden et al., 2001).

The asymmetry in gray matter myelination is directly relevant to proposals that the left hemisphere is preferentially involved in the processing of rapid temporal changes in acoustic signals. These proposals come from studies of brain function using various techniques. For example, deficits in rapid temporal processing have been observed in patients with left, but not right temporal lobe lesions (Efron, 1963, Robin et al, 1990,

Ehrle et al, 2001). In normal subjects, greater PET activation on the left Heschl's gyrus was observed for tasks that tested subject's ability to process rapid changes in the temporal aspects of non-speech sounds, while greater activation on the right side was observed for tasks that tested subject's ability to process rapid changes in pitch information (Zatorre and Belin, 2001). Intracerebral recordings in epilepsy patients showed that left temporal regions are able to follow temporal transitions in speech and non-speech sounds better than right temporal regions (Liegeois-Chauvel et al, 1999). Our data indicating hemispheric differences in gray matter myelination suggest a structural substrate for the functional findings. Since myelin plays a crucial role in maintaining the timing of neural activity, greater myelination on the left may increase the precision of neural timing, thus providing the left hemisphere with an enhanced ability (over the right hemisphere) to discriminate and follow rapid acoustic changes.

Increased myelin within the neural circuitry of the gray matter is only one way that enhanced neural timing in the left hemisphere might be achieved. For example, well-documented larger volume of the left planum temporale and Heschl's gyrus (Geschwind and Levitsky, 1968, Galaburda et al., 1978, Penhune et al., 1996) suggests left-right differences in the number of fibers that carry information to the gray matter of these regions. A greater number of inputs could enhance timing of neural processing by, for example, increasing confidence in the particular outcome that, in turn, could allow resolving closely spaced (in time) events with higher accuracy. Thus, the asymmetry in gray matter myelination identified here may be one of two or more substrates for specialized temporal processing in the left hemisphere.

The gray matter asymmetry observed in the present study may also play a role in the left hemispheric specialization for speech and language in humans. The reasons for suggesting this are two-fold. First, the observation of greater gray matter on the left was only seen in regions of the temporal lobe heavily implicated in language processing (PT, STG, STS) (Zatorre et al, 1992, Binder et al, 2000, Hickok and Poeppel, 2000), or in regions supplying inputs (directly or indirectly) to those more specialized regions (HGpm; Kaas et al., 1999). Second, behavioral studies in clinical populations (e.g., dyslexics and aphasics) have indicated that accurate temporal processing may be crucial to normal speech and language functions (Efron, 1963; Robin et al., 1990; Tallal, 1980,

Tallal and Stark, 1981). Thus, the leftward bias in gray matter myelination, if it is indeed a substrate for higher fidelity temporal processing, may by extension be an important substrate for the left-hemispheric specialization for speech and language.

Implications and significance

The present study demonstrates that a putative marker for a particular auditory area (koniocortex) can be identified using structural MRI. However, at a broader level it provides a proof of concept that delineation of auditory cortical areas based on anatomical criteria used in histology is feasible in individual, living humans using MRI. In contrast to histological examinations, techniques described here can be used in-vivo, avoid major limitations introduced by labor-intensive nature and technical difficulties of working with postmortem tissue, and provide mapping capabilities that allow examining cortical surface in a continuous manner.

There are many implications of having an ability to distinguish auditory cortical areas (and auditory koniocortex, in particular) in-vivo. On one hand, it can provide a common framework for interpreting functional neuroimaging work on auditory cortex and understanding its functional organization. On the other hand, it may also enable future studies to assign specialized functions to particular areas, as it has been done in animals for decades, and, thus, provide the structural underpinnings to understand the organizational principles of auditory cortical processing. Importantly, the technique described here can be included in any neuroimaging study because data acquisition time is short and it uses conventional scanners and protocols.

The clinical significance of being able to assess and quantify myelination in living humans is evident when one considers that aging and many brain pathologies (e.g., multiple sclerosis and dyslexia) have been linked to atrophy or congenital deficiency in myelin (Tallal and Stark, 1981, Mottershead et al., 2003, Laule et al., 2004, Schmierer et al., 2004, Fernando et al., 2004). Approaches such as one used in this study may provide objective (and practical) measure of the pathology, understanding of its structural underpinnings, as well as allow tracking of structural changes associated with therapy and learning.

References

- Anderson, B., B. D. Southern, et al. (1999). "Anatomic asymmetries of the posterior superior temporal lobes: a postmortem study." Neuropsychiatry Neuropsychol Behav Neurol **12**(4): 247-54.
- Barbier, E. L., S. Marrett, et al. (2002). "Imaging cortical anatomy by high-resolution MR at 3.0T: detection of the stripe of Gennari in visual area 17." Magn Reson Med **48**(4): 735-8.
- Belin, P., R. J. Zatorre, et al. (2000). "Voice-selective areas in human auditory cortex." Nature **403**(6767): 309-12.
- Bellis, T. J., T. Nicol, et al. (2000). "Aging affects hemispheric asymmetry in the neural representation of speech sounds." J Neurosci **20**(2): 791-7.
- Binder, J. R., J. A. Frost, et al. (2000). "Human temporal lobe activation by speech and nonspeech sounds." Cereb Cortex **10**(5): 512-28.
- Brodman, K. (1909). Brodman's "Localisation in the cerebral cortex". London, Smith-Gordon.
- Buxhoeveden, D. P., A. E. Switala, et al. (2001). "Lateralization of minicolumns in human planum temporale is absent in nonhuman primate cortex." Brain Behav Evol **57**(6): 349-58.
- Buxhoeveden, D. P., A. E. Switala, et al. (2001). "Morphological differences between minicolumns in human and nonhuman primate cortex." Am J Phys Anthropol **115**(4): 361-71.
- Campbell, A. W. (1905). Histological studies on the localization of cerebral function. Cambridge, Cambridge University Press.
- Cho, S., D. Jones, et al. (1997). "Establishing norms for age-related changes in proton T1 of human brain tissue in vivo." Magn Reson Imaging **15**(10): 1133-43.
- Dale, A. M., B. Fischl, et al. (1999). "Cortical surface-based analysis. I. Segmentation and surface reconstruction." Neuroimage **9**(2): 179-94.
- Draganski, B., C. Gaser, et al. (2004). "Neuroplasticity: changes in grey matter induced by training." Nature **427**(6972): 311-2.
- Efron, R. (1963). "Temporal Perception, Aphasia and D'ej'a Vu." Brain **86**: 403-24.
- Ehrle, N., S. Samson, et al. (2001). "Processing of rapid auditory information in epileptic patients with left temporal lobe damage." Neuropsychologia **39**(5): 525-31.
- Eickhoff S., W. N., Schleicher A., Malikovic A., Egan G., Watson J., Zilles K., Amunts K. (2003). Comparison of the cortical architecture of in vivo, high resolution structural MR with mylo- and cytoarchitectonic histological sections. Human Brain Mapping, New York City, USA.
- Estes, R. I., J. Jerger, et al. (2002). "Reversal of hemispheric asymmetry on auditory tasks in children who are poor listeners." J Am Acad Audiol **13**(2): 59-71.
- Fernando, M. S., J. T. O'Brien, et al. (2004). "Comparison of the pathology of cerebral white matter with post-mortem magnetic resonance imaging (MRI) in the elderly brain." Neuropathol Appl Neurobiol **30**(4): 385-95.
- Fischl, B. and A. M. Dale (2000). "Measuring the thickness of the human cerebral cortex from magnetic resonance images." Proc Natl Acad Sci U S A **97**(20): 11050-5.

- Fischl, B., M. I. Sereno, et al. (1999). "Cortical surface-based analysis. II: Inflation, flattening, and a surface-based coordinate system." Neuroimage **9**(2): 195-207.
- Galaburda, A. and F. Sanides (1980). "Cytoarchitectonic organization of the human auditory cortex." J Comp Neurol **190**(3): 597-610.
- Galaburda, A. M., M. LeMay, et al. (1978). "Right-left asymmetries in the brain." Science **199**(4331): 852-6.
- Galaburda, A. M., F. Sanides, et al. (1978). "Human brain. Cytoarchitectonic left-right asymmetries in the temporal speech region." Arch Neurol **35**(12): 812-7.
- Galuske, R. A., W. Schlote, et al. (2000). "Interhemispheric asymmetries of the modular structure in human temporal cortex." Science **289**(5486): 1946-9.
- Gelman, N., J. M. Gorell, et al. (1999). "MR imaging of human brain at 3.0 T: preliminary report on transverse relaxation rates and relation to estimated iron content." Radiology **210**(3): 759-67.
- Geschwind, N. and A. M. Galaburda (1985). "Cerebral lateralization. Biological mechanisms, associations, and pathology: III. A hypothesis and a program for research." Arch Neurol **42**(7): 634-54.
- Geschwind, N. and W. Levitsky (1968). "Human brain: left-right asymmetries in temporal speech region." Science **161**(837): 186-7.
- Griffiths, T. D., C. Buchel, et al. (1998). "Analysis of temporal structure in sound by the human brain." Nat Neurosci **1**(5): 422-7.
- Hackett, T. A., T. M. Preuss, et al. (2001). "Architectonic identification of the core region in auditory cortex of macaques, chimpanzees, and humans." J Comp Neurol **441**(3): 197-222.
- Hickok, G. and D. Poeppel (2000). "Towards a functional neuroanatomy of speech perception." Trends Cogn Sci **4**(4): 131-138.
- Hopf, A. (1968). "Photometric studies on the myeloarchitecture of the human temporal lobe." J Hirnforsch **10**(4): 285-97.
- Hutsler, J. J. and M. S. Gazzaniga (1996). "Acetylcholinesterase staining in human auditory and language cortices: regional variation of structural features." Cereb Cortex **6**(2): 260-70.
- Kaas, J. H. and T. A. Hackett (2000). "Subdivisions of auditory cortex and processing streams in primates." Proc Natl Acad Sci U S A **97**(22): 11793-9.
- Kaas, J. H., T. A. Hackett, et al. (1999). "Auditory processing in primate cerebral cortex." Curr Opin Neurobiol **9**(2): 164-70.
- Kennedy, D. N., N. Lange, et al. (1998). "Gyri of the human neocortex: an MRI-based analysis of volume and variance." Cereb Cortex **8**(4): 372-84.
- Kimura, D. (1961). "Some effects of temporal-lobe damage on auditory perception." Can J Psychol **15**: 156-65.
- Kulynych, J. J., K. Vldar, et al. (1994). "Gender differences in the normal lateralization of the supratemporal cortex: MRI surface-rendering morphometry of Heschl's gyrus and the planum temporale." Cereb Cortex **4**(2): 107-18.
- Kuperberg, G. R., M. R. Broome, et al. (2003). "Regionally localized thinning of the cerebral cortex in schizophrenia." Arch Gen Psychiatry **60**(9): 878-88.

- Laule, C., I. M. Vavasour, et al. (2004). "Water content and myelin water fraction in multiple sclerosis. A T2 relaxation study." *J Neurol* **251**(3): 284-93.
- Laule, C., I. M. Vavasour, et al. (2004). "Water content and myelin water fraction in multiple sclerosis. A T2 relaxation study." *J Neurol* **251**(3): 284-93.
- Leblanc, R., E. Meyer, et al. (1992). "Language localization with activation positron emission tomography scanning." *Neurosurgery* **31**(2): 369-73.
- Leonard, C. M., C. Puranik, et al. (1998). "Normal variation in the frequency and location of human auditory cortex landmarks. Heschl's gyrus: where is it?" *Cereb Cortex* **8**(5): 397-406.
- Leonard, C. M., K. K. Voeller, et al. (1993). "Anomalous cerebral structure in dyslexia revealed with magnetic resonance imaging." *Arch Neurol* **50**(5): 461-9.
- Liegeois-Chauvel, C., J. B. de Graaf, et al. (1999). "Specialization of left auditory cortex for speech perception in man depends on temporal coding." *Cereb Cortex* **9**(5): 484-96.
- Liegeois-Chauvel, C., K. Giraud, et al. (2001). "Intracerebral evoked potentials in pitch perception reveal a functional asymmetry of the human auditory cortex." *Ann N Y Acad Sci* **930**: 117-32.
- Merzenich, M. M., W. M. Jenkins, et al. (1996). "Temporal processing deficits of language-learning impaired children ameliorated by training." *Science* **271**(5245): 77-81.
- Morel, A., P. E. Garraghty, et al. (1993). "Tonotopic organization, architectonic fields, and connections of auditory cortex in macaque monkeys." *J Comp Neurol* **335**(3): 437-59.
- Morosan, P., J. Rademacher, et al. (2001). "Human primary auditory cortex: cytoarchitectonic subdivisions and mapping into a spatial reference system." *Neuroimage* **13**(4): 684-701.
- Mottershead, J. P., K. Schmierer, et al. (2003). "High field MRI correlates of myelin content and axonal density in multiple sclerosis--a post-mortem study of the spinal cord." *J Neurol* **250**(11): 1293-301.
- Nicholls, M. E., J. Gora, et al. (2002). "Hemispheric asymmetries for visual and auditory temporal processing: an evoked potential study." *Int J Psychophysiol* **44**(1): 37-55.
- Penhune, V. B., R. J. Zatorre, et al. (1996). "Interhemispheric anatomical differences in human primary auditory cortex: probabilistic mapping and volume measurement from magnetic resonance scans." *Cereb Cortex* **6**(5): 661-72.
- Poremba, A., R. C. Saunders, et al. (2003). "Functional mapping of the primate auditory system." *Science* **299**(5606): 568-72.
- Rademacher, J., V. S. Caviness, Jr., et al. (1993). "Topographical variation of the human primary cortices: implications for neuroimaging, brain mapping, and neurobiology." *Cereb Cortex* **3**(4): 313-29.
- Rademacher, J., P. Morosan, et al. (2001). "Probabilistic mapping and volume measurement of human primary auditory cortex." *Neuroimage* **13**(4): 669-83.
- Rivier, F. and S. Clarke (1997). "Cytochrome oxidase, acetylcholinesterase, and NADPH-diaphorase staining in human supratemporal and insular cortex: evidence for multiple auditory areas." *Neuroimage* **6**(4): 288-304.
- Robin, D. A., D. Tranel, et al. (1990). "Auditory perception of temporal and spectral events in patients with focal left and right cerebral lesions." *Brain Lang* **39**(4): 539-55.

- Rosas, H. D., A. K. Liu, et al. (2002). "Regional and progressive thinning of the cortical ribbon in Huntington's disease." Neurology **58**(5): 695-701.
- Rupp, A., S. Hack, et al. (2000). "Fast temporal interactions in human auditory cortex." Neuroreport **11**(17): 3731-6.
- Sailer, M., B. Fischl, et al. (2003). "Focal thinning of the cerebral cortex in multiple sclerosis." Brain **126**(Pt 8): 1734-44.
- Salat, D. H., R. L. Buckner, et al. (2004). "Thinning of the cerebral cortex in aging." Cereb Cortex **14**(7): 721-30.
- Schmierer, K., F. Scaravilli, et al. (2004). "Magnetization transfer ratio and myelin in postmortem multiple sclerosis brain." Ann Neurol **56**(3): 407-15.
- Schneider, P., M. Scherg, et al. (2002). "Morphology of Heschl's gyrus reflects enhanced activation in the auditory cortex of musicians." Nat Neurosci **5**(7): 688-94.
- Schwartz, J. and P. Tallal (1980). "Rate of acoustic change may underlie hemispheric specialization for speech perception." Science **207**(4437): 1380-1.
- Seldon, H. L. (1981). "Structure of human auditory cortex. I. Cytoarchitectonics and dendritic distributions." Brain Res **229**(2): 277-94.
- Seldon, H. L. (1981). "Structure of human auditory cortex. II. Axon distributions and morphological correlates of speech perception." Brain Res **229**(2): 295-310.
- Seldon, H. L. (1982). "Structure of human auditory cortex. III. Statistical analysis of dendritic trees." Brain Res **249**(2): 211-21.
- Shah, N. J., H. Neeb, et al. (2003). "Quantitative T1 mapping of hepatic encephalopathy using magnetic resonance imaging." Hepatology **38**(5): 1219-26.
- Shapleske, J., S. L. Rossell, et al. (1999). "The planum temporale: a systematic, quantitative review of its structural, functional and clinical significance." Brain Res Brain Res Rev **29**(1): 26-49.
- Sled, J. G., I. Levesque, et al. (2004). "Regional variations in normal brain shown by quantitative magnetization transfer imaging." Magn Reson Med **51**(2): 299-303.
- Sowell, E. R., B. S. Peterson, et al. (2003). "Mapping cortical change across the human life span." Nat Neurosci **6**(3): 309-15.
- Steen, R. G., W. E. Reddick, et al. (2000). "More than meets the eye: significant regional heterogeneity in human cortical T1." Magn Reson Imaging **18**(4): 361-8.
- Steen, R. G., D. Spence, et al. (2001). "Effect of therapeutic ionizing radiation on the human brain." Ann Neurol **50**(6): 787-95.
- Symms, M., H. R. Jager, et al. (2004). "A review of structural magnetic resonance neuroimaging." J Neurol Neurosurg Psychiatry **75**(9): 1235-44.
- Talairach, J. and P. Tournoux (1988). Co-planar stereotaxic atlas of the human brain, Thieme Medical Publishers, New York.
- Tallal, P. (1980). "Auditory temporal perception, phonics, and reading disabilities in children." Brain Lang **9**(2): 182-98.

- Tallal, P., S. L. Miller, et al. (1996). "Language comprehension in language-learning impaired children improved with acoustically modified speech." Science **271**(5245): 81-4.
- Tallal, P. and R. E. Stark (1981). "Speech acoustic-cue discrimination abilities of normally developing and language-impaired children." J Acoust Soc Am **69**(2): 568-74.
- Taub, J. M., P. E. Tanguay, et al. (1976). "Electroencephalographic and reaction time asymmetries to musical chord stimuli." Physiol Behav **17**(6): 925-30.
- von Economo, C. (1929). The cytoarchitectonics of the human cerebral cortex. London, Oxford University Press.
- Wallace, M. N., P. W. Johnston, et al. (2002). "Histochemical identification of cortical areas in the auditory region of the human brain." Exp Brain Res **143**(4): 499-508.
- Walters, N. B., G. F. Egan, et al. (2003). "In vivo identification of human cortical areas using high-resolution MRI: an approach to cerebral structure-function correlation." Proc Natl Acad Sci U S A **100**(5): 2981-6.
- Warrier, C. M. and R. J. Zatorre (2004). "Right temporal cortex is critical for utilization of melodic contextual cues in a pitch constancy task." Brain **127**(Pt 7): 1616-25.
- Yoshiura, T., S. Higano, et al. (2000). "Heschl and superior temporal gyri: low signal intensity of the cortex on T2-weighted MR images of the normal brain." Radiology **214**(1): 217-21.
- Zatorre, R. J. (2001). "Neural specializations for tonal processing." Ann N Y Acad Sci **930**: 193-210.
- Zatorre, R. J. and P. Belin (2001). "Spectral and temporal processing in human auditory cortex." Cereb Cortex **11**(10): 946-53.
- Zatorre, R. J., P. Belin, et al. (2002). "Structure and function of auditory cortex: music and speech." Trends Cogn Sci **6**(1): 37-46.
- Zatorre, R. J., A. C. Evans, et al. (1992). "Lateralization of phonetic and pitch discrimination in speech processing." Science **256**(5058): 846-9.

Figure Captions

Figure 3.1. Coronal slice through the temporal lobe showing the spatial distribution of R1 at the resolution of the original images (1 x 1 x 1.3 mm). The grayscale value for each pixel indicates the magnitude of R1 (estimated from multiple image data sets). Black and white lines indicate the gray matter/CSF and gray matter/white matter borders, respectively, as determined by the segmentation procedure. For the R1 maps in figure 3, a single R1 value was obtained at individual points on the cortical surface by averaging R1 across the depth of the gray matter in 3-D, and using a line always perpendicular to the cortical surface.

Figure 3.2. ROIs displayed on a 3-D reconstruction of the right superior temporal lobe in one subject (#5).

Figure 3.3. Typical maps of gray matter R1 on the superior temporal lobe. The maps correspond to the left and right hemispheres of one subject. R1 is indicated in color on a red (low R1) to yellow (high R1) scale. Here, R1 map was spatially smoothed using iterative (number of steps = 2) approximation to isotropic Gaussian smoothing ("width" of the mask \approx square root (# of iterations * 2 / pi)). The distribution of R1 suggests that gray matter myelin content is generally smallest anteriorly (in planum polare), intermediate posteriorly (on planum temporale), and greatest on Heschl's gyrus.

Figure 3.4. Mean gray matter R1 for different ROIs on the superior temporal lobe. Error bars indicate one standard error.

Figure 3.5. Regions of high R1 on the superior temporal lobe. Each panel shows either the right (top) or left (bottom) superior temporal lobe of a given subject. The high R1 regions (white) overlap first Heschl's gyrus in all cases, but also differ across cases in position relative to Heschl's gyrus. There were no regions of high R1 on the lateral face of the temporal lobe or within sulci (i.e. in regions of the superior temporal lobe that cannot be seen). Dashed vertical line separates subjects (#1-3) in whom gray matter segmentation was more accurate than in subjects #4 and 5 because of the better tissue contrast.

Figure 3.6. Degree of R1 asymmetry on the superior temporal lobe. For each ROI and subject, an asymmetry index was calculated as the difference in R1 between the left and right sides divided by the sum. Each black circle indicates the index for a particular subject. Gray bars indicate the mean across subjects. Dashed horizontal line at zero indicates no asymmetry. HGpm, PT, STG, and STS showed significant asymmetry whereas ROIs located anteriorly on the superior temporal plane (AMA, HGal) did not (based on a statistical comparison of left vs. right R1 values; paired t-test). No data are given for HG2 since none of the subjects had a second Heschl's gyrus on both the left and right sides.

Coronal View of R1 Image (temporal lobe)

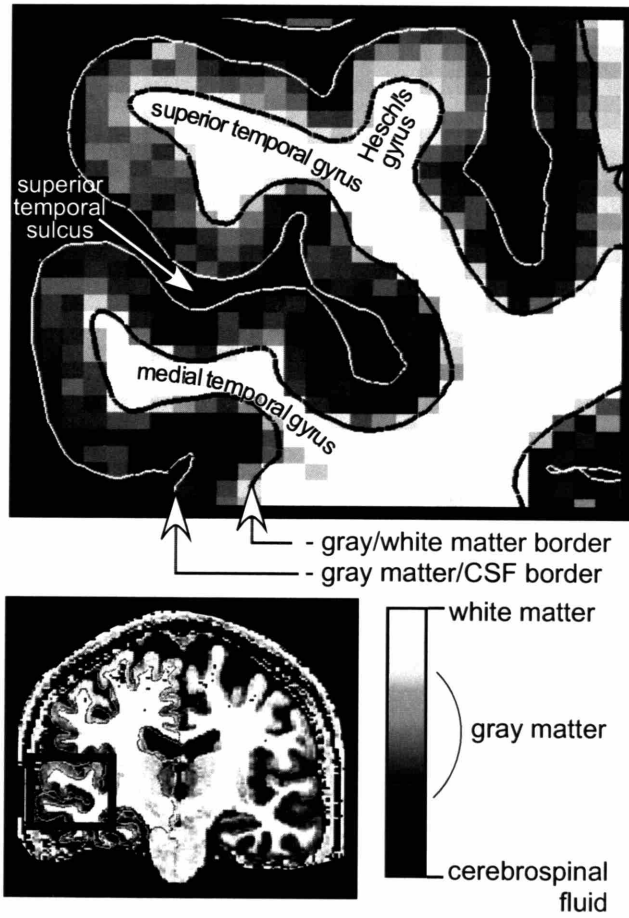


Figure 3.1.



Temporal Lobe (view from above)

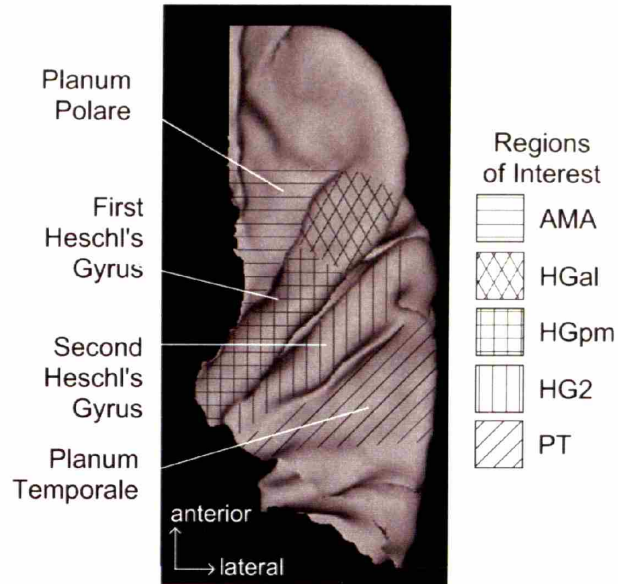


Figure 3.2.

Spatial Maps of Gray Matter R1 (subj. #1)

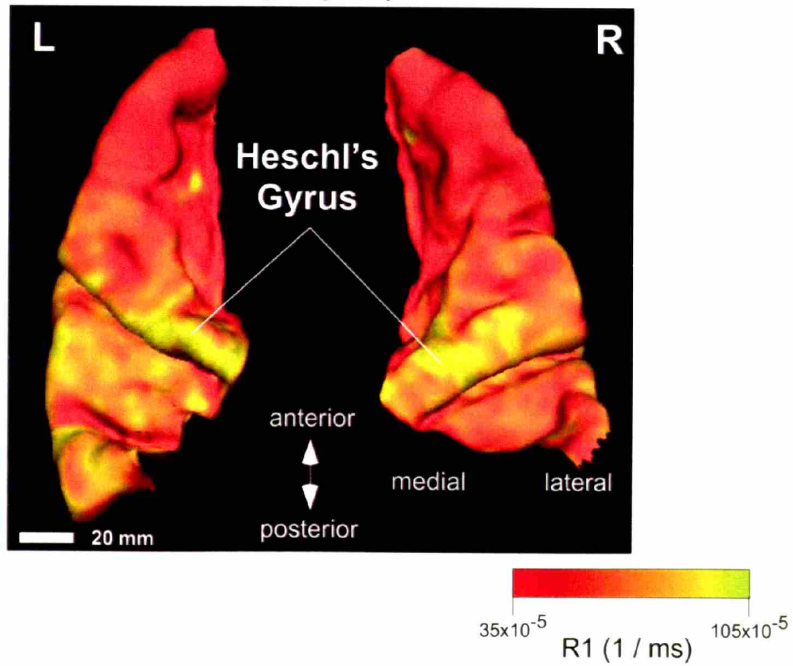


Figure 3.3.



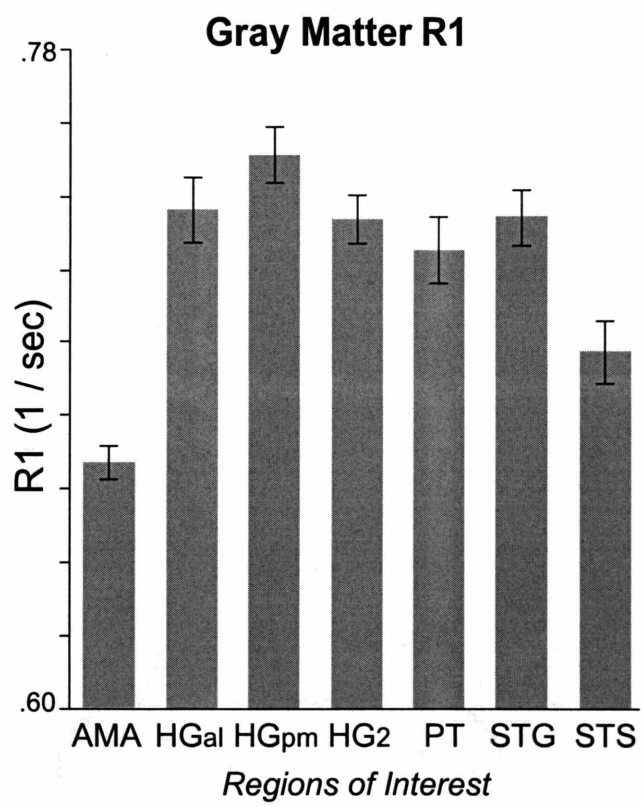


Figure 3.4.

High R1 regions on the temporal lobes of individual subjects

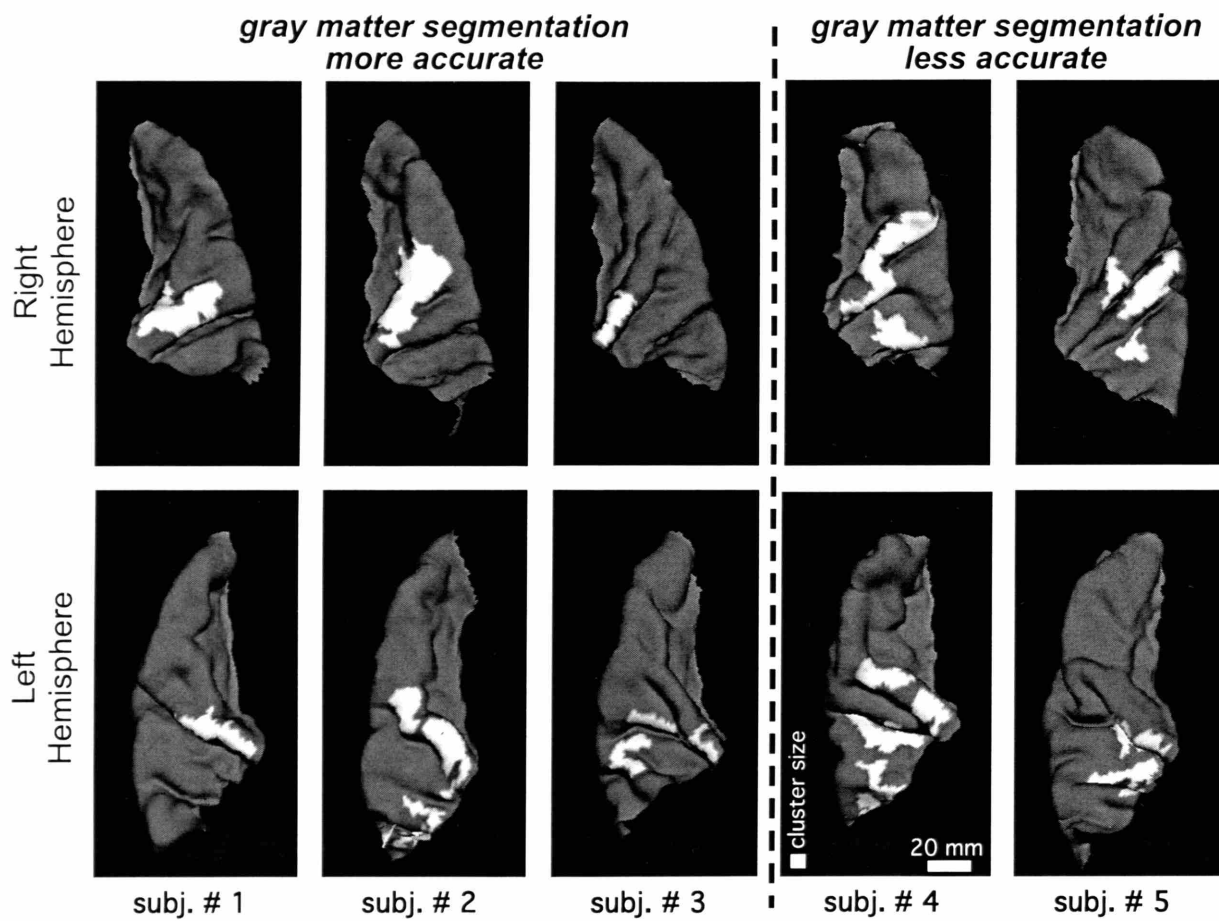


Figure 3.5.

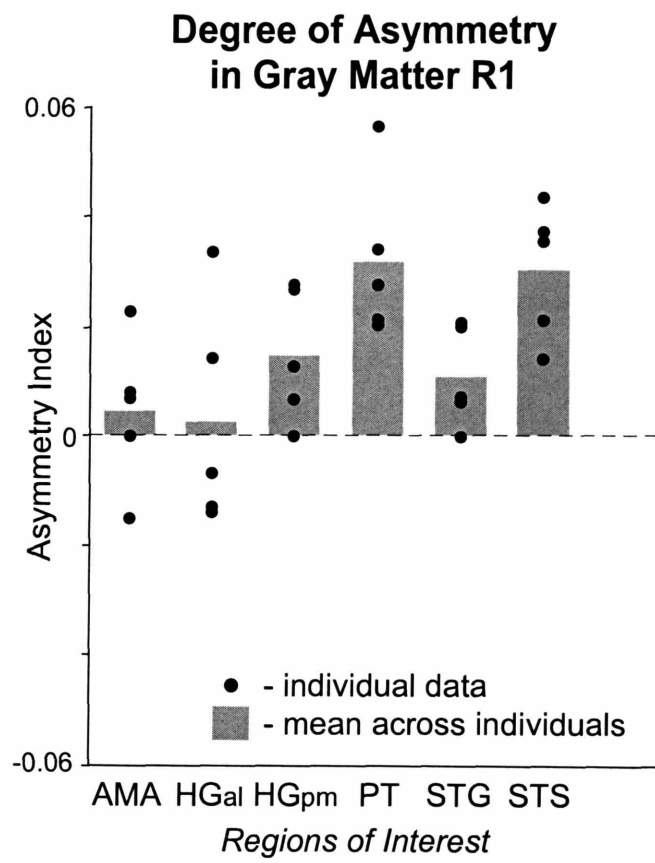


Figure 3.6.

Chapter IV.

Imaging auditory gray matter thickness

Introduction

The present study uses structural MRI to quantify and map auditory cortical gray matter thickness. Our examination of gray matter thickness is motivated by the following. Gray matter thickness is an indicator of cortical neural architecture (e.g., number, size and packing density of cortical neurons) and changes with aging, learning, development, sensory deprivation and disease (Rosas et al., 2002, Kuperberg et al., 2003, Sailer et al., 2003, Sowell et al., 2003, Draganski et al., 2004, Salat et al., 2004). This raises the possibility that thickness changes also occur, for instance, during language acquisition, auditory training or following changes in the auditory periphery. In quantifying and mapping the thickness of auditory cortex in normal human subjects, we set the stage for examining these possibilities.

MRI methods for measuring gray matter thickness (including segmentation of the gray matter and spatial mapping) have been described and tested previously (Fischl et al., 2000, Rosas et al., 2002). Important to our examination of gray matter thickness are the 3D segmentation, estimation and mapping techniques. Our approach, which takes into consideration the full three-dimensionality of the gray matter ribbon, has an advantage over a typical histological way of using 2-D brain slices. Two-dimensional brain slices (either histological or MRI) provide misleading estimates of gray matter thickness unless they are perpendicular to the cortical surface. The highly folded nature of the human brain does not allow cutting two-dimensional slices always or even most often perpendicular to the cortical surface. Here, we will use a 3D method that allows measurements that are always perpendicular to the cortical surface and has been shown to

provide gray matter thickness estimates with sub-millimeter accuracy by directly comparing this method and manual measurements from histological tissue.

Methods

Subjects

Five subjects (24 to 39 years, mean = 30 yrs.; 3 male; all right-handed) each participated in one imaging session. Subjects had no known neurological disorders and no tinnitus. Hearing thresholds of all subjects were normal (< 20 dB HL) at all standard audiological frequencies from 250 to 8000 Hz.

This study was approved by the institutional committees on the use of human subjects at the Massachusetts Institute of Technology, Massachusetts Eye and Ear Infirmary, and Massachusetts General Hospital. All subjects gave their written informed consent.

Imaging

See Chapter III.

Segmentation of the cortical gray matter

See Chapter III.

Estimating and mapping gray matter thickness

Gray matter thickness was estimated at finely-spaced points (vertices) covering the cortical surface. The thickness of the gray matter at each vertex was estimated as the shortest distance between the gray/white matter border and the gray matter/CSF border, always perpendicular to the cortical surface (Fischl et al., 2000).

For each subject, gray matter thickness was mapped over the cortical surface and viewed on reconstructions of the temporal lobes (created from the segmented gray matter using FreeSurfer, Fischl et al., 1999). The thickness maps were also viewed in a format

that computationally inflates the cortex so that the cortical surface on gyri and in sulci can be viewed simultaneously (inflation performed using FreeSurfer; Dale et al., 1999; Fischl et al., 1999). However, all quantifications were performed on the original folded cortex in order to avoid errors introduced by such distortions.

The fact that gyri of the cortical gray matter are generally thicker than sulci has been well known for decades (von Economo, 1929, Blinkov and Glezer, 1968). In order to examine regional variations in gray matter thickness beyond those explained by this correlation, the correlation between gray matter thickness and local curvature of the cortical surface was mathematically removed in every hemisphere as follows. First, the local curvature (average convexity or concavity) at every point on the cortical surface was determined as described in Fischl et al (1999). Then, for every point on the cortical surface, we plotted gray matter thickness (T) vs. local curvature at that point (C). This relationship was fitted by a line described by

$$T = C * A + B,$$

where A is a correlation coefficient between gray matter thickness and curvature of the cortical surface and B is DC offset. Finally, for every point on the cortical surface, “gray matter thickness, correlation with curvature removed” (T’) was estimated as

$$T' = T - C * A.$$

Defining Regions of Interest (ROIs):

Gross anatomical landmarks were used to delineate ROIs on the superior surface of the temporal lobe (see description and Figure 3.2 in Chapter III)

Results

Sample maps of gray matter thickness on the surface of the superior temporal plane are shown for the left and right hemispheres of one subject in Figure 4.1. These maps are typical in that gyri are thicker than sulci and there is an overall increase in gray matter thickness towards the temporal pole. For all subjects, the overall increase in

thickness was more evident in the right hemisphere than the left in that, besides local inhomogeneities, the overall difference in thickness between the posterior and anterior parts of the temporal lobe was greater in the right hemisphere. Visual inspection also revealed that gray matter of the temporal lobe was thicker than the rest of the cerebral gray matter.

Superimposed on the global change in thickness, there were more local regional differences as shown in Figure 4.2A. Most of these differences reflect correlation between gray matter thickness and curvature of the cortical surface ($r = -0.56$), which, in turn, reflects a well-known fact that gray matter is thicker on gyri than in sulci as seen in Figure 4.1. For example, sulcal regions AMA, PT and STS are thinner than gyral regions HGal and STG. Consistent with this, regional differences were considerably diminished when correlation was mathematically removed except for AMA, which became significantly thicker than other ROIs (Figure 4.2B).

Visual inspection of gray matter thickness maps (original and with correlation removed) did not reveal spatial patterns that were consistent across subjects beyond those described above.

There was no hemispheric difference in gray matter thickness for any ROI ($p = 1$ in left/right comparison of each ROI).

Discussion

Consistent with a well-documented fact that gray matter of gyri is thicker than in sulci (von Economo, 1929, Blinkov and Glezer, 1968), we found that gray matter thickness correlated with curvature of the temporal lobe. In addition to this, we observed that gray matter thickness of the temporal lobe increased in the postero-anterior direction towards the temporal pole (this was especially apparent in the right hemisphere) and that temporal lobe is thicker compared to the rest of the brain. While histological literature on the thickness of the auditory gray matter is sparse, von Economo notes both of these trends in his 1925 tractate.

It is worth noting that von Economo's estimates (~3 mm) for the temporal region are greater than those observed in this paper. This is most likely due to an inherent overestimation caused by measuring thickness from the 2-D slices of the tissue used in his studies. In order to measure gray matter thickness accurately from the 2-D slices of the human brain, one has to always cut perpendicular to the cortical surface, which is impossible due to the highly folded nature of the brain. As a result, most of the brain in 2-D slices is cut obliquely which results in the overestimation of gray matter thickness. In contrast, methods such as the one used in this study provide accurate estimates of gray matter thickness by utilizing 3-D reconstructions of the brain, which allows measuring gray matter thickness always perpendicular to the cortical surface.

Our data did not reveal spatial patterns in gray matter thickness that would be indicative of the spatial arrangements of anatomically distinct auditory areas described using cyto- and myelo-architecture. This suggests that gray matter thickness might not be especially useful for delineating auditory areas using classical parcellation scheme (e.g., core, belt and parabelt). On the other hand, certain trends in the distribution of the auditory gray matter thickness (e.g., hemispheric asymmetry in the increase in thickness towards temporal pole and the trend of thicker gray matter in auditory cortex compared to the rest of the brain) may have functional significance yet to be established.

Quantitative assessment of gray matter thickness has already provided objective measure of the effects of aging, learning and disease on the human brain (Rosas et al., 2002, Kuperberg et al., 2003, Sailer et al., 2003, Sowell et al., 2003, Draganski et al., 2004, Salat et al., 2004). Being able to assess and compare gray matter thickness of different auditory areas in different populations (e.g., professional musicians and people with no musical training, dyslexics and people with normal reading abilities) may improve our understanding of the structural basis for a wide range of auditory abilities and dysfunction in the population.

References

- Blinkov, S. and I. Glezer (1968). The human brain in figures and tables: a quantitative handbook. New York, Basic Books, Inc., Plenum Press (p. 181).
- Dale, A. M., B. Fischl, et al. (1999). "Cortical surface-based analysis. I. Segmentation and surface reconstruction." Neuroimage **9**(2): 179-94.
- Draganski, B., C. Gaser, et al. (2004). "Neuroplasticity: changes in grey matter induced by training." Nature **427**(6972): 311-2.
- Fischl, B. and A. M. Dale (2000). "Measuring the thickness of the human cerebral cortex from magnetic resonance images." Proc Natl Acad Sci U S A **97**(20): 11050-5.
- Fischl, B., M. I. Sereno, et al. (1999). "Cortical surface-based analysis. II: Inflation, flattening, and a surface-based coordinate system." Neuroimage **9**(2): 195-207.
- Kuperberg, G. R., M. R. Broome, et al. (2003). "Regionally localized thinning of the cerebral cortex in schizophrenia." Arch Gen Psychiatry **60**(9): 878-88.
- Rosas, H. D., A. K. Liu, et al. (2002). "Regional and progressive thinning of the cortical ribbon in Huntington's disease." Neurology **58**(5): 695-701.
- Sailer, M., B. Fischl, et al. (2003). "Focal thinning of the cerebral cortex in multiple sclerosis." Brain **126**(Pt 8): 1734-44.
- Salat, D. H., R. L. Buckner, et al. (2004). "Thinning of the cerebral cortex in aging." Cereb Cortex **14**(7): 721-30.
- Sowell, E. R., B. S. Peterson, et al. (2003). "Mapping cortical change across the human life span." Nat Neurosci **6**(3): 309-15.
- von Economo, C. (1929). The cytoarchitectonics of the human cerebral cortex. London, Oxford University Press.

Figure Captions

Figure 4.1. Typical maps of gray matter thickness (left) and corresponding anatomy (right) on the superior temporal lobe (inflated view) for two right hemispheres (Subjs. 1 and 2). Thickness is indicated in color on a light blue (thick) to dark blue (thin) scale. Black outlines on the maps of gray matter thickness indicate gyral/sulcal borders for the purposes of orientation. On the images on the right, light gray indicates gyral and dark gray indicates sulcal regions.

Figure 4.2. **A.** Mean gray matter thickness for different ROIs on the superior temporal lobe. **B.** Mean gray matter thickness for different ROIs after correlation between thickness and curvature was mathematically removed in every hemisphere. Error bars indicate one standard error.

Spatial Map of Gray Matter Thickness (right temporal lobe, inflated view)

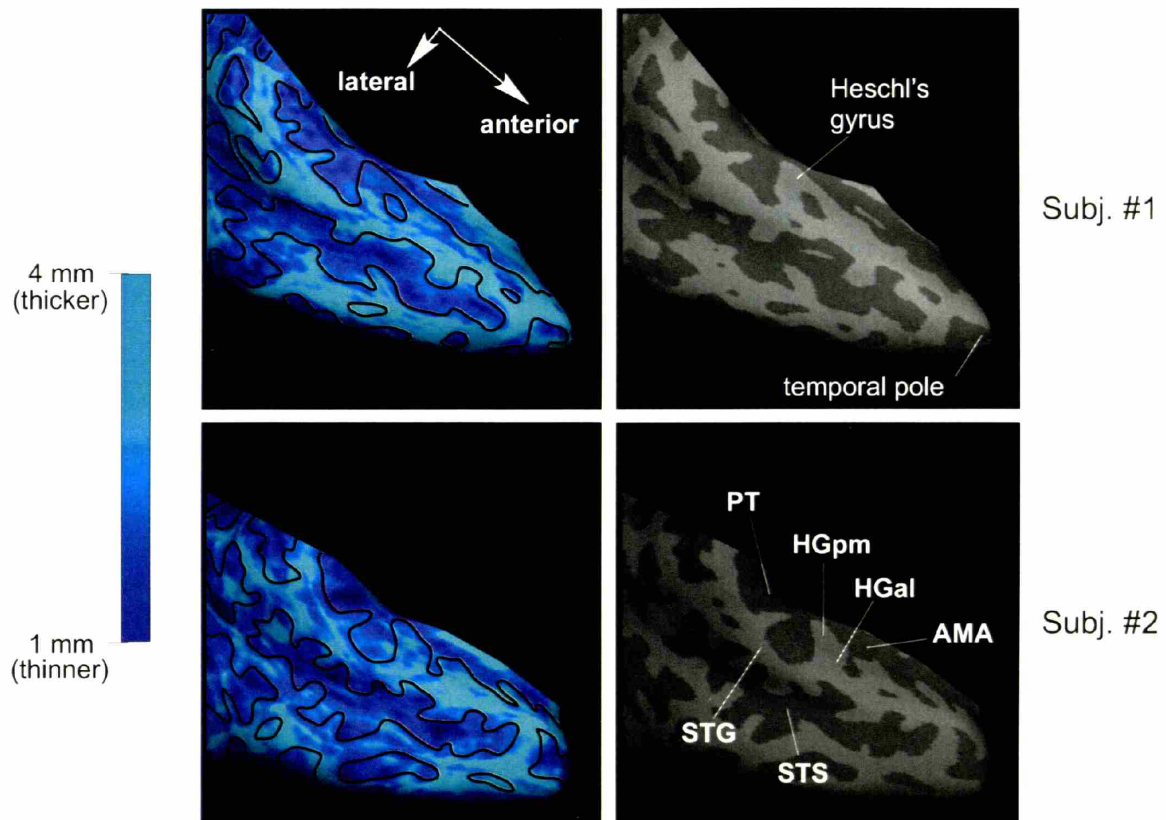
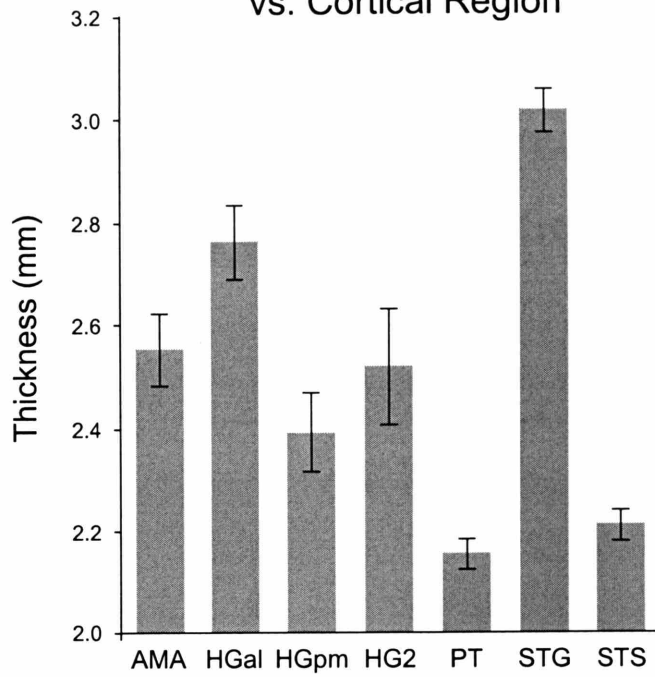


Figure 4.1.



A. Gray Matter Thickness vs. Cortical Region



B. Gray Matter Thickness vs. Cortical Region

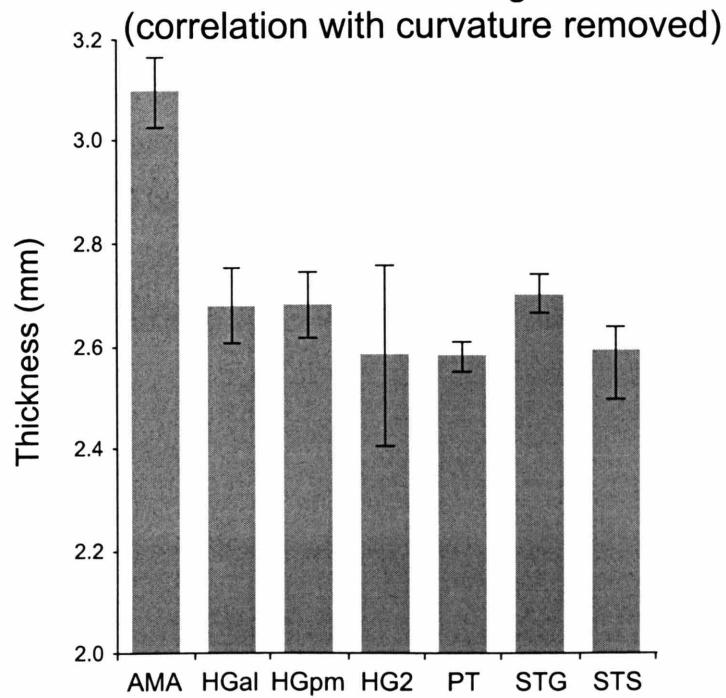


Figure 4.2.

Chapter V.

Contrasting sensitivity of inferior colliculus and auditory cortex to music and continuous noise studied using fMRI

Introduction

This fMRI study was designed to examine relative sensitivity to temporal characteristics of the stimulus in the inferior colliculus and auditory cortex using broadband, non-speech stimuli. Sensitivity to temporal characteristics was examined by considering the temporal waveshape and the magnitude of activation in response to two stimuli: broadband continuous noise and orchestral music. These two broadband stimuli differed in several respects. The primary physical difference was in their temporal characteristics (they were similar in total energy and spectral shape). They also differed in their behavioral relevance (music can carry emotional weight and meaning).

Methods

Subjects

Six subjects (25 to 37 years; 2 male; all right-handed) each participated in either two (5 subjects) or one imaging session. Subjects had no known neurological disorders and no tinnitus. Hearing thresholds of all subjects were normal (< 20 dB HL) at all standard audiological frequencies between 200 and 8000 Hz.

This study was approved by the institutional committees on the use of human subjects at the Massachusetts Institute of Technology, Massachusetts Eye and Ear Infirmary, and Massachusetts General Hospital. All subjects gave their written informed consent.

Acoustic Stimulation

All stimuli were presented binaurally at levels referenced to threshold (measured in the scanner room separately for each ear). Broadband continuous noise was presented at 35, 45, 55, 65 or 75 dB SL (55 - 104 dB SPL) in six imaging sessions with 3-4 levels per session always including 55 dB SL. In five separate sessions, orchestral music (1st 30 sec. of Beethoven Symphony No. 7 in A Major, 4th movement) was presented at 30, 50 and 60 dB SL (54 - 96 dB SPL) with all three levels per session. Stimuli at all levels were clearly audible during functional imaging and did not exceed the subject's comfort level.

Stimuli were alternately turned on for 30 s and off for 30 s in a standard fMRI block paradigm. Four on/off repetitions constituted a scanning "run". Subjects were presented with either (1) 3 runs of noise for every noise level (360 images per level) and 1 run of music at 55dB SL, or (2) 2 runs of music for every music level (235-240 images per level). Stimuli were generated by a digital-to-analog board (running under LabVIEW), amplified, and fed to a pair of audio piezoelectric transducers housed in earmuffs worn by the subject.

Task

Subjects were instructed not to move and to attend to the stimuli. Subjects turned an array of lights on each time the stimulus went on and turned them off when the stimulus went off (this task has origins in a separate study on tinnitus).

Mitigation of scanner acoustic noise

The effects of the acoustic noise produced by the scanner gradient coils during functional imaging were reduced by (1) imaging a single, rather than multiple slices, and (3) using earmuffs that attenuated the gradient noise by ~30 dB SPL at the ear. The earmuffs also attenuated background noise produced by the scanner coolant pump. (Note that the pump noise was on-going and therefore present during the threshold measurements, as well as functional imaging).

Imaging

Subjects were imaged using a transmit/receive head coil and a 1.5 Tesla (General Electric LX) scanner. In each imaging session: (1) Contiguous sagittal images of the whole head were acquired. (2) The brain slices to be functionally imaged were selected based on the sagittal images. The single imaged slice intersected the IC and the posterior aspect of HG in both hemispheres. (3) T1-weighted, high resolution anatomical images were acquired of the selected brain slices for subsequent overlay of the functional data (thickness = 7mm; in-plane resolution = 1.6x1.6mm; TI = 930ms; TR = 4s; TE = 12ms). (4) Functional images were acquired using a blood oxygenation level-dependent (BOLD) sequence (asymmetric spin echo, TR ~ 2s, TE = 70 ms, τ offset = -24 ms, flip = 90°, slice thickness = 7mm, in-plane resolution = 3.125x3.125mm). Functional imaging was performed using cardiac gating which increases the detectability of activation in the brainstem structures (Guimaraes et al. 1998). Image acquisitions were synchronized to every other QRS complex thus yielding a TR of approximately 2s. The TRs were recorded so that the precise timing of the image acquisitions relative to the sound stimulus could be taken into account in subsequent analyses. Fluctuations in heart rate lead to variations in TR that result in image-to-image variations in image signal strength

for short TRs (i.e., T1 effects). Using the measured TR values, image signal was corrected to account for these variations (Guimaraes et al., 1998).

Detecting activation

The functional image data were first corrected for any head movements that may have occurred over the course of the imaging session using standard software (SPM95; Friston et al., 1995). Activation was then detected using a general linear model which operated on a set of basis functions designed to reflect different temporal components of fMRI activation in the auditory system (Harms and Melcher, 2003). Activation maps were created for each stimulus and sound level by estimating (using an F-statistic; Fomby et al., 1984), for every voxel, whether the amplitude of any of the basis functions is significantly different from zero.

Defining regions of interest

Responses were analyzed quantitatively within the following anatomically defined regions of interest (ROIs): IC, HG and PT. We used gross anatomical landmarks to define ROIs for IC and auditory cortex. The ICs were readily identified as distinct anatomical circular areas in the near-coronal plane. Cortical areas were defined as follows. In the near-coronal slice, the HGpm area was defined on the “mushroom” of Heschl’s gyrus protruding from the surface of the superior temporal plane. The PT area was defined as cortex lateral to the Heschl’s gyrus and was limited laterally by the middle of the lateral surface of the superior temporal gyrus. All ROIs were first identified in the high-resolution T1-weighted MRI images (in-plane resolution 1.6 x 1.6 mm) for each hemisphere of every subject. These “high-resolution” ROIs were then down-sampled to the lower resolution of the functional images (3.1 x 3.1 mm) to yield the ROIs used for all subsequent analyses.

Calculating response waveforms:

Response waveforms were calculated from the raw functional data by (1) interpolating the data for each run to a constant inter-image interval of 2 s, (2) averaging

across stimulus presentations on a time-point by time-point basis, and (3) temporally smoothing using a three-point filter (details in Harms and Melcher, 2002).

Response quantification

In the IC, response amplitude was quantified for a single voxel with lowest p-value within IC ROI. In cortex, response amplitude was quantified as mean response amplitude for all active ($p < 0.001$) voxels. For all structures, response amplitude was calculated from time courses as the time-average percent change over the 30 s stimulus presentation.

Results

Activation was reliably evoked in all auditory structures intersected by the imaging plane, IC and posterior aspect of HG and PT, for both stimuli at all sound levels.

Effect of stimulus type on response waveshape:

Stimulus type had a substantial effect on response waveshape in cortex at all stimulus levels. Consistent with previously published data (Harms et al., 2004), responses to music were largely sustained in contrast to noise, which produced phasic responses in the auditory cortex (Figure 5.1A and B for PT). While responses to music were similarly sustained in HG and PT, responses to noise were more phasic in PT than in HG (not shown). In contrast to cortex, response waveshape in the IC did not depend on stimulus type: response waveshape was sustained for both music and noise (Figure 5.1C and D).

Effect of stimulus type on response amplitude:

In the IC, music consistently produced less ($p < 0.01$) activation (i.e., smaller amplitude of the response) than noise throughout stimulus presentation when equated in

either dB SL (Figure 5.2, left) or dB SPL (not shown). In contrast to the IC, music produced considerably more activation than noise in the auditory cortex (Figure 5.2, middle and right). This difference was even more pronounced in PT ($p < 0.00001$) compared to HG ($p < 0.001$). This “reversal” of more potent stimulus for IC and cortex was true at all stimulus levels.

Discussion

We examined sensitivity to stimulus type in two structures, inferior colliculus and auditory cortex, using orchestral music and continuous noise. Our results show that auditory cortex shows strong sensitivity to stimulus type in two respects. First, the waveshape of the fMRI response changed drastically from sustained to phasic depending on whether music or noise was used as a stimulus. Second, response amplitude was significantly greater when music, as compared to noise, was used as a stimulus. In contrast to auditory cortex, IC did not show strong sensitivity to stimulus type. The waveshape of the fMRI responses in the IC was similarly sustained for both music and noise. While noise produced greater response amplitude in the IC compared to music, this difference was far less significant than the difference between responses to noise and music in the auditory cortex.

Music and continuous broadband noise differ in two major respects: temporal characteristics and behavioral relevance. It is, therefore, possible that either one or both of these parameters dominate the waveshape of the fMRI response. Harms et al (2005) showed that stimulus temporal characteristics are strongly represented in the temporal envelope of neural activity in auditory cortex by demonstrating that response waveshape shifts from sustained to phasic when stimulus rate and/or continuity increase. Music has discontinuities and amplitude modulations at relatively low rates and produced sustained responses in our study. White noise, on the other hand, has amplitude modulations at very high rates (i.e., is perceived as continuous stimulus) and produced phasic responses.

Thus, our findings are consistent with Harms et al and suggest that temporal characteristics are reflected in the waveshape of fMRI responses in the auditory cortex.

Our results also show that music produced greater response amplitude than noise and this difference was greater in the non-primary PT area than in the primary HG area. These findings would be consistent with the general notions that (1) more behaviorally relevant and engaging stimulus produces more activation in cortex, and (2) behavioral relevance of the stimulus would be represented to a greater degree in the non-primary compared to the primary auditory areas. Thus, our data suggest that, in the auditory cortex, behavioral relevance and/or subject's state are represented in the fMRI response amplitude.

Our results also show that auditory cortex and IC showed reversed sensitivity to stimulus type: music produced greater response amplitude than noise in the auditory cortex, but reverse was true for the IC. This indicates that the “most potent” stimulus may be different depending on the auditory structure. This information may come useful when designing experiments aimed at optimizing activation in a particular structure. For example, temporally complex stimuli such as music and speech are generally thought to be among the most potent activators of auditory cortex. However, our results illustrate that this idea does not always extend to lower centers. Broadband continuous noise, on the other hand, would be a relatively bad choice to elicit strong cortical activation, but a great choice to elicit strong IC activation.

To conclude, our results, combined with previous studies, suggest that, in the auditory cortex, fMRI response waveshape is dominated by the stimulus temporal characteristics. Our results also suggest that temporal characteristics and behavioral relevance are represented to a greater degree in the fMRI responses of the auditory cortex than inferior colliculus.

References

Fomby, T. B., Hill, R.C., Johnson, S.R. (1984). Advanced econometric methods. New York, Springer-Verlag.

Friston, K. J., Ashburner, J., Frith, C.D., Poline, J.-B., Frackowiak, R.S.J (1995a). "Spatial registration and normalization of images." Hum Brain Mapp **2**: 165-189.

Friston, K. J., Holmes, A.P., Worsley, K.J., Poline, J.-P., Frith, C.D., Frackowiak, R.S.J. (1995b). "Statistical parametric maps in functional imaging: A general linear approach." Hum Brain Mapp **2**: 189-210.

Guimaraes, A. R., J. R. Melcher, et al. (1998). "Imaging subcortical auditory activity in humans." Hum Brain Mapp **6**(1): 33-41.

Harms, M. P. and J. R. Melcher (2002). "Sound repetition rate in the human auditory pathway: representations in the waveshape and amplitude of fMRI activation." J Neurophysiol **88**(3): 1433-50.

Harms, M. P. and J. R. Melcher (2003). "Detection and quantification of a wide range of fMRI temporal responses using a physiologically-motivated basis set." Hum Brain Mapp **20**(3): 168-83.

Harms, M. P., J. J. Guinan Jr, et al. (2005). "Short-term sound temporal envelope characteristics determine multisecond time-patterns of activity in human auditory cortex as shown by FMRI." J Neurophysiol. **93**(1): 210-22

Figure Captions

Figure 5.1. Response waveshape for IC and PT in response to music (A, C) and noise (B, D). Each waveform is an average across subjects. Response waveshapes for HG are not shown because they are qualitatively similar to those of PT.

Figure 5.2. Response amplitude vs. sound level for music (open symbols) and noise (black symbols) for IC (left) and auditory cortex (middle and right). Bars indicate OSE.

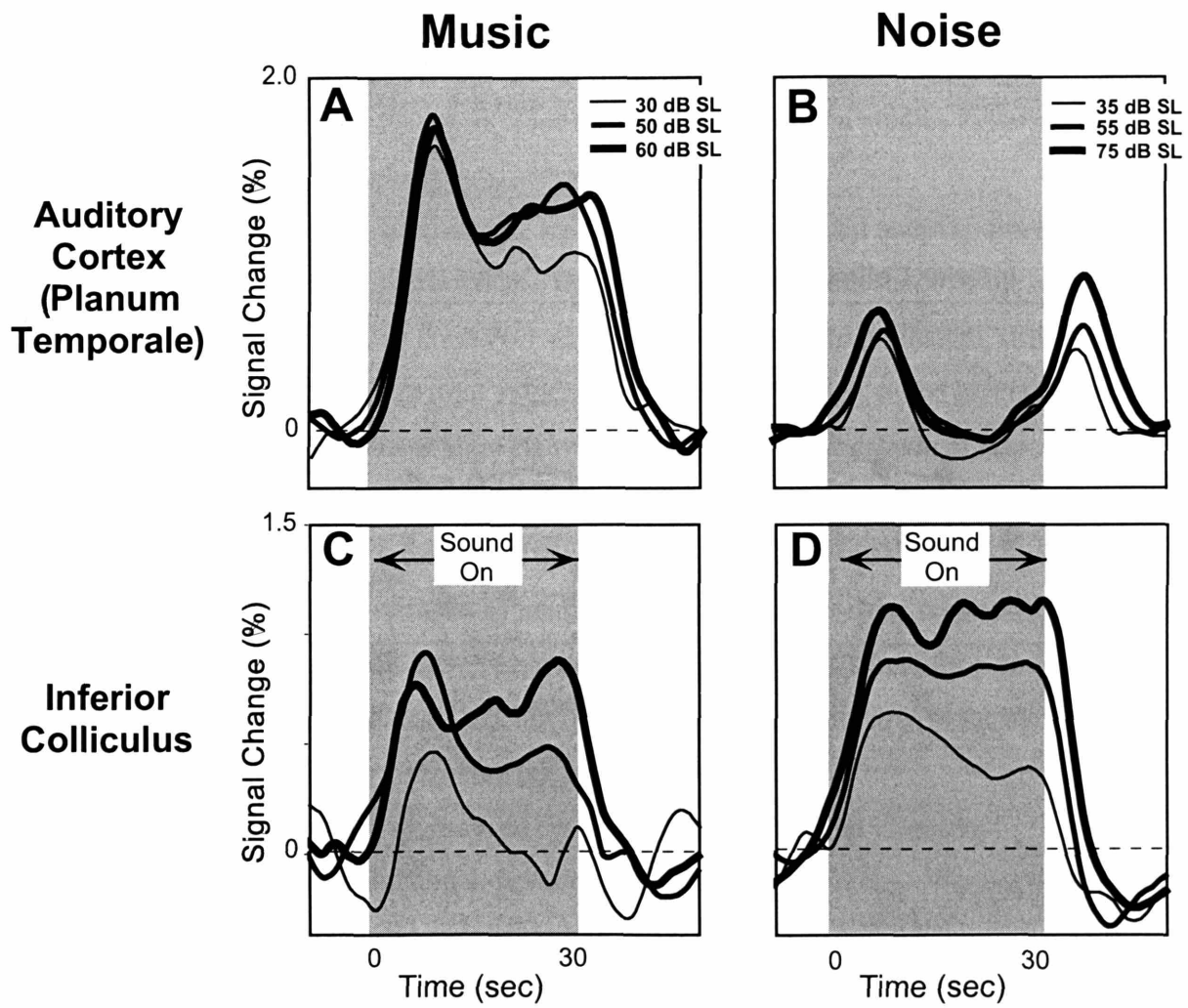


Figure 5.1.

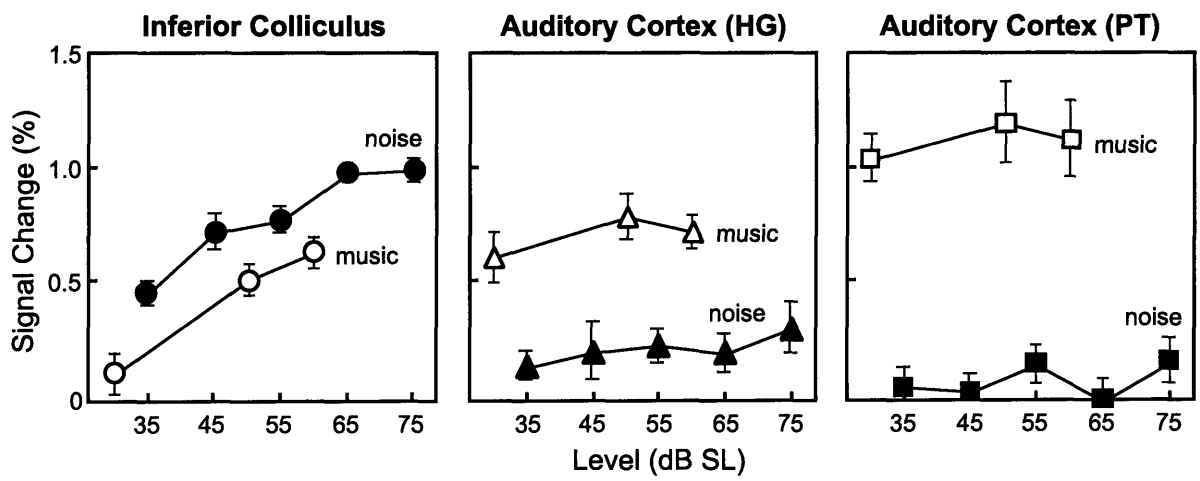


Figure 5.2.

Chapter VI.

SUMMARY

From brainstem to thalamus to cortex, the human auditory pathway includes many functionally and structurally distinct centers in which sound is processed. In animals, invasive neurophysiology and histology revealed these distinctions, and, consequently, organizational principles behind sound processing and perception. In humans, however, comparable demonstrations are sparse. This thesis includes several studies that used MRI to reveal distinctions between auditory centers in living humans.

To summarize our main findings, we found in Chapter I that auditory brainstem and cortex exhibit contrasting sensitivities to sound level in that the shape of the level function was different between these two stages of processing. In brainstem, fMRI activation increased and then showed evidence of saturation at high sound levels. In contrast, cortical fMRI activation showed evidence of accelerated growth at high sound levels. This result, in combination with other data from our group, suggests the following: as more sound is presented to the ear, more activity is observed in the auditory brainstem structures up to a limit set by saturation. In contrast, cortical responses exhibit complexities that might reflect sub-ordination of representation of sound level to other sound characteristics in the overall amount of population neural activity in the auditory cortex (Harms and Melcher, 2002, Hawley and Melcher, 2002).

In Chapters II and III we focused on the auditory cortex and examined differences, structural and functional, between different auditory areas. We proposed two candidate markers for primary auditory cortex (PAC). One, a physiological marker, was suggested by the region of the sustained responses on Heschl's gyrus. Comparison to anatomical literature indicated that the region of sustained responses may also include primary-like auditory areas immediately adjacent to PAC. Another marker, an anatomical one, was suggested by the region of high gray-matter R1 on Heschl's gyrus. While intriguing and promising, neither proposal has been validated beyond being consistent with descriptions of PAC in the classical anatomical literature.

In the future, our candidate structural marker for PAC can be directly validated by comparisons of MRI data (gray matter R1 maps) and myelin-stained tissue from the same sample in postmortem tissue (e.g., Walters et al., 2003, Barbier et al., 2002, Mottershead et al., 2003, Eickhoff et al., 2004). However, this approach cannot be applied to validate functional candidates for PAC.

In living subjects, one possible way to proceed is to examine how well the two candidate markers for PAC correlate with one another (or with other possible markers). For example, one can examine to what degree the region of high R1 on Heschl's gyrus (structural marker) overlaps with the region of sustained responses on Heschl's gyrus (functional marker). The idea is that a consistent pattern of overlap across subjects would increase our confidence that either one of these candidates corresponds to PAC. Unfortunately, we cannot examine how the region of high R1 correlates with the region of sustained responses because the data for Chapters II and III were acquired in different subjects.

However, a different type of functional data, a tonotopic map of the auditory cortex, is available for some of the subjects imaged in Chapter III. Tonotopic gradients are often used in animal auditory neurophysiology to locate PAC. In our study, the maps of tonotopic representation in auditory cortex were acquired as pilot data for four left hemispheres (Subjs. 2-5, Chapter III) using sweeps of AM narrowband noise (bandwidth = 1/3 octave) with center frequencies from 250 to 8000 Hz. Using these tonotopic maps, we will qualitatively illustrate in Figure 6.1 how structural and functional data could be combined in the future investigations to understand how the candidate markers of PAC relate to PAC as it would be defined histologically (or physiologically).

Figure 6.1 (left column) shows the regions of high R1 (white) on Heschl's gyrus for four left hemispheres in the inflated view (the advantages of this view for data presentation are discussed in Chapter IV). A region of high R1 on the postero-medial part of Heschl's gyrus (most probable location of PAC based on histological evidence) is outlined in red. An inflated view is used here to show sulcal (dark gray) and gyral (light gray) regions simultaneously. Figure 6.1 (middle column) shows color-coded tonotopic maps in the same hemispheres (also in the inflated view). Gradations of color from dark

(high frequencies) to light (low frequencies) blue indicate tonotopic arrangements on and in the vicinity of Heschl's gyrus. Consistent with previous studies in humans (e.g., Talavage et al., 2004), these maps show that there are several tonotopic gradients on the surface of the superior temporal plane (solid and dashed black arrows). In all cases, one of the gradients (gradient "PAC", solid black arrow) begins with high frequencies at the postero-medial edge of the Heschl's gyrus (first, if there are two) and moves in the antero-lateral direction to end with low frequencies off the lateral side of the Heschl's gyrus. Unlike in animals, the tonotopic arrangements in the human auditory cortex have not been established as to be used as a "gold standard" for delimiting auditory cortical areas. For example, some previous studies have noted medial-to-lateral gradient on Heschl's gyrus (e.g., Talavage et al., 2000), while others have noted variation in frequency along the crown of the gyrus (e.g., Formisano et al., 2003). Interestingly, our tonotopic maps in Figure 6.1 include elements of both (i.e., somewhat concentric mapping) and suggest a way to reconcile these two seemingly contradictory views. Nevertheless, the location (postero-medial Heschl's gyrus) and direction of the gradient may suggest that it coincides with primary auditory cortex in humans (Wessinger et al., 1997, Bilecen et al., 1998, Talavage et al., 2000, Formisano et al., 2003, Talavage et al., 2004). Below, we will use this tonotopic gradient "PAC" as an approximate functional marker of the primary auditory cortex.

Superimposing the region of high R1 (red outline) on the tonotopy map for each hemisphere illustrates that the high R1 region (1) overlaps with the "PAC" gradient in all four cases and only includes another gradient in one hemisphere (Subj. 3), and (2) consistently overlaps with the medial part and less consistently with the lateral part of the "PAC" gradient (Figure 6.1, right). In particular, in all four cases, the region of high R1 on the postero-medial part of Heschl's gyrus overlaps high and middle frequency regions of the "PAC" gradient. Only in two cases (Subjs. 3 and 5) the high R1 region also overlaps low frequencies of the "PAC" gradient. These data suggest that the region of high R1 on Heschl's gyrus may specifically coincide with the medial part of PAC and less reliably with its lateral part.

Consistent with this proposal, the histological literature suggests that while the medial border of the auditory koniocortex is well defined, its lateral border is more

elusive (Galaburda and Sanides, 1980, Penhune et al., 1996). Histological literature also suggests differences between the medial and lateral parts of the auditory core (Galaburda and Sanides, 1980, Hackett et al., 2001). In particular, there is evidence that the medial part of the auditory koniocortex may be more heavily myelinated than its lateral part (Hackett et al., 2001). This evidence suggests that the probability of “hitting” the medial part of auditory koniocortex may be greater compared to its lateral part in general, but especially if using parameters that are sensitive to myelin.

To conclude, the qualitative comparison of structural (gray matter R1) and functional (tonotopic) data (1) support our previous proposal that the high gray matter R1 region on Heschl’s gyrus may present a marker for primary auditory cortex in humans, and (2) suggests that the high R1 region consistently marks the more heavily myelinated medial part of the auditory koniocortex, but only sometimes includes the less heavily myelinated lateral part. While neither gray matter R1 nor tonotopy data alone provide means to delineate PAC at present, combining these data illustrates how, with further improvements, the auditory MRI field should converge on establishing a marker for PAC.

In the end of this final chapter, I would like to discuss which one of the two proposed markers for the primary auditory cortex (high gray matter R1 or sustained fMRI responses) is more promising from practical and theoretical considerations. In my opinion, delimiting auditory cortical areas using intrinsic MR tissue parameters (structural marker) is both more practical and conceptually “cleaner” than using temporal properties of the fMRI responses (functional marker) for the following reasons: (1) the concept behind our structural marker is simple and based on prominent and well-documented features of the auditory gray matter myelination (whereas there is no direct physiological correlate for our functional marker in either animal or human physiology); (2) the structural MRI technique is practical because it is easy to implement (once developed) and the necessary data take short time to acquire so that it can be included as a standard scan in any neuroimaging study (in contrast, auditory fMRI experiments are several hours long and are relatively complex); (3) the mapping of structural parameters is continuous along the cortical surface (whereas functional data are limited to voxels that

respond to sound); and finally, (4) the concept and implementation of gray matter R1 mapping is in its infancy and holds plenty of room for improvement.

References

- Barbier, E. L., S. Marrett, et al. (2002). "Imaging cortical anatomy by high-resolution MR at 3.0T: detection of the stripe of Gennari in visual area 17." Magn Reson Med **48**(4): 735-8.
- Bilecen, D., K. Scheffler, et al. (1998). "Tonotopic organization of the human auditory cortex as detected by BOLD-fMRI." Hear Res **126**(1-2): 19-27.
- Eickhoff, S., N. B. Walters, et al. (2004). "High-resolution MRI reflects myeloarchitecture and cytoarchitecture of human cerebral cortex." Hum Brain Mapp **24**(3): 206-215.
- Formisano, E., D. S. Kim, et al. (2003). "Mirror-symmetric tonotopic maps in human primary auditory cortex." Neuron **40**(4): 859-69.
- Galaburda, A. and F. Sanides (1980). "Cytoarchitectonic organization of the human auditory cortex." J Comp Neurol **190**(3): 597-610.
- Harms, M. P. and J. R. Melcher (2002). "Sound repetition rate in the human auditory pathway: representations in the waveshape and amplitude of fMRI activation." J Neurophysiol **88**(3): 1433-50.
- Hawley, M. L. and J. R. Melcher (2002). Representation of sound bandwidth in the human auditory system using fMRI. Assoc Res Otolaryngology.
- Hackett, T. A., T. M. Preuss, et al. (2001). "Architectonic identification of the core region in auditory cortex of macaques, chimpanzees, and humans." J Comp Neurol **441**(3): 197-222.
- Mottershead, J. P., K. Schmierer, et al. (2003). "High field MRI correlates of myelin content and axonal density in multiple sclerosis--a post-mortem study of the spinal cord." J Neurol **250**(11): 1293-301.
- Penhune, V. B., R. J. Zatorre, et al. (1996). "Interhemispheric anatomical differences in human primary auditory cortex: probabilistic mapping and volume measurement from magnetic resonance scans." Cereb Cortex **6**(5): 661-72.
- Talavage, T. M., P. J. Ledden, et al. (2000). "Frequency-dependent responses exhibited by multiple regions in human auditory cortex." Hear Res **150**(1-2): 225-44.
- Talavage, T. M., M. I. Sereno, et al. (2004). "Tonotopic organization in human auditory cortex revealed by progressions of frequency sensitivity." J Neurophysiol **91**(3): 1282-96.
- Walters, N. B., G. F. Egan, et al. (2003). "In vivo identification of human cortical areas using high-resolution MRI: an approach to cerebral structure-function correlation." Proc Natl Acad Sci U S A **100**(5): 2981-6.
- Wessinger, C., M. Buonocore, et al. (1997). "Tonotopy in human auditory cortex examined with functional magnetic resonance imaging." Human Brain Mapping **5**: 18-25.

Figure Caption

Figure 6.1. Combining structural and functional data in individual subjects supports our proposal that the high gray matter R1 on Heschl's gyrus may coincide with primary auditory cortex. Each row includes data from the same hemisphere.

LEFT: Regions of highest gray matter R1 on Heschl's gyrus (white) superimposed on an inflated view of the anatomy of the superior temporal plane in the vicinity of Heschl's gyrus (gyri). The region of high R1 on the postero-medial part of Heschl's gyrus, a proposed site of the primary auditory cortex, is outlined in red. Light gray indicates gyral and dark gray indicates sulcal regions. Yellow arrow indicates Heschl's gyrus (first, if there are two).

MIDDLE: Tonotopy maps superimposed on the anatomy of the superior temporal plane in the vicinity of Heschl's gyrus (gyri). Activation to the sweeps of narrowband noise (color) is thresholded at the liberal $p < 0.05$ cutoff so that the continuity in the best frequency gradations could be appreciated. Best frequency is indicated in color on a light blue (low frequency) to dark blue (high frequency) scale. Black arrows indicate major tonotopic gradients in the vicinity of Heschl's gyrus (gyri). Thin black outlines indicate gyral/sulcal borders for the purposes of orientation. The same methods for scanner noise reduction, that were used in Chapters I and II (clustered volume acquisition and staggered sampling) were used to acquire tonotopy maps data.

RIGHT: The region of high R1 (red outline) is superimposed on the tonotopic maps. In every case, a high-to-low frequency gradient (solid black arrow) lies within the high R1 region.

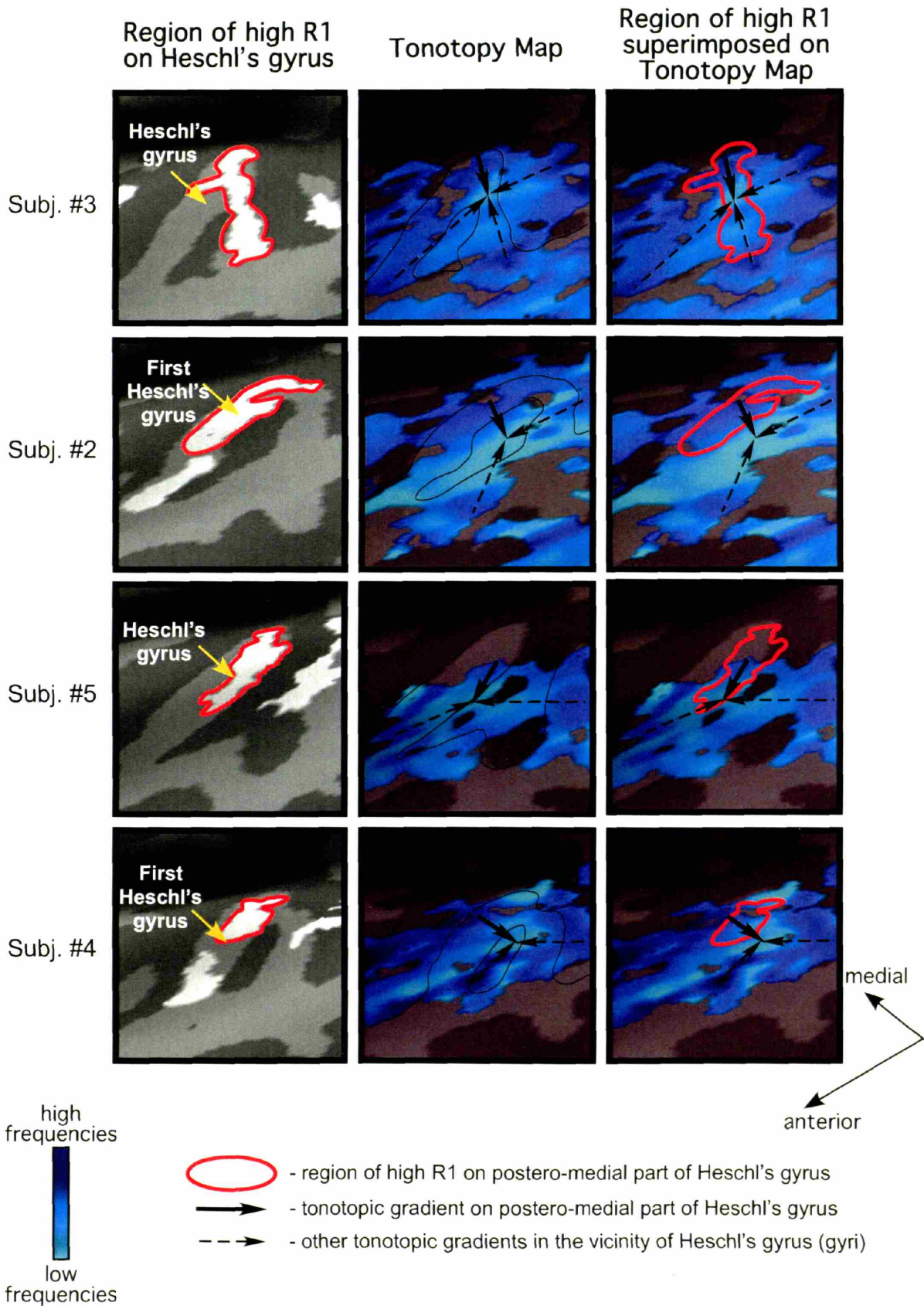
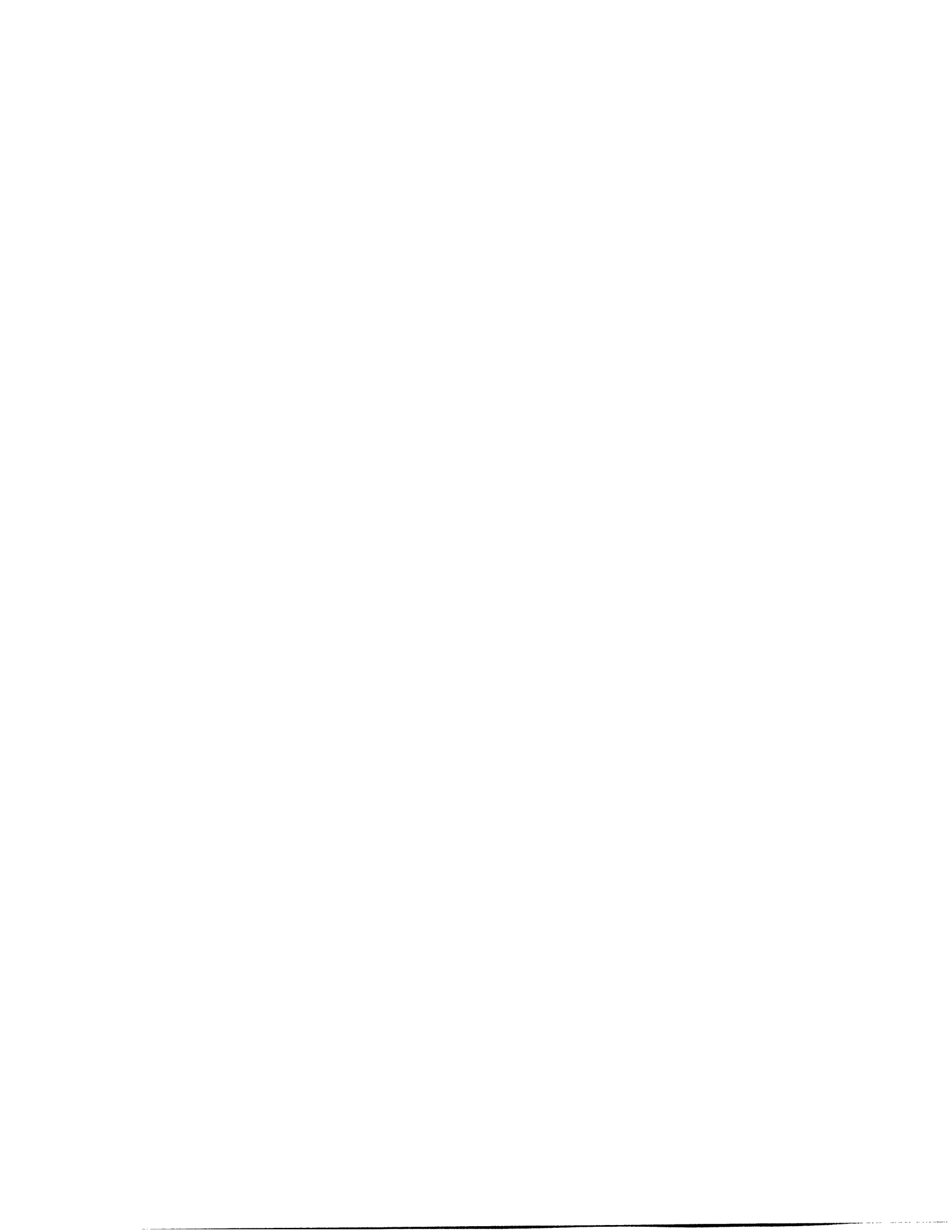


Figure 6.1.



Biography

Irina S. Sigalovsky

EDUCATION

- 1996 - 2005 - Massachusetts Institute of technology, Cambridge, MA
Ph.D. in Speech and Hearing Biosciences and Technology, Harvard-MIT
Division of Health Sciences and technology
- 1993 - 1996 - Boston University, Boston, MA
B.S. in Biomedical Engineering

HONORS AND AWARDS

- 2004 - Helen Carr Peake Research Prize
- 1999, 2002, 2003 - Athinoula A. Martinos Research Scholarship
- 1995 - Alpha Eta Mu Beta Biomedical Engineering Honor Society, Secretary
- 1995 - Biomedical Engineering Society (BMES)
- 1994 - Tau Beta Pi Engineering Honor Society

TEACHING EXPERIENCE

- 2003 - Guest Lecturer, "Neural Basis of Vision and Audition" (HST.722)
MIT, Cambridge, MA
- 2003 - Guest Lecturer, "Quantitative Physiology of the Auditory System" (BE 509)
Boston University, Boston, MA
- 2002 - Guest Lecturer, "Neural Basis of Vision and Audition" (9.04)
MIT, Cambridge, MA
- 2002 - Guest Lecturer, "Biophysics of the Hearing Mechanism" (SAR CD 846)
Boston University, Boston, MA
- 2001 - Teaching Assistant, "Functional MRI: Data Acquisition and Analysis"
MIT/Harvard HST, Cambridge MA
- 1999 - Guest Lecturer, " Auditory Psychophysics and Physiology",
Harvard University, Cambridge, MA

PROFESSIONAL EXPERIENCE

- 1993-1996 - Research Assistant, Auditory-Neurophysiology Laboratory,
Dept. of Biomedical Engineering, Boston University, MA
- 1995 - Research Assistant, Clinical Engineering Dept.,
Brigham and Women's Hospital, Boston, Ma.

PUBLICATIONS

- Sigalovsky, I.S., Fischl, B., Wald, L.L., Dale, A.M. and Melcher, J.R. (in preparation) Imaging gray matter myelin content of human auditory cortex suggests that a major architectonic division can be resolved in-vivo.
- Sigalovsky, I.S., Guinan, J.J, Harms, M.P., Melcher, J.R. (in preparation) Spatio-temporal patterns of fMRI activation in the human auditory cortex.
- Sigalovsky, I.S., Guinan, J.J, Melcher, J.R. (in preparation) Sound level representations in the auditory brainstem, thalamus and cortex of humans as seen with fMRI.
- Harms, M.P., Melcher, J.R., Sigalovsky, I., Guinan, J.J. (2005) Sound temporal envelope determines the time-pattern of fMRI responses in human auditory cortex. *J. Neurophys.* 93(1): 210-22.

- Melcher, J.R., Sigalovsky, I., Guinan, J.J., Levine, R.A. (2000) Lateralized tinnitus studied with functional magnetic resonance imaging: abnormal inferior colliculus activation. *J. Neurophys.* 83: 1058-1072.
- Sigalovsky, I.S., Melcher, J.R., Levine, R.A. (1999) Growth of fMRI activation with stimulus level in the inferior colliculi: implications for understanding tinnitus-related abnormalities. *Proceedings of the Sixth International Tinnitus Seminar.* 317-322.
- Melcher, J.R., Sigalovsky, I.S., Levine, R.A. (1999) Tinnitus-related fMRI activation patterns in human auditory nuclei. *Proceedings of the Sixth International Tinnitus Seminar.* 166-170.

ABSTRACTS

- Sigalovsky, I.S., Melcher, J.R. (2003) Coding of sound in the human central auditory system: Examinations using structural and functional MRI. *International Conference on Auditory Cortex.* Invited talk.
- Sigalovsky, I.S., Fischl, B., Wald, L.L., Dale, A.M. and Melcher, J.R. (2003) Imaging the Internal Architecture of Auditory Cortical Gray Matter in Living Humans. *Abstracts of Assoc. Res. Otolaryngol.*
- Harms, M.P., Sigalovsky, I.S. and Melcher, J.R. (2002) Temporal dynamics of fMRI responses in human auditory cortex: primary vs. non-primary areas. *Abstracts of Assoc. Res. Otolaryngol.*
- Sigalovsky, I.S., Hawley, M., Harms, M.P., Melcher, J.R. (2001) Sound level representations in the human auditory pathway investigated using fMRI. *Abstracts of the Organization for Human Brain Mapping.*
- Sigalovsky, I.S., Hawley, M., Harms, M.P., Levine, R.A., Melcher, J.R. (2001) Sound level representations in the human auditory pathway investigated using fMRI. *Abstracts of Assoc. Res. Otolaryngol.*
- Harms, M.P., Sigalovsky, I.S., Guinan, J.J.Jr. and Melcher, J.R. (2001) Temporal dynamics of fMRI responses in human auditory cortex: dependence on stimulus type. *Abstracts of Assoc. Res. Otolaryngol.*
- Melcher, J.R., Sigalovsky, I., Levine, R.A., Guinan, J.J.Jr., Talavage, T.M., Ravicz, M.E., Rosen, B.R., Benson, R.R. and Fullerton, B.C. (1998) Tinnitus studied using functional magnetic resonance imaging: preliminary findings. *Abstracts of Assoc. Res. Otolaryngol.*
- Sigalovsky I., Hancock, K.E. and Voigt, H.F. (1995) The effects of stimulus duration on the response maps of the neurons in the dorsal cochlear nucleus in the anesthetized gerbil. *Annals of Biomed. Eng.* 23: S-87